Università degli Studi di Firenze

DIPARTIMENTO DI FARMACOLOGIA PRECLINICA E CLINICA
"MARIO AIAZZI MANCINI"

Tesi di Dottorato di Ricerca
In Neuroscienze XXI ciclo
Settore Disciplinare BIO/14

"A STUDY ON CELLULAR AND MOLECULAR MECHANISMS OF NEUROINFLAMMATION, CHOLINERGIC DEFICITS AND NOVEL CHOLINESTERASE INHIBITORS FOR THE MEMORY IMPAIRMENTS"

Coordinatore del ciclo:
Prof. Luca Massacesi

Candidato:
Dott.ssa Francesca Cerbai

Tutore Scientifico:
Dott.ssa Maria Grazia Giovannini

Tutore Teorico:
Prof. Renato Corradetti

Anno Accademico 2008/2009

INDEX

1. INTRODUCTION

1.1 Learning and memory

Behaviour is the result of the interaction between genes and the environment. In humans the most important mechanisms through which the environment alters behaviour are learning and memory. Learning is the process by wich we acquire knowledge about the world, while memory is the process by which that knowledge is encoded, stored and retrieved.

Memory is a process that can last a second or forever, and it can be classified (Baddeley, 1992) from a time-space point of view in:

SHORT TERM MEMORY: is a working memory and its duration is at maximum 5 sec. It needs repetition over time.

LONG TERM MEMORY: involves more complicate memory processes to remember facts long time after the acquisition. Long term memory strongly correlates to new protein synthesis.

IMPLICIT OR NON DECLARATIVE MEMORY: does not depend on conscious process and does not require a conscious search of memory. This type of memory builds up slowly, through repetition over many trials, and is expressed primarily in performance, not in words. Examples of implicit memory include perceptual and motor skills and the learning of certain types of procedures and rules.

EXPLICIT OR DECLARATIVE MEMORY: it depends on conscious and deliberate processes. Example of explicit memory is the factual knowledge of people, places, and

things. It can be classified as *episodic*, a memory for events and personal experiences, or *semantic,* a memory for fact, objects and concepts.

The analysis of the effects of lesions is the oldest, and still most widely used, approach to the problem of determining the neuroanatomy of memory systems in the brain. In humans, the behavioural effects of lesions resulting from head injury, tumors, vascular accidents or neurosurgery are compared to the behaviour of normal subjects on a variety of standardized behavioural tasks (Steinberg and Augustine, 1997;Harrison et al., 1999). Similar research has been carried out in nonhuman species like primates and rodents (Aggleton and Mishkin, 1985) (Mumby et al., 1993).

Studies performed on patients with Korsakoff's syndrome have shown a linkage between the medial dorsal thalamic nucleus, region consistently injured in these patients, and impaired explicit memory (Graff-Radford et al., 1990;Winocur et al., 1984). This syndrome is associated with a severe anterograde and retrograde amnesia.

Patients with medial dorsal thalamic damage following cerebrovascular infarctions also demonstrate significant memory impairment (Graff-Radford et al., 1990; Winocur et al., 1984).

Hippocampus may mediate the representation of spatial and temporal memories. Experimental supports for these ideas has come from many different approaches to the study of hippocampal function. When the hippocampus is damaged, animals show profound impairment in the ability to store information across a delay interval. The most sensitive task that is used to demonstrate memory impairments related to the hippocampus is the spatial task that requires the animal to move in the environment (O'keefe and Nadel, 1978). In monkeys, hippocampal lesions also impaire memory for the spatial location of objects. The hippocampus may temporarily store information that has been recently obtained (working memory).

The cerebellum is responsible for implicit memories of sensorimotor learning.

Pharmacological studies in numerous species, using a variety of experimental paradigms, have linked ACh to learning and memory processes. In general cholinergic agonists, like physostigmine, improve memory whereas cholinergic antagonists, like scopolamine, impair memory (Bartus et al., 1985).

Classic lesion studies have identified a particular set of cholinergic neurons and projections that is critical for learning and memory. These neurons are located in the basal forebrain and project to the hippocampus and neocortex. The basal forebrain region includes the medial septal areas (MSA) and the vertical limb of the diagonal band of Broca (dbB), which project primarily to the hippocampus, and the horizontal limb of the dbB and nucleus basalis magnocellularis (NBM), which project to the neocortex. Lesions of the MSA and NBM in rodents impair performance on a variety of mnemonic tasks including spatial reference and working memory tasks such as Morris water maze and T-maze alternation (McDonald et al., 1997).

All these observations confirm that a good functioning of the cholinergic system is important for memory and learning, and a therapy to ameliorate the cholinergic system could be the key for treatment of Alzheimer's Disease (AD) and other forms of dementia.

1.2 Cholinergic system

The chemical mediator of the cholinergic system in the mammalian brain is acetylcholine (ACh).

The central cholinergic system was characterized in the eighties using an anti-choline acetyltransferase (ChAT) antibody (Kimura et al., 1980) and it was divided into 10

relatively well defined populations of cholinergic neurons termed Ch1-Ch10 (Mesulam et al., 1983){Mesulam, 1983 753 /id}. Most of these clusters of cholinergic cells are formed by projecting neurons, although there are some well characterized populations of interneurons (Fig. 1). The most studied central cholinergic neurons are those found in the basal forebrain because they undergo degeneration in AD. They constitute an aggregate of discontinuous cell islands of large, multipolar cells with extensive dendritic trees. The cholinergic neurons of the basal forebrain, named Ch1-Ch4, give rise to the main cholinergic input to the cortical mantle and hippocampus, (MS/DBB projecting primarily to the hippocampus but also to the cortex, and NB, corresponding to the nucleus basalis of Meynert in primates, that projects diffusely to the cortex and to the amygdala).

Other cholinergic projection neurons include cells extending from the peduncolopontine tegmental nuclei to the floor of the fourth ventricle (Ch5-Ch8). These cells have widespread projections to the forebrain nuclei and to the thalamus, as well as descending projections to the spinal cord. These neurons do not show substantial degeneration in AD {Schliebs, 1998 2100 /id}.

The striatum contains large aspiny cholinergic interneurons whose dysfunction plays a pathogenetic role in Parkinson's disease. The existence of cortical cholinergic interneurons has been confirmed in the rat cerebral cortex by means of immunohistochemical staining for the vesicular ACh transporter {Schafer, 1994 2172 /id}. Their role needs to be defined.

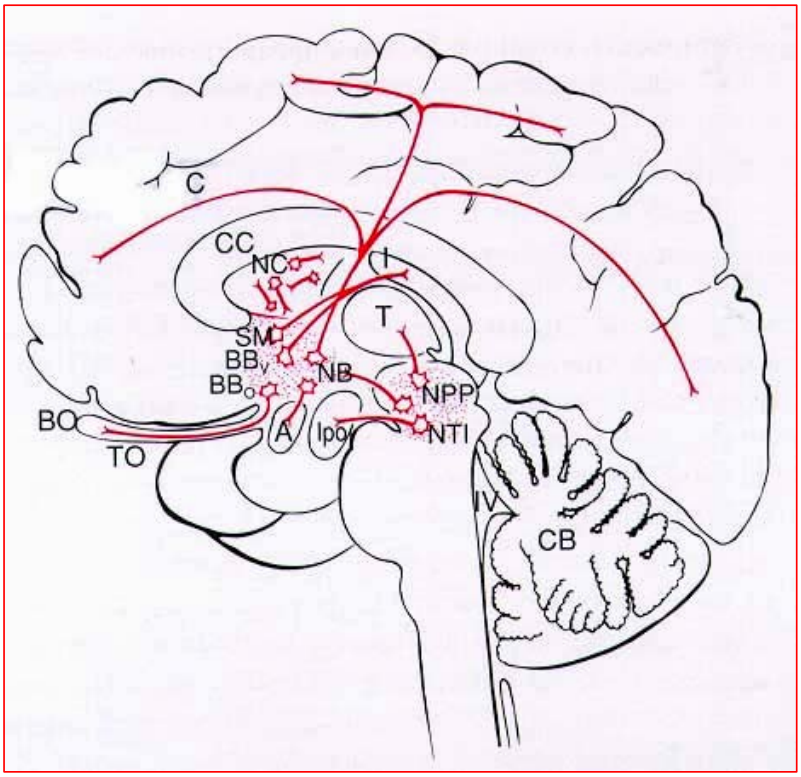

Fig. 1 Cholinergic pathways in human brain. From Pepeu, G.(1999) In: Farmacologia Generale e Molecolare. F. Clementi e G. Fumagalli (Eds.), IIa ed, UTET, Torino, p. 386

1.3 Nicotinic receptors

Nicotinic acetylcholine receptors (nAChRs) are a family of ACh-gated ion channels consisting of different subtypes, each of which has a specific pharmacology, physiology and anatomical distribution in brain and ganglia. Are found on skeletal muscle at the neuromuscolar junction, in autonomic ganglia of the peripheral nervous system, on sensory nervs and some peripheral nerve terminals, and at numerous sites in the spinal cord and brain. The nAChR found on mammalian skeletal muscle is analogous to the receptors from electric organ of *Torpedo* and *Electrophorus* (Unwin, 1996). This receptor consists on five protein subunits (two α and one each of β, γ and δ) surrounding a central ion channel (Fig. 2).

To date, 12 neuronal subunits have been described including nine α (α2-α10) and three β (β2-β4) subunits. The α subunits contain two adjacent cysteine residues for binding of ACh, whereas the β subunits lack them (Alkondon and Albuquerque, 1993). The combination of these subunits defines the function and affinity of the receptor for specific ligands (Sudweeks and Yakel, 2000). Nicotinic receptors are stimulated by nicotine and ACh.

It is generally accepted that the predominant nAChR in the CNS which binds [^{3}H]nicotine with high affinity is composed of α4 and β2 subunits (α4β2). This conclusion is based on immunoprecipitation studies (Flores et al., 1992), comparison of cloned amino acid sequences to immunopurified receptor subunits (Boulter et al., 1987;Whiting et al., 1991), and correlation of autoradiography data with results from in situ hybridization experiments (Clarke and Pert, 1985) (Harfstrang A et al., 1988). There is a decreased number of these receptors in the human cortex associated with AD

(Perry et al., 1995;Nordberg, 1994), supporting a possible role in cognitive function. Radioligand binding, using [^{3}H]nicotine, in mice shows moderate binding in may areas of the brain, including hippocampus, amygdala, frontal cortex, thalamus, substantia niagra, ventral tegmental area (VTA).

Initial studies comparing the pharmacology of ACh release in rat hippocampus with responses from recombinant chick α4β2 nAChRs suggested the possible involvment of this subtype in ACh release (Wilkie et al., 1996).

Studies on the participation of nAChRs in developmental processes suggest that α4β2 nAChRs may have a role in neuronal migration (Moser et al., 1996;Zheng et al., 1994).

Whereas in many neurotransmitter systems prolonged or excessive agonist exposure leads to receptor down-regulation (Lohse, 1993), a unique feature of some neuronal nAChRs is their up-regulation following chronic treatment with nicotine and other nAChR agonist (Schwartz and Kellar, 1985;Gopalakrishnan et al., 1997). Although this effect is observed for other subtypes of nAChRs, including the α7 subtype, only the α4β2 nAChRs appear to be upregulated by physiologically relevant concentrations of nicotine (Lukas, 1995). The extent of up-regulation of presumed α4β2 nAChRs is variable by brain region (Collins et al., 1996).

α-Bungarotoxina (α-Bgt) is a 75-amino acid peptide isolated from a species of East Asian snake (*Bungarus multicinctus*) and has been recognized historically for its high affinity to muscle-type nAChRs (Lee, 1979). An additional class of nAChRs in the CNS is identified by propensity to bind [^{125}I]-α-Bgt with high affinity and nicotine with relatively low affinity (Marks et al., 1986). The overall population of these sites is similar to that for α4β2 nAChRs, but the localization is different and varies according to species (Williams M. et al., 1994). The subunit composition of this nAChR subtyoes has

not been estabilished, but evidence supports the hypothesis that most native mammalian α-Bgt receptors are α7 homo-oligomers. The α7 nAChRs have an unusually high permeability to calcium compared to other sutypes (Delbono et al., 1997) and exhibit a rapid desensitization following exposure to agonists (Castro and Albuquerque, 1993;Alkondon et al., 1994). Like α4β2, up-regulation of α7 is selective by brain region when elicited *in vivo* (Collins A.C. and Marks MJ., 1996).

Among the nAChRs, the α7nAChR has major clinical and pharmacological implication for AD. In neuronal cells activation of the α7nAChR causes an increase in intracellular Ca^{2+} directly through voltage activated channels (activation of ERK1/2 in a Ca^{2+} and PKA dependent manner) (Dajas-Bailador et al., 2002b) and indirectly from intracellular sources following ryanodine receptor channels activation (Dajas-Bailador et al., 2002a). In astrocytes, the α7nAChR appears to modulate Ca^{2+} release from intracellular stores (Sharma and Vijayaraghavan, 2001).

α7nAChR are widely distributed in the brain. Radioligand binding of [I^{125}]α-bungarotoxin shows a high distribution of the α7nAChR in the CA1 region of the hippocampus and enthorinal cortex (Court JA et al., 2000). In the prefrontal and motor cortex, the α7nAChR localizes in the pyramidal neurons of the layer II/III, V and VI (Wevers et al., 1994). Decline in nicotinic receptors, particularly the α7nAChR in the frontal cortex, is associated with aging (Utsugisawa et al., 1999). Decline of α7nAChR is also observed in AD patients. These deficits appears early in the disease and correlate with the progressive loss of cognitive abilities (Nordberg, 1994;Nordberg, 2001;Whitehouse and Kalaria, 1995). In AD patients, the α7nAChR protein levels are reduced in the cortex and hippocampus (Burghaus et al., 2000;Guan et al., 2000;Martin-Ruiz et al., 1999).

Epidemiological studies show that nicotine decreases the risk of Parkinson's disease (PD) and AD (Fratiglioni and Wang, 2000). This negative association is in agreement with postmortem studies showing diminutions of amyloid plaque deposition in former smokers with AD (Hellstrom-Lindahl et al., 2004b). Nicotine treatment appears to interfere with the formation of the amyloid plaques *in vitro* and *in vivo* (Hellstrom-Lindahl et al., 2004a;Ono et al., 2002;Utsuki et al., 2002) and to reduce the accumulation of Aβ42 peptides (Nordberg et al., 2002) through a mechanism mediated by α7nAChR (Hellstrom-Lindahl E. et al., 2004a).

Nicotine seems to protect against the development of AD and PD through anti-inflammatory mechanisms. Both AD and PD are characterized by local inflammation sustained by activated microglial cells (Fiszer et al., 1994;Hirsch et al., 2003;Rogers et al., 2007;Barger and Harmon, 1997;Aisen, 1997;Rogers and Shen, 2000). Nicotine induces anti-inflammatory mechanisms that diminish local inflammatory responses (Streit, 2002) Wang H.Y. et al., 200a, b).

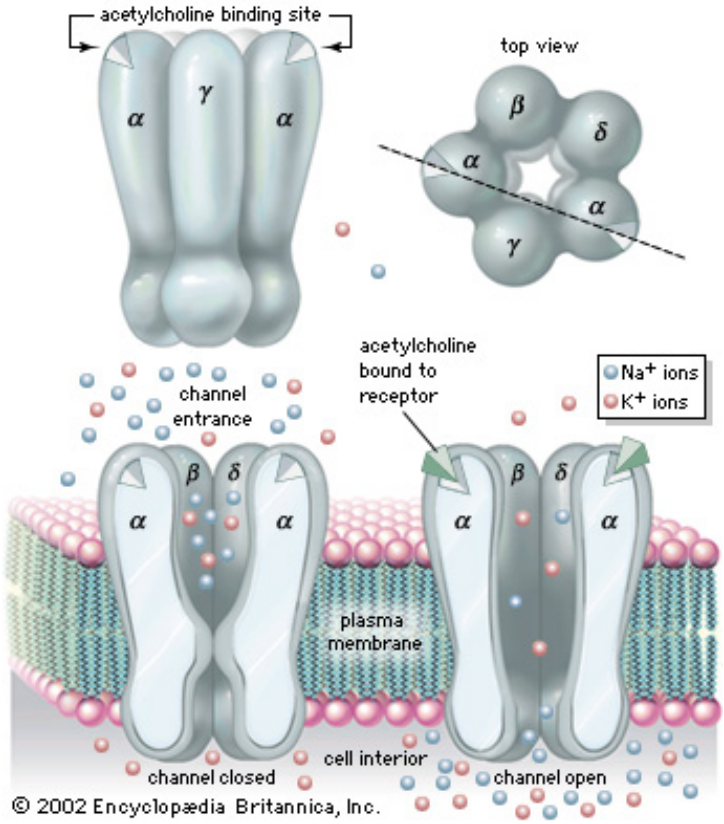

Fig. 2 Nicotinic receptor. Made up five subunits (2α, 1β, 1γ, 1δ) surrounding a central ion channel. From 2002 Encyclopaedia Britannica, Inc.

1.4 Muscarinic receptors

Muscarinic acetylcholine receptors (mAChRs) are the targets of ACh released from the cholinergic nerve endings and in some cases are located on cholinergic neurons and nerve endings (autoreceptors). In the mammalian central nervous system (CNS) both nicotinic and mAChRs are present but the density of the muscarinic receptors is much larger (Clarke, 1993).

The first evidence of the existence of more than one muscarinic receptor subtype was given by the work of {Riker, 1951 2001 /id} showing the cardioselective action of gallamine, but it was only at the end of the '70s that the use of the muscarinic receptor antagonist pirenzepine, with higher selectivity for ganglionic than cardiac muscarinic receptors (Hammer et al., 1980){Hammer, 1980 2003 /id}, clearly demonstrated the existence of more than one receptor subtype.

At present, pharmacological, biochemical, immunological, and molecular biological evidence indicates the existence of five mammalian genes (m1-m5) encoding muscarinic receptors (M_1-M_5). The cloning (Kubo et al., 1986;Peralta et al., 1987){Peralta, 1987 2133 /id}{Kubo, 1986 2134 /id} and expression of these receptor subtypes in cell lines shed light on their function, potential physiological role as well as their signal transduction mechanisms. Recently a gene for a putative sixth muscarinic receptor (m6) was cloned and patented by Millennium Pharmaceuticals Inc. (P1); no details on its pharmacological or potential physiological role are available yet (Eglen et al., 1999){Eglen, 1999 2005 /id}. The five subclasses of mAChRs so far best characterized all have the structural features of the seven-transmembrane helix G-protein-coupled receptor superfamily (Fig. 3). Much of the diversity in the structure between the M_1/M_3/M_5 sequences compared with the M_2/M_4 sequences resides in the

postulated third intracellular loop (i3), responsible for the specificity of coupling to G proteins and which probably determines the quite specific coupling preferences of these two groups (Wess, 1993). The "odd-numbered" $M_1/M_3/M_5$ mAChRs predominantly couple via the α subunits of the $G_{q/11}$ proteins that activate the enzyme phospholipase Cβ, while the "even-numbered" M_2/M_4 subtypes couple via G_i and G_o α subunits that inhibit adenyl cyclase, as well as to G proteins that directly regulate Ca^{2+} and K^+ channels.

While a great diversity of behavioral, physiological and biochemical effects mediated by mAChRs have been observed, the identities of the molecular subtypes responsible for any given neuronal function remain elusive. The complex pharmacology of the mAChR subtypes, together with the lack of drugs with high selectivity has made it difficult to determine the individual roles of m1-m5 receptors in the brain. Identification of the mAChR subtypes in the brain has been accomplished using *in situ* hybridization to localize their mRNAs (Brann et al., 1988;Vilaro et al., 1993), or highly selective antibodies to directly localize the proteins (Levey et al., 1991;Van der Zee and Luiten, 1999b). All subtypes appear to be present in the brain, although with different densities, localization and relative abundance. In the forebrain, the region of interest for AD, the major mAChRs subtypes found are the m1, m2 and m4 proteins. For example, quantitative immunoprecipitation studies showed that in the hippocampus and several areas of human brain neocortex, the m1 receptor accounts for 35-60% whereas the m2 and m4 each accounts for about 15-25% of all binding sites (Flynn et al., 1995). In contrast, m2 is the most prominent subtype in the basal forebrain and m4 is the most abundant in caudate-putamen. Immunocytochemistry with specific antibodies has enabled researchers to define a detailed regional and cellular localization of mAChRs in different brain structures. In the medial temporal lobe, the expression of the m1-m4

subtypes shows differences in the regional and laminar patterns (Levey et al., 1995b). In neocortical areas and hippocampus, the m1 subtype is expressed on all pyramidal neurons, where it is localized in somatodendritic regions, primarily at a postsynaptic level. The pattern of cellular staining for mAChRs in the neocortex is characterized by a clear laminar distribution (Buwalda et al., 1995), with strong immunoreactivity present predominantly in layer 5. Less numerous immunopositive neurons are present in layers 2, 3 and 6, see {Van der Zee, 1999 2015 /id}. Postsynaptic mAChR subtypes modulate excitatory synaptic transmission in the hippocampus (Halliwell, 1990){Halliwell, 1990 2024 /id}, and an example of this modulation is the enhanced responsiveness of NMDA receptors in area CA1 by activation of M_1 receptors (Markram and Segal, 1990). Double labeling electron microscopic immunocytochemistry has shown that the m1 subunit colocalizes with the NR1 subunit of NMDA receptors in CA1 pyramidal neurons, indicating an appropriate localization for m1 to modulate the activity of the NMDA receptor (Rouse et al., 1999). The m1 receptor has a similar postsynaptic distribution at excitatory synapses in the striatum (Hersch et al., 1994){Hersch, 1994 2028 /id} and increases the excitability of striatal spiny neurons to the application of NMDA (Calabresi et al., 1998), suggesting that this subunit might play a general role in the modulation of glutamatergic neurotransmission.

The m2 subtype, with its prevalent presynaptic localization in the CNS (Mash et al., 1985), is generally believed to act as an autoreceptor inhibiting ACh release. Recently, however, this issue has become controversial. {Levey, 1995 13 /id} using molecular and immunocytochemical approaches demonstrated that the m2 subtype is present in the basal forebrain not only as a presynaptic cholinergic autoreceptor, but it is also expressed by the remaining population of cells (possibly GABAergic) projecting to the cortex and hippocampus. Also, electron microscopic analysis has shown that in the

hippocampus the m2 receptors are present on axons and axon terminals (Levey et al., 1995a). The m2 receptor is presynaptic in other regions of the brain, including the neocortex (Mrzljak et al., 1993), where most of the m2 receptors are located on intrinsic noncholinergic neurons {Levey, 1995 13 /id}, because complete lesion of the projecting cholinergic neurons almost completely spare the m2 receptors in the terminal field. In the striatum the majority of the m2 receptor acts as an autoreceptor {Hersch, 1994 2028 /id}.

Much less is known about the localization of the other mAChR subtypes in the CNS. The m3 receptor is present throughout the brain (Levey et al., 1994), particularly in the basolateral and central amygdala {Levey, 1994 2032 /id}, while the m4 is mostly abundant in the hippocampus and striatum. GABA and glutamate release is inhibited in the basolateral amygdala through m_3-like receptors (Sugita et al., 1991){Sugita, 1991 2034 /id}, suggesting a function of these m_3 receptors as heteroreceptors. In the hippocampus the m_3 and m_4 subtypes are predominantly postsynaptic to the septohippocampal cholinergic terminals (Zang and Creese, 1997). However, the m4 subtype seems to also be presynaptically located on hippocampal associational and commissural projection pathways where it might regulate glutamate release {Levey, 1995 2020 /id}. The distribution profile of the m_5 receptor is distinct from the other four subtypes and is enriched in the outer layers of the cortex, specific subfields of the hippocampus, caudate putamen, olfactory tubercle and nucleus accumbens (Reever et al., 1997). These studies also demonstrated that the levels of m_5 receptor protein expression are apparently higher and more widespread than anticipated from previous *in situ* hybridization and immunoprecipitation studies. Taken together, the results suggest a unique and potentially physiologically important role for the m_5 receptor subtype in modulating the actions of ACh in the brain.

The mAChRs mediate both excitation and inhibition, depending on the receptor subtype, distribution, subcellular localization, etc. These receptors are found both presynaptically and postsynaptically and, ultimately, their main neuronal effects appear to be mediated through alterations in the properties of ion channels. Excitatory effects result principally from closure of one or more of a number of different K^+ channels (Brown et al., 1997), though instances of cation channel openings have also been described (Delmas et al., 1996;Haj-Dahmane and Andrade, 1996), while inhibitory effects include opening of K^+ channels and closure of voltage-gated Ca^{2+} channels. The presynaptic auto- and hetero-receptors constitute important feedback loops that control ACh release in an inhibitory manner and represent an important regulatory mechanism for short-term modulation of neurotransmitter release.

Investigations on the physiological role of the various mAChR subtypes are hampered by the lack of selective agonists or antagonists for the specific receptor subtypes. Over the last few years several knockout mice strains have been developed for the M_1 (Hamilton et al., 1997), M_2 (Gomeza et al., 1999a){Gomeza, 1999 2201 /id} , M_3 (Matsui et al., 2000) and M4 receptors (Gomeza et al., 1999b){Gomeza, 1999 2203 /id}. The use of knockout animals might help to elucidate the physiological functions and pathophysiological implications of each receptor subtype. From these studies it appears that mAChR subtypes are involved in different physiological functions in the CNS, the M_2 receptor being involved in movement, temperature control and nociception {Gomeza, 1999 2201 /id}, the M_3 in facilitation of food intake (Yamada et al., 2001), the M_4 in locomotor activity {Gomeza, 1999 2203 /id}, and the M_5 in water intake, and rewarding brain stimulation (Yeomans et al., 2001){Yeomans, 2001 2229 /id}. Studies on M_1 receptor knockout mice have given contradictory results concerning their role in cognitive mechanisms. (Hamilton et al., 2001) reported that $M_1R^{-/-}$ mutant mice showed

defects in LTP induction in hippocampal CA1 neurons and severe impairment in the consolidation of contextual conditioning. On the other hand, it was shown (Miyakawa et al., 2001) that $M_1R^{-/-}$ mutant mice have normal working memory, tested with a radial arm maze, normal spatial memory, tested using a Morris water maze, and normal freezing levels during contextual fear conditioning. The possibility that compensatory mechanisms occurring during development may help maintaining proper cognitive functions in $M_1R^{-/-}$mice must be considered.

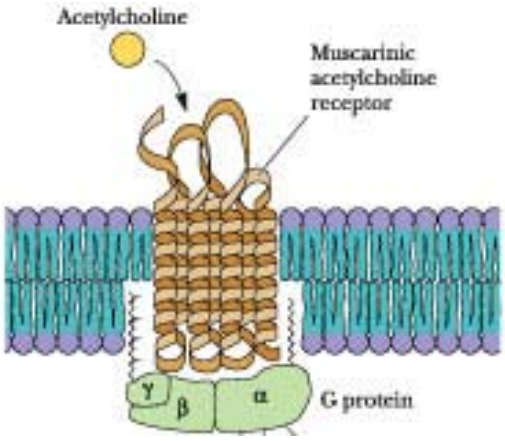

Fig. 3 Muscarinic receptor.

1.5 The brain cholinergic system in the mechanisms of learning and memory.

A consensus exists that brain cholinergic neurotransmission plays a critical role in the processes underlying attention, learning, and memory (Everitt and Robbins, 1997b;Sarter and Bruno, 1997b). Two main cholinergic nuclei of the basal forebrain, the medial septum and the NBM projecting to the hippocampus and neocortex subserve attentional functions and are considered of crucial importance in learning and memory processes (Zola-Morgan and Squire, 1993).

Experiments with lesions of the forebrain cholinergic neurons made by different neurotoxins have helped to enlighten the role of ACh in learning and memory and have demonstrated that the decrease in ACh extracellular levels is accompanied by specific behavioral deficits. Excitotoxic lesions of the NBM induce a longlasting, significant decrease in cortical ACh release both at rest and under K+ depolarization, paralleled by disruption of a passive avoidance conditioned response (Casamenti et al., 1988) and working memory (Bartolini et al., 1996;Casamenti et al., 1998).

Disruption of the septo-hippocampal projections impairs choice accuracy in short-term memory (Flicker et al., 1983) and results in deficits in a T-maze performance (Rawlins and Olton, 1982). The most selective procedure for the disruption of the cholinergic neurons is the use of 192IgG-saporin, which, injected intracerebrally (Heckers et al., 1994), causes an almost complete cholinergic differentiation to the cortex and hippocampus and a significant decrease in ACh release from these structures (Rossner

et al., 1995). All behavioral studies performed in rats with i.c.v. injections of 192IgG-saporin indicate that only very extensive lesions involving >90% of cholinergic neurons result reliably in severely impaired performances (Wrenn and Wiley, 1998). Impairments in water-maze acquisition (Leanza et al., 1995), delayed matching (Leanza et al., 1996), and nonmatching to position task (McDonald et al., 1997), as well as acquisition, but not retention, of an object discrimination (Vnek and Rothblat, 1996) or of spatial working memory (Shen et al., 1996) have been reported in the rat. (Ballmaier et al., 2002) demonstrated in rats that bilateral 192IgG-saporin lesions of the NBM reduce cortical ACh release below detection limits and abolish prepulse inhibition. Restoration of ACh levels to normal levels by a cholinesterase inhibitor was associated with reappearance of prepulse inhibition, a finding indicating a role of the forebrain cholinergic system in the sensory motor gating.

Activation of basalocortical cholinergic afferents may foster the attentional processing that is central to the memory-related aspects of anxiety caused by threat-related stimuli and associations (Berntson et al., 1998). Intraparenchymal injections of 192IgGsaporin have been used to study the effects of basal forebrain cholinergic lesions on attentional processing (Stoehr et al., 1997).

Most of the studies report disrupted attentional processing in NBM- or MS-injected animals (McGaughy et al., 1996) ((Wrenn and Wiley, 1998), thus confirming the role of the cholinergic system in attention. However, a correlation between attentional effort, required by the task difficulties, and ACh release has not always been found (Passetti et al., 2000).

A novel environment represents a stressful condition, and the first exposure to it causes pronounced behavioral activation (Ceccarelli et al., 1999)(Aloisi et al. 1997;, which provides one of the most elementary forms of learning. Rats placed in novel

environments, either an arena with objects or a Y maze, showed a 150%–200% increase in ACh release from the cerebral cortex (Giovannini et al., 1998). If the rats were placed in the arena for only 2 min, no habituation occurred. However, if the rats were left for 30 min in the arena, habituation developed, as demonstrated by a much smaller increase in motor activity and ACh release when the rats were placed again in the arena 60 min later, in comparison with the first exposure (Giovannini et al., 2001e).The maximum increase was 64% in the cortex and 200% in the hippocampus in the first exploration of the arena and 37% and 51%, respectively, in the second exploration. Hippocampal ACh release increases during performance of a learned spatial memory task (Stancampiano et al., 1999)(; Stancampiano et al. 1999), and, interestingly, the improvement in radial arm maze performance is positively correlated to the increase in ACh release during 12 days of task learning (Fadda et al., 2000). These results show that the learning of the spatial task modifies the function of cholinergic neurons projecting to the hippocampus, which become progressively more active. In a behavioral paradigm investigating spatial orientation, (Van der Zee et al., 1995) showed that spatial discrimination learning selectively increases muscarinic ACh receptor immunoreactivity in cell bodies of CA1–CA2 pyramidal neurons. Changes were also observed in the neocortex, but not in the amygdala (Van der Zee and Luiten, 1999a). During the habituation, that is, the learning period, exploration-associated synaptic changes are likely to occur, and variations in ACh release accompanied by alterations in mAChRs density might reflect these changes.

Memory processes are mediated, in the intact brain, by parallel, sometimes interdependent, but other times independent and even competing, neural systems (White and McDonald, 2002). It has recently been demonstrated that hippocampal ACh release increases both when rats are tested in a hippocampal dependent spontaneous alternation

task and in an amygdala dependent conditioned place preference (CPP) task (McIntyre et al., 2002). Interestingly, the magnitude of hippocampal ACh release is negatively correlated with good performance in the CPP task, indicating not only a competition between the two structures in this type of memory, but also that activation of the cholinergic hippocampal system adversely affects the expression of an amygdala-dependent type of memory (McIntyre et al., 2002). However, competition is not the only interaction between the hippocampus and the amygdala, because it has been demonstrated (McIntyre et al., 2003) that ACh release in the amygdala is positively correlated with performance in a hippocampal spatial working memory task. The two structures seem to have a nonreciprocal interaction in that the hippocampus competes with the amygdala, whereas the amygdala cooperates with the hippocampus during learning.

1.6 Mitogen Activated Protein Kinase pathways

The components of the Mitogen Activated Protein Kinase (MAPK) signal transduction pathways are ubiquitous and well conserved protein kinases involved in relaying extracellular signals into intracellular responses. In 1990, among the members of the MAPK family, Extracellular signal Regulated Kinases-1 and -2 (ERK1/2) were the first to be cloned by Cobb and coworkers (Boulton et al., 1990b). Later, several additional members of the MAPK family were cloned and characterized, including p38/HOG (Hafner et al., 1994;Han et al., 1994), JNK/SAPK (c-jun N-terminal kinase/stress activated protein kinase) (Kaang et al., 1993b;Kyriakis et al., 1994b;Kyriakis et al., 1994a;Kaang et al., 1993a)), and ERK5 (Zhou et al., 1995b;Lee et al., 1995;Zhou et al., 1995a). The classic MAPK pathway consists of a three-layered cascade of protein

kinases which starts with the kinases Raf-1 or B-Raf. Phosphorylation by either of these kinases activates the MAP kinase kinase (MEK) which, in turn, is a dedicated dual-specificity kinase that phosphorylates and thereby activates only ERK (Seger and Krebs, 1995b;Seger and Krebs, 1995a).

1.7 Role of extracellular signal regulated kinase pathway in learning and memory

Two isoforms of ERK have been described, the so called ERK1 (p44 MAPK) and ERK2 (p42MAPK). The two isoforms seem to have similar distribution in the brain, although, as reported, the amount of ERK1 in rat hippocampus appears to be considerably less than ERK2 (Kanterewicz et al., 2000;Giovannini et al., 2001a). Furthermore, although it is known that the two isoforms share about 90% homology (Boulton et al., 1990a) and have the same substrate specificity *in vitro*, their specific role *in vivo* remains to be understood. In particular, it has not yet been made clear whether the two isoforms subserve different functions and whether either one or both isoforms are involved in the learning and memory mechanisms. Several groups have found that in neurons the two isoforms seem to be selectively regulated by different stimuli (English and Sweatt, 1996;Bading and Greenberg, 1991;Giovannini et al., 2001c;Fiore et al., 1993c). Possible explanations for selective activation of ERK2 are specific activation by upstream kinases, compartmentalization, and binding to scaffolding proteins through highly specific docking sites (Sharrocks et al., 2000;Enslen and Davis, 2001),but there is no compelling evidence for any of these. Knockout mice lacking either ERK1 or ERK2 have been created and, while ERK1 knockout mice are viable and appear to be neurologically normal (Selcher et al., 2001b;Selcher et al.,

2001a), ERK2 knockout mice are embryonic lethal at day 6.5 (Saba-El-Leil et al., 2003c;Saba-El-Leil et al., 2003b;Yao et al., 2003). Therefore the two isoforms must have some important differential functions, at least early in mouse development after the implantation stage (Saba-El-Leil et al., 2003a). In the following paragraphs I will be using the terminology "ERK1" or "ERK2", depending upon which isoform I would be referring to or "ERK", referring to both isoforms.

ERK, first identified and studied extensively as a mediator of cell differentiation and proliferation in mitotic cells, was later shown to be highly expressed in the postmitotic neurons of the adult mammalian brain (Boulton et al., 1991;Fiore et al., 1993a). In particular, immunohistochemistry demonstrated that ERK is localized to the soma and dendritic trees of neurons in the neocortex, hippocampus, striatum, and cerebellum (Fiore et al., 1993b). ERK was then demonstrated to be required for different types of synaptic plasticity, learning and memory (Atkins et al., 1998a;Kaminska et al., 1999;Blum et al., 1999d;Walz et al., 2000d;Cammarota et al., 2000b).

All types of memory depend on the integrated activity of various brain structures and neurotransmitter systems and involve more than one receptor, signal transduction pathways and postsynaptic mechanism (Izquierdo et al., 1998b). Among neurotransmitter systems, the cholinergic neurons of the basal forebrain, projecting to the hippocampus and neocortex, subserve attentional functions and are considered of crucial importance in learning and memory processes (Zola-Morgan and Squire, 1993;Muir et al., 1996;Everitt and Robbins, 1997a;Sarter and Bruno, 1997a;Sarter and Bruno, 2000;Sarter and Bruno, 1997c;Sarter and Bruno, 2000), while those projecting to the amygdala are required for both acquisition and expression of Pavlovian fear responses (LeDoux, 1995;Maren, 1996a;Maren, 1996b). Nevertheless, much evidence indicates that several other neurotransmitters, including glutamate, noradrenaline,

serotonin, GABA, and histamine, are involved in the modulation of attention/learning processes (Decker and McGaugh, 1991;Passani et al., 2000). Activation of the forebrain cholinergic system has been demonstrated in many tasks in which the environment requires the analysis of novel stimuli which may represent a threat or offer a reward (revised in Pepeu and Giovannini, 2006). As it is well known that cholinergic activation subserves the mechanisms of memory encoding (see references in (Sarter et al., 2003) and (Pepeu and Giovannini, 2004)), the question is how the increase in ACh release resulting from activation of the cholinergic neurons contributes to the learning and memory processes. Recent research has shown that many of the neurotransmitters that play crucial roles in learning and memory activate ERK, among which ACh *via* muscarinic (Berkeley et al., 2001) or α7 nicotinic receptors (Dineley et al., 2001), glutamate *via* metabotropic (Peavy and Conn, 1998) or ionotropic glutamate receptors (Zhu et al., 2002;Krapivinsky et al., 2003), norepinephrine *via* β-adrenergic receptors (Williams et al., 1998;Winder et al., 1999;Watabe et al., 2000b), and histamine *via* the H3 receptor (Drutel et al., 2001;Giovannini et al., 2003b). Thus, each of these neurotransmitter systems, alone or in combination, provides a possible mechanism for the activation of ERK which can function as biochemical signal integrator and coincidence detector (Watabe et al., 2000a) in response to extracellular signals in neurons, subserving processes such as synaptic plasticity and learning in the adult brain. Thus, the ERKs are poised at a critical position allowing cross-talk between a different array of signals and signal transduction pathways.

The first direct evidence that the ERK cascade is involved in memory processes *in vivo* was reported by the group of Sweatts' (Atkins et al., 1998b), who showed that ERK activation is required for the expression of Long Term Memory (LTM) induced by a cued- and cued-contextual fear-conditioning paradigm in the rat. Atkins found that

ERK2 phosphorylation was increased in the rat hippocampus 1 h after training. Additional studies (Giovannini et al., 2003a;Apergis-Schoute et al., 2005) showed that the ERK cascade is required for long-term fear memory, as inhibitors of ERK activation caused blockade of memory formation upon testing. In fear conditioning, rats are taught to associate a foot shock either with a cue (a tone), a context, or both. Later, the extent of the animal's memory to the cue or the context is quantified by fear-associated "freezing" upon testing with either the cue or the context. Contextual fear conditioning is dependent on both the amygdala and the hippocampus, while cued fear conditioning is dependent only on the amygdala. The initial findings by Atkins were confirmed and greatly expanded using intraventricular injection (Schafe et al., 1999a), intra-amygdalar infusion of an inhibitor of ERK activation in the rat (Schafe et al., 2000b), and using systemic administration in the mouse (Selcher et al., 1999d). Interestingly, fear conditioning caused a transient and significant activation of both ERK1 and ERK2 isoforms 60 min after training in the basolateral amygdala (Schafe et al., 1999b;Schafe et al., 2000a). The authors asserted in their paper that the increased activation of both isoforms was specifically associated to the pairing of tone and shock. Pretraining inhibition of ERK dose-dependently impaired LTM of Pavlovian fear conditioning, leaving STM intact.

The formation of long-term Conditioned Taste Aversion (CTA) memory in the Insular Cortex (IC) requires multiple neuromodulatory and signal transduction mechanisms (Berman et al., 1998a;Berman et al., 2000;Naor and Dudai, 1996a;Rosenblum et al., 1997a) involving cholinergic and β-adrenergic receptors, the ERK cascade, the transcription factor Elk-1, and protein synthesis. Berman et al. (Berman et al., 1998b), using the CTA paradigm, showed that the ERK cascade is involved in the formation of long-term memories for taste in the IC. Indeed, an unfamiliar taste leads to activation of

ERK in the IC within 30 min of its presentation and microinjection of a reversible inhibitor of MEK shortly before exposure to the novel taste attenuates long-term taste aversion memory without significantly affecting short-term memory or the sensory, motor, and motivational faculties (Berman et al., 1998c). These data suggest that ERK is involved in IC–dependent LTM. The authors propose that activation of the ERK signalling cascade is salient for the encoding of novelty during acquisition and initiation of long-term storage of taste memory in the IC. A model proposed by the authors to explain information encoding involves neuromodulatory systems such as the basal forebrain cholinergic pathway (Naor and Dudai, 1996b). The authors propose that activation of this cholinergic pathway during acquisition, and the subsequent release of ACh in the cortex, possibly leads to activation of muscarinic receptors that in turn trigger ERK activation either via PKC (Yasoshima and Yamamoto, 1997) or PYK2 (Lev et al., 1995). Ca^{2+} influx via NMDA receptors, necessary for the encoding (but not the retrieval) of taste memory in the IC (Rosenblum et al., 1997b), might also act synergistically with the cholinergic-dependent signal transduction cascades to activate ERK. Thus, not only does ERK appear to be involved in hippocampus-dependent LTM, but evidence now also implicates ERK in insular cortex–(taste) and entorhinal cortex–dependent LTM. On the other hand, CTA memory extinction is dependent on protein synthesis and β-adrenergic receptors in the IC, but independent of muscarinic receptors and MAPK, since it is not blocked by muscarinic receptor antagonists and by MEK inhibition. This indicates that the muscarinic receptors and the MAPK cascade in the IC are not essential for the taste-malaise association, further corroborating the notion that they play a role in encoding the novelty dimension of the taste stimulus in CTA (Berman and Dudai, 2001).

Later it was demonstrated that ERK is essential for long term spatial memory (Blum et al., 1999c;Selcher et al., 1999c), measured with the Morris water maze. In this task animals learn to locate a hidden escape platform in a pool of opalescent water using various visual cues. Blum et al. (Blum et al., 1999b) reported that behavioural training in the Morris water maze increases ERK phosphorylation in pyramidal cells of the CA1/CA2 subfield of the dorsal, but not ventral, hippocampus and that ERK activation is necessary for long-term spatial memory in rats. The authors (Blum et al., 1999a) showed that MEK inhibition, 20 min before training or immediately after training did not interfere with acquisition of the task, but attenuated long term memory retention on the first trial determined 48 h after training. These results are at variance with those published by (Selcher et al., 1999b) who showed that ERK activation is necessary for spatial learning in the mouse, since when administered post training in animals that had already learned the task blockade of ERK activation had no effect on recall, thus indicating that ERK activation is required for memory formation, but not for memory maintenance or recall. The authors explain this discrepancy with the different training or testing paradigms applied, species of test used, differences in the efficacy and time course of ERK inhibition, or in drug administration protocols. Nevertheless, the result obtained by (Selcher et al., 1999a) are consistent with the LTP studies involving ERK performed by English et al. (English and Sweatt, 1997) and Giovannini et al. (Giovannini et al., 2001d) in which MEK inhibition before stimulation blocks LTP induction, but when applied 30 min after stimulation MEK inhibition has no effect on the expression of established LTP. It seems however that a time-window for ERK inhibition to be efficacious must exist, since it has been demonstrated that, at least in spatial memory, delayed infusion of MEK inhibitors does not interfere with long term spatial memory retention. Akirav and coworkers (2001) demonstrated a differential

activation of ERK in the hippocampus and amygdala following spatial learning in stressful conditions (Akirav et al., 2001). In CA1 region of the dorsal hippocampus activation of ERK2 was present in those animals that had acquired the task, while in the amygdala significant activation of ERK2 was found in animals that had acquired the task under very stressful conditions, suggesting that this pathway in the amygdala is activated in learning situations that are highly arousing, such as fear conditioning.

ERK is also necessary for step-down inhibitory avoidance (IA) (Walz et al., 2000c;Cammarota et al., 2000a). Inhibitory avoidance is a paradigm that involves learning an association between a footshock and an electric grid on the floor. It differs from the Pavlovian contextual fear conditioning in that, although both are emotionally-arousing paradigms (Izquierdo et al., 1997;Maren, 2001), the step-down inhibitory avoidance also entails working memory, as the animal may choose to avoid the aversive stimulus (Wilensky et al., 2000). In the step down IA task rodents, put on an elevated platform placed by one wall of an arena, learn to associate exploration of the adjacent compartment with a foot shock delivered through the floor grid. On a subsequent exposure to the same environment, the animal will avoid to step down, or will increase the latency before 'stepping down' onto the floor grid. Thus, the step-down IA is a form of associative learning that is acquired in one trial and involves several sensorial stimuli including spatial and visual perceptions, sensitivity to pain, and emotional components (Izquierdo, 1989;Izquierdo and Medina, 1997). The IA response is a learning task which depends upon the activation of the cholinergic system, as it is impaired by pre- (Giovannini et al., 1999;Izquierdo et al., 1998c) or post-training administration of muscarinic receptor antagonists (Giovannini et al., 1999;McGaugh and Izquierdo, 2000;Izquierdo et al., 1998d), and is enhanced by muscarinic receptor agonists (Barros et al., 2002;Baratti et al., 1979). Recall can be performed 60 min after acquisition, a

time sufficient for short term memory to be formed (Izquierdo et al., 1998a;Izquierdo et al., 1998e).

Work from the group of Izquierdo (Cammarota et al., 2000) demonstrated that learning of IA is associated with a similar activation of both isoforms ERK1 and ERK2 in the rat hippocampus. Immediate post-training administration of the NMDA receptor antagonist APV into the hippocampus blocks ERK activation and causes amnesia for this task, indicating that NMDA receptors are necessary upstream activators of ERK intracellular cascade in this memory. In a further series of papers by the same group (Walz et al., 1999;Walz et al., 2000b) the authors found that inhibition of ERK activation in the area CA1 of the dorsal hippocampus, entorhinal cortex, parietal cortex or in amygdala impaired retention of the avoidance when tested up to six hours after training, with a differential time course in the different brain regions. The authors thus concluded that the ERK cascade is time-dependently involved in the posttraining memory processing of IA, with a different time-course in the hippocampus, amygdala, entorhinal cortex, or parietal cortex of rats (Walz et al., 2000a). It seems that activation of ERK correlates mostly with the aversive, emotional, component of IA acquisition since it has been previously found that ERKs are activated by mild electric footshocks similar in intensity and length to that employed during IA training (Bevilaqua et al., 2005a;Bevilaqua et al., 2005b), but not simply by exposure to the training box in the absence of footshock (Alonso et al., 2002b;Alonso et al., 2002a).

More recently work from the same group (Igaz et al., 2004) demonstrated that single trial step down IA caused an increase of total ERK mRNA 3 h and protein upregulation 24 h after training. ERK1 protein was neither changed at 3 nor 24 h. These results are interesting in that they reveal that ERK activity can possibly be modulated not only by activation, but also by increased protein expression in different behavioural tasks.

Kelly et al., (2003) (Kelly et al., 2003) found that ERK is activated in distinct hippocampal circuits following either consolidation or reconsolidation of an object recognition memory in the rat. The task, first developed by Ennaceur and Delacour (1987) (Ennaceur and Delacour, 1987), relies on rat innate propensity to explore novel objects. This task is run in an open box and does not involve the use of reinforcement and does not require any training. Rats are placed in an open box and exposed for a limited period of time to two identical objects and then returned to their home cage. After a delay rats are returned to the open box where they are exposed to two different objects, one identical to the one previously encountered in the previous phase, therefore now familiar (***F***), and the other one novel (***N***). The times spent in exploration of the familiar ***F*** and of the new object ***N*** are recorded separately and a discrimination index ***D*** is calculated. A value of ***D*** significantly above zero describes animals exploring more the novel than the familiar object. A value of ***D*** significantly below zero describes animals exploring more the familiar than the novel object. Object discrimination depends on cholinergic activity since it is impaired by the cholinergic hypofunction induced by anticholinergic drugs administration (Ennaceur and Meliani, 1992) and by lesions of the cholinergic neurons innervating the cortex (Bartolini, 1996). It was demonstrated that ERK1 activation is necessary for consolidation and reconsolidation of object recognition memory and a transient activation of ERK1 occurrs in the dentate gyrus and CA1 during both processes Kelly et al., (2003).

1.8 p38MAPK and JNK

Extracellular Regulated Kinase1,2 (ERK1,2) typically regulates growth, proliferation and differentiation, whereas p38MAPK and Stress Activated Protein Kinase/JunKinase

(JNK), are activated in response to osmotic shock, UV irradiation, inflammatory cytokines, oxidative stress (Haddad, 2004). MAP kinases are implicated in various cellular processes (Raman et al., 2007), and dysfunction of specific MAP kinases is associated with diseases such as cancer and immunological disorders. While it is suggested that dysregulation of the MAPK pathway(s) might play a role in the intracellular mechanisms of neurodegeneration, their effective involvement is still controversial. In the nervous system, as well as in other tissues, activation of JNK and p38MAPK has often been correlated with death in various cell types, including neurons (Xia et al., 1995;Kummer et al., 1997;Willaime-Morawek et al., 2003). Nevertheless, the genuine *in vivo* physiological functions of MAPK still remain to be fully unravelled. Others report that β-amyloid causes mitochondrial impairment in neurons, and generates oxidative species (Butterfield and Boyd-Kimball, 2004) that decrease ERK activity and activate p38MAPK and JNK (Troy et al., 2001); (Hensley et al., 1999;Ferrer et al., 2001;Zhu et al., 2000), leading to cell death (Daniels et al., 2001). Indeed, given that activated p38MAPK is both upstream and downstream of proinflammatory agents, it appears that conditions exist in the AD brain for a self-propagating cycle of stimulation (Hull et al., 2002;Sun et al., 2003), in which p38MAPK plays a prominent role through the production of pro-inflammatory cytokines, IL-1β and others, cyclooxygenase-2, iNOS, (Gonzalez-Scarano and Baltuch, 1999;Harris et al., 1995;Markesbery, 1999;Kaminska, 2005).

A near complete overlap between activated JNK and p38MAPK in severe AD cases is reported, implying that both are activated by the same signals and seem to work synergistically *in vivo* (Zhu et al., 2001a). Three genes encoding for JNKs have been identified (JNK1, JNK2 and JNK3). Neurons from JNK3$^{-/-}$ mice are more resistant than

normal mice neurons to β-amyloid-induced apoptosis (Morishima et al., 2001) and to glutamate-induced excitotoxicity. In human *postmortem* brains from AD patients, JNK phosphorylation is markedly increased and there is pronounced redistribution of JNK compared with age-matched controls. JNK2 and JNK3 are associated with neurofibrillary pathology, and JNK upregulation has a complete overlap with phosphorylated tau (Zhu et al., 2001b). Indeed, increased activation of JNK and p38MAPK has been found in brain homogenates in all the tauopathies (Ferrer et al., 2005b) and aberrantly activated p38MAPKs and JNK have been reported to be associated with cells that contain filamentous tau in AD (Atzori et al., 2001) (Ferrer et al., 2001), suggesting that β-amyloid triggers activation of stress kinases which may phosphorylate tau in neurites surrounding β-amyloid deposits and form tau fibrils (Churcher, 2006). Moreover, activated JNK and p38MAPK phosphorylate c-Jun, AP1 and their target genes in AD (Ferrer et al., 2005a).

1.9 Alzheimer's disease

In 1907, Alois Alzheimer (Alois Alzheimer, 1983-1915) described the case of a 51 year old woman with dementia and prominent behavioural disturbances. At autopsy, the brain was found to be atrophied and microscopic examination with silver staining revealed widespread senile plaques and neurofibrillary tangles. Senile plaques were seen as dystrophic neuritic processes around a central core and neurofibrillary tangles as intensely staining intraneuronal perikaryal inclusions. It was only in 1910 that Emil Kraepelin, a famous German psychiatrist, gave a name to the dementia discovered by Alzheimer, calling it with his name (Emil Kraepelin, 1856-1926).

Alzheimer's disease (AD) is a cerebral degenerative disorder with gradual loss of memory, reasoning, orientation and judgment. The diagnosis of Alzheimer's disease remains clinical unless histological confirmation is available at autopsy. Diagnostic criteria have been developed that allow a diagnosis of probable Alzheimer's disease. Many classifications have been proposed based on age of onset, presence of a family history, presence of extrapyramidal features and focal cortical disease. One of the most widely considered distinctions has been that based on age of onset. Patients with an onset below the age of 65 are considered to have presenile dementia in contrast to later onset cases of senile dementia of the Alzheimer type. Clinically, it has been suggested that early onset cases have a more severe disease with rapid progression, together with a predominance of language disturbances. A family history is also more readily apparent in young onset cases. A related group are patients with Down's syndrome trisomy 21 who develop Alzheimer histopathology and, in many instances, a super-added dementia in their third and fourth decade of life.

The clinical features of Alzheimer's disease can be divided in two groups: cognitive and behavioural deficits.

Cognitive deficits: the most prominent cognitive deficit in Alzheimer's disease is memory impairment, and this is often the presenting feature. At the beginning of the disease there appears a failure of short term memory (STM) but with the ongoing of the disease long term memory (LTM) is also affected, and particularly the explicit, episodic or autobiographical memory, while the implicit memory is well conserved until the late stage of the disease.

Language deficits and visuospatial deficits appear as the disease progresses. Early language preservation may allow the patient to maintain a social façade that can mask the cognitive impairment. It is usually clear, however, that although speech may be

fluent it is rather empty of meaning or the patient may present with some difficulties finding words (*anomia*).

Behavioural deficits: non-cognitive symptoms are common and about 40% have depression features, usually early in the disease. Delusion, hallucinations, and aggression are commonly encountered and can present considerable management problems for relatives and caretakers. AD patients also show anxiety and insomnia.

The above features and the characteristic progression have been incorporated into clinical criteria (the NINCDS/ADRDA criteria), which provide levels of probability of diagnosis. It goes from *Possible* to *Definite* Alzheimer's disease.

Possible Alzheimer's disease: a dementia syndrome with atypical onset, presentation or progression, and of an unknown etiology is present. No co-morbid diseases capable of producing dementia are believed to be at its origin.

Probable Alzheimer's disease: dementia has been established by clinical and neuropsychological examination. Also, cognitive impairments must be progressive and must be present in two or more areas of cognition. The onset of the deficits is between the age of 40 and 90 years and, finally, there must be an absence of other diseases capable of producing a dementia syndrome.

Definite Alzheimer's disease: the patient meets the criteria for probable Alzheimer's disease and has histopathologic evidence of AD, demonstrated *via* biopsy or autopsy.

There are several risk factors for AD: age, family history, lifestyle. Only 10% of AD cases are familial (FAD) and start before 60 years of age and are caused by autosomic dominant mutation on genes that codify for the protein precursor of amyloid (APP), and for the presenilin 1 and presenilin 2. These genes are localized in chromosomes 21, 14 and 1, respectively.

1.10 Neuropathology of Alzheimer's disease

Alzheimer's disease is characterized by atrophy in the cerebral cortex with loss of synapses and neurons, gliosys, presence of intraneuronal accumulation of paired helical filaments in the form of neurofibrillary tangles (NFT), and senile plaques (SP) (Fig. 4). Neurofibrillary tangles consist of aberrantly phosphorylated microtubule-associated protein (MAP) tau. Tau proteins consist of a developmentally regulated family of proteins which *in vivo* are known to stabilize the microtubule network (Cleveland et al., 1977;Drubin and Kirschner, 1986). The hyperphosphorilation of MAP tau renders the protein insoluble, which thus aggregates in filaments that precipitate (Hanger et al., 1991). Their presence signifies the failure of the neuron to properly maintain its cytoskeleton. Senile plaques are more complex; they consist of extracellular deposit of amyloid material and are associates with swollen, distorted neuronal processes called dystrophic neurites. The specificity of cerebral amyloid is provided by its major peptide component, β-amyloid (Aβ), a short 40-42 amino-acid fragment of the transmembrane protein, β-amyloid precursor protein (β-APP). Plaques start as innocuous deposit if nonaggregated, putative non-neurotoxic Aβ (diffuse plaques). With time, they undergo an orderly sequential transformation into the mature senile neuritic plaques that are associated with the development of AD. The neuritic plaques are more diffuse in the cerebral cognitive areas like cortex, hippocampus and amygdala.

The amyloid is predominantly in the core of senile plaques, surrounded by abnormal neurites from degenerated neuronal cells and by glial cells: microglial cells in the centre

of the plaque and astrocytes in the periphery (Selkoe, 1999). It is believed that activation of glial cells and production of cytochines, nitric oxygen (NO) and reactive Oxygen Species (ROS) leads to plaque maturation (Sheng et al., 2000;Ramirez et al., 2008). Amyloid deposits are not homogeneous. They are made up for more than 90% of Aβ, but they also contain α-1-antichimotrypsin (ACT), apolipoprotein E2 and E4 (apoE2 and apoE4), heparin sulphate proteoglycane (HSPG) and proteins of the complement (Selkoe, 1999).

1.11 Role of amyloid-β peptide in Alzheimer's disease

APP is a 105-130 kDa secretory protein and is involved in cell-cell or cell-matrix interaction. It may also be a component of the acute phase response and accumulates in astroglial cells in response to injury and is influenced by cytokines (Kushner, 1991;Trejo et al., 1994). In 1991 the gene for APP was localized to chromosome 21 by John Hardy, at St. Mary's Medical School, within the region that, when trisomic, is responsible for Down's syndrome (REF). There is a known association between Down's syndrome and AD (Patterson et al., 1988). The level of APP mRNA in the fetal brain with trisomy 21 is 50% higher than normal. By the fourth decade all patients with Down's syndrome have preamyloid plaques, containing APP-derived material. The APP gene is made of 19 exons and, after alternative splicing, different isoforms are obtained. The principal isoforms known are APP 695, APP 751 and APP 770. The APP 695 is the predominant isoform expressed in the Central Nervous System, the other isoforms are expressed also in other tissues (Selkoe, 1994). The amyloid-β (Aβ) is the product of an abnormal cleavage of APP operated by specific enzymes. It is delimitated by aa 672 and 712-715 of APP and part of it is localized in the transmembranarian tract and the other

part in the extracellular tract of the APP. Two different processing pathways of the APP have been described: *non amyloidogenic* and *amyloidogenic*. Under physiological conditions, APP is converted to soluble β-amyloid precursor protein via the non amyloidogenic pathway, since the hydrolysis is operated by α-secretases at the aa Lys687-Leu688, at the level of the transmembranarian tract of the β-amyloid (Fig. 4). Currently, three different enzymes with α-secretase activity have been described: ADAM 9, ADAM 10 and ADAM 17. After the cleavage, two different fragments are generated, one that origins from the N-terminal tract of the APP (sAPPα) that is secreted in the extracellular space, and the other one is a fragment of 83 aa (C83) that contains the C-terminal of the APP (CTF, C-terminal fragment), that remains in the plasma membrane, and than is hydrolyzed by γ-secretases to give a smaller fragment (p3) (Haass et al., 1993;Haass and Selkoe, 1993). The amyloidogenic pathway leads to the formation of Aβ. In this case the cleavage is operated by β-secretase at aa Met671-Asp672 with the release of sAPPβ in the extracellular space and the formation of a transmebranarian fragment of 99 aa (C99), where the N-terminus correspond to the first aa of the Aβ peptide (Fig. 5). The enzyme responsible for the cleavage is BACE1 (β-site APP cleaving enzyme) that is a membranarian protein (Vassar et al., 1999;Sinha and Lieberburg, 1999). The γ-secretase produces the other extremity of the Aβ by the hydrolysis of the aa nearby the residue 712, producing the amyloid peptide and the short intracellular fragment AICD (APP intracellular domain) (Fig. 5) (Steiner, 2004;Comery et al., 2005). If the cleavage by γ-secretase is at the link 712-713 or 713-714 there is the formation of short Aβ (39-40 aa), while the cleavage after the residue 714 leads to the formation of a longer Aβ peptide (42-43 aa) (Fig. 5) that is the major component of the

neuritic plaques since it is more amyloidogenic than the shortest peptide, with a greater propensity to form amyloid fibrils.

The genetic basis of AD have been studied on patients with a family history. Four different mutated genes have been identified, localized on chromosomes 21, 14,1 and 19, that are able to cause FAD (familial AD). There are different forms of AD based on the age onset:

-Early onset (EOFAD) when pathology starts before age 65.

-Late onset (LOFAD) when the pathology starts after age 65.

This classification is important since different genes are involved in the EOFAD as compared to the LOFAD. Studying different families with EOFAD, researchers have found that a "missense" mutation at the exon 17 of the APP gene is the cause of the disease. The most common mutation is the substitution of an adenine with a guanine with the consequent conversion of the Valine 717 to Isoleucine. Other familial forms are known, in which there is a mutationof Val to Gly or Phe. This kind of substitution makes the transmembranarian domain of the Aβ more hydrophobic, stabilizing the deposited form of the peptide.

Two Swedish families show a different double mutation (Mullan et al., 1992) with the substitution of a Lys and a Met, at the N-terminal of the Aβ, with an Asn and a Leu, respectively. This substitution facilitates the hydrolysis of APP operated by β-secretase.

The cleavage of APP can also be operated by a different family of proteases associated to apoptosis, the caspases. This cleavage leads to the formation of Aβ, and correlates the cellular death with Aβ deposition. Gervais et al. (1999) have demonstrated that the cytoplasmatic domain of APP can be cleaved by caspase 3 with the consequent formation of Aβ (Gervais et al., 1999).

Studies have demonstrated that mutations at the genes for presenilin 1 and 2, localized on chromosome 14 and 1, respectively, enhance the probability of apoptosis of different types of cells.

In 1992 three different groups demonstrated independently that there is a linkage between the central region of the long arm of chromosome 14 and AD (Van Broeckhoven et al., 1992;George-Hyslop et al., 1992;Mullan et al., 1992). In 1995 the gene on this chromosome was cloned (PS-1). This gene seems to be responsible for 70% of the EOFAD. Families with PS-1 show the disease at early age (around 45 years of age).

In the same year, another gene similar to PS-1 was found on chromosome 1, and it was called PS-2. Seven families from Volga region and one family from North of Italy have shown mutations on this gene.

In 1994, Potter coined the term "pathological chaperones" (REF), referring to apolipoprotein E (ApoE) and α_1-antichymotrypsin (αACT). *In vitro* ApoE and αACT act as catalysts, increasing amyloid filament formation by 10-20 fold (Jianyi et al., 1994). In an oxidant-dependent process, ApoE binds to Aβ in the region delimited by amino acids 12-18, the same region that is responsible for fibril formation.

ApoE is a 34kDa glycosylated protein, and is one of the major risk factor (other than age) for the development of AD. It is involved in synaptic repair, particularly in response to tissue injury and it has an important role in the maintenance of neuronal structure and cholinergic function. In the brain it is produced by microglial cells and astrocytes, but not by neurons. ApoE is a major component of lipoprotein and lipid complexes in the cerebrospinal fluid. In peripheral nerve regeneration, ApoE redistributes lipids to axons during neurite extension and Swann cells during

remyelinization (Yankner et al., 1990). The ApoE gene is localized on chromosome 19 and exists in 3 allelic forms: ε2, ε3 and ε4 with frequencies of 8%, 78% and 14% respectively. The ε4 allele increases the risk of developing late and sporadic AD by 5-15 fold. The prevalence of ApoEε4 appears to vary by population according to the prevalence of AD; it is increased in the Finnish, Sudanese, Aborigines and decreased in the Chinese and Japanese (Harrington et al., 1994). *In vitro* ApoEε4 binds more rapidly to Aβ than does ApoEε3, forming a denser matrix of monofibrils. On the other hand ApoEε3 seems to bind to the protein tau.

In contrast the ApoEε2 allele has been associated with a reduced risk of AD and longevity (Rebeck et al., 1994). *In vitro* ApoE ε2 inhibits fibrillar aggregation.

The familial forms of AD are correlated to mutations of the APP gene and other genes that alter the metabolism of this precursor, including the increased production of the Aβ (1-42) peptide that is the predominant form in the senile plaques. The crucial event for the pathogenesis of the disease is the amyloid-β peptide deposition. Studies on transgenic mice that present some of the AD alterations, have shown that the immunization with Aβ (1-42) interferes with the accumulation and deposition of Aβ and with the activation of glial cells, leading to cognitive improvement (Schenk et al., 1999). The immunization of transgenic mice with Aβ (1–.42) before the onset of AD, prevents the formation of plaques and the activation of microglial cells and astrocytes.

The *in vivo* injection of Aβ (1-40) in the cortex of a rat produces necrosis around the site of the injection, neuritic degeneration and neuronal loss (Scali et al., 1999).

Aβ binds also to metals like Cu^{2+}, Zn^{2+} and Fe^{2+}. In this case the Aβ toxicity is induced by the production of hydrogen peroxide that induces the aggregation of the peptide.

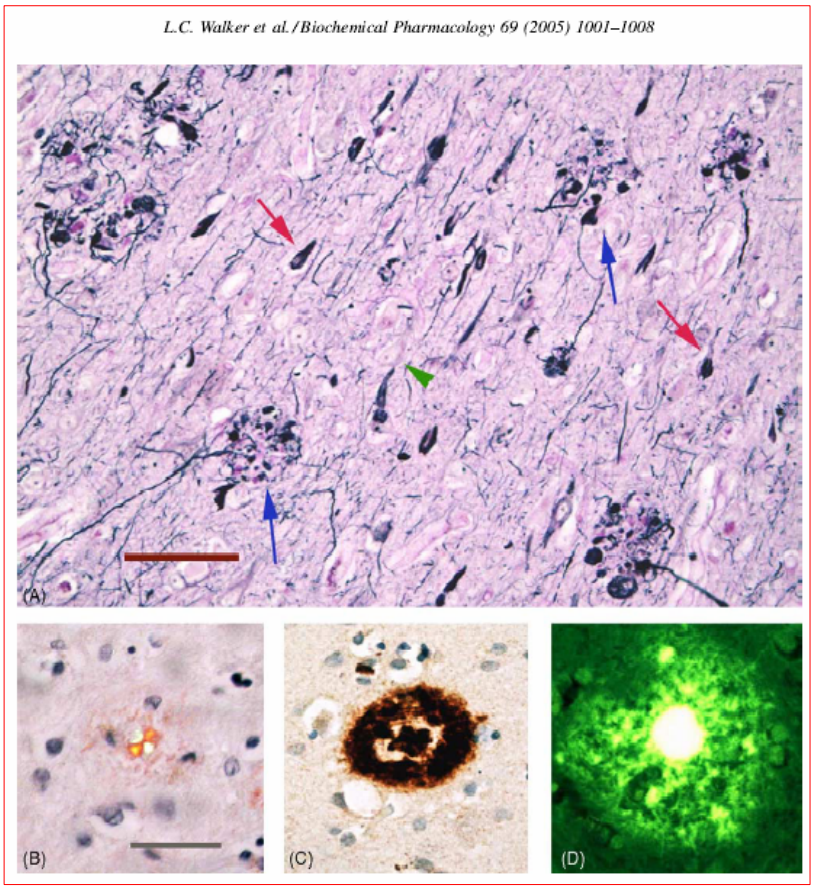

Fig. 4 The canonical pathology of Alzheimer's disease. (A) senile plaques and neurofibrillary tangles in a hippocampal section stained with the Naoumenko-Feigen silver impregnation method and counterstained with periodic acid-Shiff (PAS). Two classical senile plaques are indicated by blue arrows, they consist of an extracellular core of amyloid (stained pinkish-red by PAS) encircled by black, distended neuronal processes (neurites). Diffuse deposition of Aβ usually lack neurites and are not stained by this method. Note also the intracellular NFT (two are marked by red arrows); a pale normal appearing neuron is designed by a green arrowhead. Bar=100μm. (B) A neocortical senile plaque stained with Congo Red, the definitive stain for classically defined "amyloid" (regardless of the identity of the protein component); the photograph was taken with crossed polarizing filters, which produce a Maltese-cruciform pattern of green orange birefringence in compact, fibrillar amyloid deposits(the plaque core, center); Nissl counterstained. (C) A cortical senile plaque immunostained with antibody 10D5 to amino acids 3-7 of Aβ. Note the central core of β-amyloid, surrounded by a halo, and then an outer ring of Aβ, which is typical of many dense-cored plaques in AD; Nissl counterstained. (D) A cortical plaque stained with Thioflavin-T, a fluorescent dye that binds to generic amyloid. The core is intensely fluorescent, and the peripheral, more diffuse deposits also bind Thioflavin. Bar in B=50μm for B, C, D.

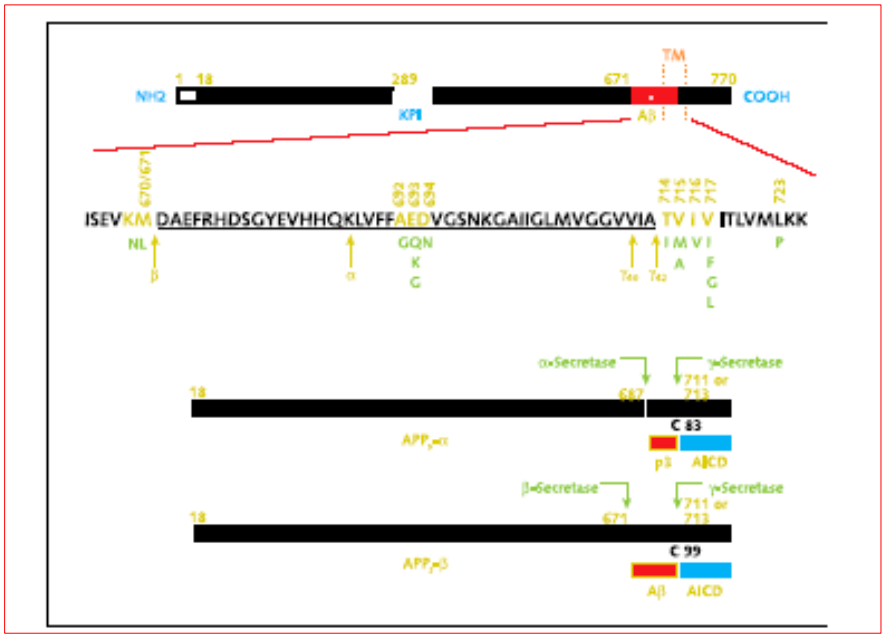

Fig. 5 Schematic diagrams of the β-amyloid precursor protein (APP) and its principal metabolic derivatives.

1.12 Role of tau protein in Alzheimer's disease

The intracellular decline that is characteristic of AD is accompanied not only by the formation of neuritic plaques, but also by the formation of neurofibrillary lesions. The presence of these lesions appears to correlate with the clinical severity of the disease and are found in cell bodies and apical dendrites as neurofibrillary tangles, in distal dendrites as neuropil threads and in the abnormal neurites that are associated with some amyloid plaques as neuritic plaques. Ultrastructurally, all three lesions contain abnormal paired helical filaments (PHFs) as their major fibrous component. Neurofibrillary lesions develop in the vast majority of nerve cells that undergo degeneration in cerebral cortex and hippocampal formation. Evidences indicate that PHFs are made entirely of microtubule-associates protein tau in a hyperphosphorylated state (Fig. 6). Tau protein is an abundant protein in both central and peripheral nervous systems. There are several neurodegenerative diseases characterized by the abnormal phosphorylation and deposition of tau in neurons and glial cells called tauopathies.

In brain tau is found predominantly in nerve cells, where it is concentrated in axons. It is a hydrophilic microtubule-associated protein. There are six adult isoforms of tau expressed in the human adult brain, which range from 352 to 441 amino acids and differ from each other by the presence or the absence of three inserts; the shortest of the six corresponds to the fetal isoform. They each contain three or four microtubule-binding domains of 31 or 32 amino acids, located at the carboxy-terminal half. These domains stabilize the microtubules and facilitate axonal transport of nutrients and neurotransmitters. The gene for the different isoforms is made of 16 exons on chromosome 17. Tau is subject to developmentally regulated alternative mRNA splicing, in that in immature brain only the transcript encoding the shortest isoform with

three repeats is expressed. The isoforms with 4 microtubule-binding domains are the most efficient in aggregating the microtubules and have more binding affinity as compared to the isoforms with 3 domains. On the long isoforms of tau protein there are 79 Serine (Ser) and Threonine (Thr) that can be phosphorylated, and the phosphorylation of 30 of these residues was observed in normal tau proteins. Phosphorylation of tau is a regulated process during growth. These phosphorylation sites are located in a region closed to the microtubule-binding domains. The phosphorylation of some of these site is fundamental for the normal function of the protein. For example the phosphorylation of Ser 262, located in the first microtubule-binding domain, leads to decrease of microtubule binding (Biernat et al., 1993). The same is obtained with the phosphorylation of Ser 396, located in the fourth microtubule-binding domain. Both these sites are phosphorylated in the fetal isoform and are hyperphosphorylated in the six isoforms present in PHFs.

Tau protein extracted from PHFs runs as three major bands of 60, 64 and 68 kDa, with a variable amount of background smear, on an immunoblots gel. These PHF-tau bands are retarded on gels relative to normal or recombinant tau. They contain intact tau, as they stain with antibodies directed against the amino- and carboxy-termini of tau. After treatment with alkaline phosphatase at high temperature the three PHF-tau bands run as six bands which align with the recombinant forms in a hyperphosphorylated state. PHF-tau has greatly reduced ability to bind to microtubules. This loss of function results from hyperphosphorilation, since dephosphorilated PHF-tau binds as well to microtubules as does normal tau. The reduced binding of PHF-tau to microtubules may destabilise microtubules in AD, resulting in the impairment of vital cellular processes, such as rapid axonal transport, and leading to the degeneration of affected nerve cells.

Hyperphosphorilation means that PHF-tau is phosphorylated at more sites than tau from adult brain and that a higher than normal percentage of tau molecules is phosphorylated. There are several classes of kinases or kinase activities that can phosphorylated tau *in vitro*. Glycogen synthase kinase-3 (GSK-3), cyclin dependent kinase-5 (cdk-5), mitogen-activated kinase, extracellular signal regulated kinase (ERK1 and ERK2), stress-activated protein kinase c-jun N-terminal kinase (SAPK/JNK) and p-38 kinase (p38MAPK). Several second messenger dependent kinases can phosphorylate tau at non Ser-Pro motifs, and this includes some sites inside the microtubule-binding domain. Examples are CaM kinase, PKA, PKC or casein kinase II.

Ser 262 is phosphorylated by microtubule-affinity regulating kinase (MARK), PKA and GSK-3 (Anderton et al., 2001).

In vivo studies have demonstrated that GSK-3 and cdk-5 are mainly implicated in the phosphorylation of tau. GSK-3 is a kinase for Ser and Thr that is abundant in the brain where it is associated to the microtubules (Ishiguro et al., 1994;Takahashi et al., 1995;Singh et al., 1995). Cdk-5 is a protein kinase fo Ser an Thr that is abundant in the cytoskeleton of neuronal cells (Baumann et al., 1993;Kobayashi et al., 1993;Lew et al., 1994).

Immunohistochemical studies have shown increased expression of several kinases, including casein kinase, Ca^{2+}/calmoduline-dependent kinase, cdk-5, GSK-3, ERK, SAPK/JNK, p38MAPK and PKA, co-localizing hyperphosphorylated tau deposits, in individual neurons in AD (Xiao et al., 1996) (Ferrer et al., 2002). Co-localization of hyperphosphorylated tau and active kinases in individual cells refers, in most cases, to the kinase phosphorylated at specific sites, as revealed with phospho specific antibodies. This is an important point since modifications in tau phosphorylation do no necessarily parallel total levels of the kinases, and rather depend on the relative abundance of their

active and inactive forms. For example the brain levels of non active kinases ERK1 and ERK2 are similar in AD and controls, whereas the levels of phosphorylated (active) ERK1 and ERK2 are markedly increased in AD brain homogenates, and phospho ERK is exclusively expressed in a percentage of neurons with phospho tau deposits in AD but not in control cases (Ferrer et al., 2001).

Several transgenic mice expressing the short and long isoforms of human tau have been generated as putative models of tauopathies (Usarek et al., 2006) (Higuchi et al., 2002). Some of these mice show axonal degeneration and tau hyperphosphorylation, thus mimicking certain aspects of tauopathies, although neurofibrillary tangles are absent.

Despite the numerous studies on PHFs formation, the basic mechanisms are not known yet. It seems that the form of tau not bound to microtubules is more resistant to degradation. This observation suggests that an enhanced interaction tau-microtubules could be positive.

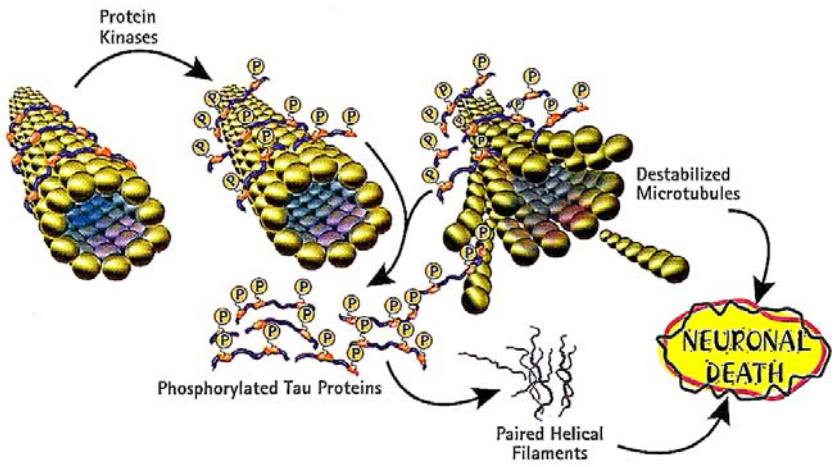

Fig. 6 Scheme of hyperphosphorylation of Tau with subsequent formation of PHF.

1.13 Inflammation in Alzheimer's disease

The inflammatory response is primarily a host defence reaction. It serves to degrade and eliminate the foreign invader. Components of the inflammatory response play essential roles when phagocytic cells remove microorganisms, necrotic host tissue and undesired deposits of abnormal substances. However, prolonged inflammation often destroys the surrounding host tissue. Such a damage is particularly serious if it occurs in brain, where regeneration and recovery take place only in a very limited degree. In neurodegenerative diseases inflammation could be caused by several events: protein aggregates deposition, molecules associated to synapsis or degenerated neurones. In AD senile plaques and tangles could be the site of sustained inflammatory response. Several studies have demonstrated that amyloid-β deposits in the neuritic plaques are associated to numerous immune system proteins, complement proteins, cytokines, protease inhibitor, binding proteins (McGeer and McGeer, 1995) (McGeer and McGeer, 1998). Activated microglia cells are associated to the neuritic plaques, producing cytokines and other neurotoxic components. The presence of molecules of immune system and of activated microglia associated to Aβ confirm the hypothesis that inflammation is the cause of neuronal degeneration in AD (Rogers et al., 2002). The activation of microglia associated with Aβ plaques in the AD brain is paralleled by similar processes in cells in culture. Exposure of cultures of white and grey matter microglia from elderly AD and non AD patients to Aβ(1-42) results in their activation. As in the AD brain, microglia cells increase their cell surface espression of MHCII (Rogers and Lue, 2001), a classic marker for the activation of scavenger cells, in addition to showing a dose-dependent increase in their secretion of the pro-inflammatory cytokines interleukin-1β (IL-1β), interleukin-6 (IL-6) and tumour necrosis factor-α (TNF-α), the chemokines interleukin-

8 (IL-8), macrophage inflammatory protein-1α (MIP-1 α), and monocyte chemoattractant peptide-1 (MCP-1) (Lue et al., 2001). The mRNAs for all these proteins have been observed in AD microglia. IL-1β is also increased after Aβ exposure to cultured AD microglia (Walker et al., 1995).

There are likely to be multiple mediators of microglia activation, chemotactic and phagocytic responses to Aβ. Evidence for complement mechanisms in microglia responses to Aβ has been reported. It seems that the peptide directly interacts with C1 complement factor that activates microglial cells (Eikelenboom et al., 1998). Activated microglia releases cytokines, proinflammatory proteins, complement proteins, reactive oxygen intermediates (Banati et al., 1993).

Inflammatory cytokines amplify and sustain inflammatory and immune responses. They are a family of glycoproteins that are important for the regulation of immune and inflammatory response. They are not only released by activated microglia but also by astrocytes. Cytokines may interact directly or indirectly with neurons, influencing their survival. Cytokines, especially IL-1, enhance the production of prostaglandin E_2 (PGE_2) in humans fibroblasts (Salvemini et al., 1993), stimulating cyclooxygenases enzyme (COX) activation. Recent studies have shown the importance of microglial IL-1 secretion in AD pathogenesis, because IL-1 not only can promote neuronal injury, but also perpetuate cycles of inflammation (Mrak and Griffinbc, 2001). IL-1 has been shown to increase APP production and subsequently increase Aβ, contributing to neuronal damage, and simultaneously, neuronal dystrophy (Goldgaber et al., 1989;Buxbaum et al., 1992). Injection of aggregated Aβ into the NB of rats caused upregulation of IL-1β, COX-2, iNOS and phospho p38MAPK in the surrounding tissue with microglial activation and cholinergic dysfunction (Giovannini et al., 2002).

Several epidemiologic studies have suggested a beneficial effect with chronic nonsteroidal anti-inflammatory drugs (NSAIDs) (McGeer et al., 1996). NSAIDs are believed to act by inhibiting COX. Two distinct isoforms of COX have now been characterized, a constitutive form, COX-1, and a mitogen-inducible form, COX-2. Studies have demonstrated that COX-2 may play a role in neurodegenerative mechanisms (Pasinetti and Aisen, 1998). A number of cross-sectional and longitudinal epidemiologic surveys also indicate that reported use of NSAID is associated with delayed onset and/or slowed cognitive decline in AD (Stewart et al., 1997;Halliday et al., 2000). However, these studies are not conclusive, and the results are controversial. Further examinations of traditional NSAIDs for the treatment of AD has been tempered by two considerations. First, NSAIDs are not the ideal class of anti-inflammatory agents to inhibit acute-phase response and complement activation, two mechanisms that contribute to neurodegeneration in AD. Second, daily use of traditional NSAIDs is associated with adverse effects, particularly on the gastrointestinal (GI) tract of elderly subjects.

Recent findings suggest that selective COX-2 inhibitors may have an advantage over nonselective NSAIDs as potential therapeutic agents in AD. Studies have shown that COX-2 may have a central role in neurodegeneration, supporting clinical evaluation of selective COX-2 inhibitors as neuroprotective agents in AD (Pasinetti and Aisen, 1998;Tocco et al., 1997;Ho et al., 2001). Studies have demonstrated that COX-2 is up-regulated in response to excitotoxic lesions in animals and cell culture systems (Yamagata et al., 1993;Adams et al., 1996). Systemic administration of kainic acid (KA) to rats induces excitotoxic neurodegeneration, which may be a model of AD. It has been demonstrated that excitotoxic lesions cause up-regulation of COX-2 expression coincident with the onset of apoptotic neuronal death. COX-2 expression has

been shown to be up-regulated in AD brain compared with controls (Pasinetti and Aisen, 1998).

Induction of COX-2 in AD may be stimulated by amyloid peptide, and may involve nuclear factor kappa b (NFkB) signalling (Pasinetti and Aisen, 1998;Lukiw and Bazan, 1998). Evidence that COX-2 is involved in AD neurodegeneration may explain the apparent protective effect of NSAIDs. It has been demonstrated that COX-2 inhibitors protect neuronal cells from amyloid toxicity in vitro and promote neuronal survival in animal models of ischemic and excitotoxic neurodegeneration (Fagarasan and Efthimiopoulos, 1996;Graham et al., 1996). Epidemiologic evidence suggests a neuroprotective effect of non-selective NSAIDs from either COX-1 or COX-2 inhibition, or inhibition of both enzymes. Because COX-1 is constitutively expressed in brain, it is plausible that COX-1 catalytic activity may also contribute to neurodegenerative mechanisms (Pasinetti and Aisen, 1998). Recent studies have demonstrated that ibuprofen therapy reduces inflammatory activity and amyloid deposition in transgenic mice (Lim et al., 2000).

Recent trials (Lim et al., 2000) have been done using two different drugs: *Naproxene*, a non-selective NSAIDs, at low doses (220 mg) to minimize the risk of serious GI toxicity, to one group of patients, and *Rofecoxib*, a selective COX-2 inhibitor at standard doses, to a second group. A third group of patients was treated with placebo. It was a one year study and the results don't show any positive effect on memory , attention, speech and orientation of treated patients as compared to controls. An explanation for the negative results obtained could be the not sufficient doses of both drugs, or the short period of time of therapy. It has been demonstrated that a two year treatment with anti-inflammatory drugs is necessary to reduce AD risk (Ruitenberg et al., 2001).

It has been shown that in AD brains there is a colocalization of hyperphosphorylated tau and phosphorylated p38 MAPK in dystrophic neurons and neurites that are associated to activated microglia that over express IL-1 (Sheng et al., 2001).

Recent studies have demonstrated that there are different molecules involved in neuron-glia intercommunication, such as CD200 and HMGB1. CD200 is a membrane glycoprotein expressed by neurons that binds to a structurally similar receptor that is expressed by microglia. Their intercommunication holds microglia in a quiescent state (Hoek et al., 2000;Lyons et al., 2007;Frank et al., 2007). HMGB1 is a non-histone DNA-binding protein that has a pro-inflammatory cytokine-like function that may influence the activation of microglia following injury or insult (Kim et al., 2006). HMGB1 levels are low in resting glia but are increased in the brains of patients with Alzheimer's disease (Takata et al., 2004). Extracellular HMGB1 has also been described as a mediator of lipopolysaccharide (LPS) toxicity (Ulloa and Messmer, 2006).

1. 14 Animal models of Alzheimer's Disease

Transgenic mice overexpressing Aβ offer a new powerful *in vivo* model to study the pathogenetic mechanisms related to Aβ neurodegeneration and allow to test possible therapeutic interventions. Among the mice strains recently developed (Hsiao et al., 1996;Masliah et al., 1996), transgenic TgCRND8 mice (Chishti et al., 2001) expressing a double mutant form of human APP (K670/M671L and V717F) have been produced. Hemizygous TgCRND8 mice exhibit extensive cerebral amyloid deposition, cortical and hippocampal atrophy and memory impairment by 3 months of age (Chishti et al., 2001) and represent one of the transgenic mouse models which more closely resemble

the human pathology. In 7-month old TgCRND8 mice, extensive Aβ deposition in the cortex, hippocampus, thalamus and basal forebrain is accompanied by significant microglia and astrocyte activation, and by cholinergic dysfunction and cognitive impairment (Bellucci et al., 2006). This transgenic line is a good model of Aβ deposition, neurodegeneration and memory defects, and can be useful to clarify involvement of MAPK dysregulation in AD and in developing new therapeutic treatments.

1.15 Alzheimer's therapy

Knowledge of the neurotransmitters disturbances in Alzheimer's disease has led to the development of drugs with symptomatic effects, which are approved in many countries. Research advances in the molecular pathogenesis of Alzheimer's disease have also led to new drug candidates with disease-modifying potential, which have now come to testing in clinical trials. Epidemiological data have suggested additional drug candidates, some of which have been investigated in randomised trials.

The cholinergic hypothesis of Alzheimer's disease states that degeneration of cholinergic neurones in the basal forebrain nuclei causes disturbances in the presynaptic memory disturbances and other cognitive symptoms.

The loss of forebrain cholinergic neurons and the ensuing reduced synthesis and release of ACh is considered a crucial pathogenetic feature of AD since the historical paper of Davies and Maloney (1976). Cholinesterase Inhibitors (ChEIs) have been considered the best tool for restoring an adequate level of ACh in the synaptic gap since they prevent the hydrolysis of the residual ACh in the brain of AD patients. The question arises as to whether ChEIs really increase brain ACh. In the rat an increase in brain ACh

extracellular levels, measured by microdialysis, has been consistently demonstrated (Rosi et al., 2004;Cerbai et al., 2007).

Since ChEIs are typically used in long-term therapy, the question has been asked whether tolerance, and consequent decrease in acetylcholinesterase (AChE) inhibition, develops after repeated administration of the inhibitor. Moreover, whether the persisting high level of ACh results in decreased ACh synthesis and modifications in cholinoceptor function. From the animal experiments investigating the effects of prolonged ChEI treatments it may be concluded that AChE, Cholineacetyltransferase (ChAT), and the transport mechanisms of choline and ACh do not undergo adaptive changes resulting in reduced AChE inhibition and ACh synthesis and ACh levels remain elevated. Muscarinic M_2 autoreceptors only appear to undergo some adaptation.

The AChE inhibitors *donepezil*, *rivastigmine* and *galantamine* are approved for clinical use in Alzheimer's disease. Donepezil and galantamine are selective AChE inhibitors, whereas rivastigmine inhibits AChE and butirrylcholinesterase (BuChE) with similar affinity. Both donepezil and galantamine are metabolised in the liver by cytochrome P450 enzymes, and can thus interact with drugs that inhibit these enzymes. Rivastigmine has a non-hepatic metabolism. The half-life of the drugs also varies thus determining the need for one or two doses per day. The efficacy of these drugs has been studied in more than 30 randomised double-blind clinical trials. Most trials have been for 3-6 months and have shown modest positive effects on cognitive symptoms. Benefits of AChE inhibitors are also seen for functional and behavioural symptoms.

Considering the mechanism of action for the AChE inhibitors, they are not expected to change the natural course of Alzheimer's disease, but only to temporarily mitigate some of the symptoms. Overall, they are safe drugs, and side-effects are generally limited to gastrointestinal symptoms, including nausea, vomiting, and diarrhoea, which however

may decrease the patient's complience. For this reason, much effort is being dedicated to the development of novel cholinesterase inhibitors that show fewer side effects.

In healthy human brain, AChE predominates over BuChE activity (Giacobini, 2003), but the latter likely has been previously underestimated (Li et al., 2000).

Whereas AChE is localized mainly to neurons, BChE is associated primarily with glial cells, as well as with endothelial cells and neurons (Darvesh and Hopkins, 2003). A possible role for brain BChE, particularly when associated with glia, is for supportive hydrolysis of ACh. The close spatial relationship of glial BChE would allow synergistic BChE-mediated hydrolysis to assist in the regulation of local ACh levels to permit the maintenance of normal cholinergic function. The survival of AChE knockout mice (Li et al., 2000) with normal levels and localization of BChE (Mesulam et al., 2002) supports the concept that BChE has a key role that can partly compensate for the action of AChE.

In AD, AChE is lost early by up to 85% in specific brain regions, whereas BChE levels (Perry et al., 1978b;Arendt et al., 1992) rise with disease progression. The ratio of BChE to AChE changes dramatically in cortical regions affected by AD from 0.2 up to as much as 11 (Giacobini, 2003). Clearly, this altered ratio in AD brain could modify the normally supportive role of BChE in hydrolyzing excess ACh only. Selective BChE inhibition may therefore be useful in ameliorating a cholinergic deficit, which likely worsens in AD due to increased activity of BChE.

Histochemical studies show that some cholinergic neurons contain BChE instead of AChE (Graybiel and Ragsdale, Jr., 1982). In fact, 10–15% of ChE-positive cells in human amygdala and hippocampus are regulated by BuChE independently of AChE (Darvesh et al., 1998). Augmenting cholinergic function by inhibiting these pathways may be of clinical value. Finally, it is pertinent to mention that BuChE is increased in

the cerebral cortex of Alzheimer's disease patients (Perry et al., 1978a;Perry et al., 1978c) and it is associated with the amyloid plaques. It has been suggested that BuChE, together with AChE (Alvarez et al., 1997), may participate in the transformation of the β-amyloid deposit into neuritic plaques (Guillozet et al., 1997a;Guillozet et al., 1997b). Inhibition of the enzyme may therefore delay plaque formation, thus suggesting the possibility to use BuChE inhibitors in the treatment of Alzheimer's disease not only to increase the availability of acetylcholine at the synapses, but also to reduce the number of plaques. Indeed, clinical studies with the dual ChEI, rivastigmine, support a role for the central inhibition of BuChE in addition to AChE inAD therapy, based on the high correlation of the former with cognitive improvement (Giacobini et al., 2002). The findings by (Bartorelli et al., 2005b;Bartorelli et al., 2005a) , that AD patients deteriorating on selective AChE inhibitor treatment can benefit from switching to a dual AChE-BuChE inhibitor, in terms of stabilization of disease and improvement in cognitive functions, has prompted the development of novel inhibitors directed towards BuChE inhibition.

Glutamate is the major excitatory neurotrasnsmitter in the brain. Under normal conditions, glutamate and the N-methyl-D-aspartate (NMDA) receptor have important roles for learning and memory processes. Under abnormal conditions, such as in Alzheimer's disease, increased glutamatergic activity can lead to sustained low-level activation of NMDA receptors, which may impair neuronal function.

Memantine is a non-competitive NMDA-receptor antagonist that is believed to protect neurons from glutamate-mediated excitotoxicity without preventing the physiological NMDA-receptor activation needed for cognitive functioning (Wilcock, 2003). Randomised double-blind clinical trials show modest positive effects on cognitive and behavioural symptoms, and improved ability to perform activities of daily living at 6

months in people with moderate to severe Alzheimer's disease (Wilcock, 2003). Additionally, in moderate to severe disease, combination therapy with donepezil and memantine show positive effects on symptoms relative to donepezil alone (Tariot et al., 2004).

Despite the theoretical rationale for neuroprotective properties of memantine, current trials are too short to asses if the drugs has any disease-modifying effects. Nevertheless, the drug is well tolerated in general, with few adverse events, and may be a useful therapeutic adjunction in patients with moderate to severe disease.

Behavioural signs, such as aggression, psychomotor agitation, and psychosis (hallucinations and delusions), are very common in patients with Alzheimer's disease, especially in the late stages of the disease. Such symptoms not only affect quality of life for patients and caregivers, but also contribute to care burden and economic cost.

Several short-term trials show efficacy of *risperidone* and *olanzapine* in reducing the rate of aggression, agitation, and psychosis (Brodaty et al., 2003;Street et al., 2000). Alternative treatments include anticonvulsants, such as *divalproate* and *carbamazepine*, and short-acting benzodiazepines, such as *lorazepam* and *oxazepam* (Materman D, 2003). Additionally, the cholinergic deficits can contribute to the development of behavioural symptoms, and treatment with AChE inhibitors also shows improvements in behavioural symptoms (Terry, Jr. and Buccafusco, 2003).

Substantial efforts have been made to translate the advances in the molecular pathogenesis of AD into therapeutic strategies. The major focus has been to inhibit brain Aβ production and aggregation, and to increase Aβ clearance from the brain.

Drugs candidates with potential disease-modifying effects are: secretase modulator, Aβ immunotherapy, anti tau-drugs.

For the first group of drugs, the finding that BACE1 knockout mice have abolished Aβ production without any clinical phenotype (Luo et al., 2001) made BACE1 inhibitors an attractive therapeutic strategy. β-secretase inhibitors have been developed to reduce brain Aβ concentrations in Alzheimer's disease transgenic mice. Drugs that stimulate α-secretase can shift APP processing towards the non-amyloidogenic pathway, thus reducing Aβ production. *Bryostatin*, a protein kinase C activator currently tested in clinical trials as an anticancer drug, substantially enhances α-secretase processing of APP and reduces brain Aβ(1–42) concentrations in AD transgenic mice (Etcheberrigaray et al., 2004).

The principal of Aβ immunotherapy was first reported in a paper showing that active immunisation of AD transgenic mice with fibrillar Aβ attenuated Aβ deposition (Schenk et al., 1999). Similar results were obtained by use of passive immunisation with antibodies against Aβ (Bard et al., 2000). The effect might be mediated by anti-Aβ antibodies that bind to Aβ plaques and induce Aβ clearance by microglia (Bard et al., 2000;Schenk et al., 2004).

These results were the basis for initiating clinical trials with active immunisation with the vaccine AN1792, composed of preaggregated Aβ42 (Schenk et al., 2004). However, the phase IIa AN1792 trial had to be interrupted because 6% of cases developed encephalitis (Orgogozo et al., 2003). This side-effect has been suggested to be due to a T-cell response against the mid-terminal and C-terminal part of the peptide. The second generation of immunotherapy , Aβ immunoconjugates composed of the N-terminal part of Aβ conjugated to a carrier protein (Schenk et al., 2004), or virus-like particles, could allow for active immunisation with reduced risk of Th-1 mediated side-effects. Both

active immunisation with N-terminal Aβ fragments and passive immunisation with N-terminal anti- Aβ monoclonal antibodies are now in phase II trials.

Drugs of the third group, candidates that reduce tau phosphorylation by inhibiting tau kinases, such as CDK5 and GSK-3β, are in the preclinical phase. However, since tau phosphorylation is regulated by the balance between multiple kinases and phosphates, inhibition of a single kinase might be insufficient to normalise tau phosphorylation.

2. AIM

Aim of the research was:

1. Evaluate the modification of different intracellular transduction pathways and extracellular intercommunicating proteins as well as activation of microglia and astrocytes in animal models of neuroinflammation, normal aging and AD-related neurodegeneration that may lead to memory deficits. To this aim different animal models were used. In particular, the molecular mechanisms involved in neuron-glia intercommunication during inflammation in the hippocampus were studied using the model of LPS-induced neuroinflammation in the rat, developed by Prof. Gary Wenk. This part of the work was carried out in Wenk's Lab, Psychology Department, Ohio State University, USA. The differential activation of MAPKs intracellular transduction pathways as well as the cellular modifications in the hippocampus during aging and AD related neurodegeneration were studied in normal aged rats and in TgCRND8 transgenic mice, an animal model of AD. This part of the work was carried out in Giovannini's Lab, Department of Pharmacology, University of Florence, Italy.

1) Evaluate the efficacy of treatment with novel compounds on differential inhibition of acetylcholinesterase/butyrilcholinesterase activity in the brain and on cortical acetylcholine release. These experiments were aimed at obtaining a proof of concept for the development of these compounds as possible drugs for the treatment of memory impairments in neurodegenerative diseases.

3. MATERIALS AND METHODS

3.1 Animals

Male Wistar rats, 220–250 g body weight (Harlan Nossan, Milano, Italy), Tg heterozygous TgCRND8 mice with a (C57)/(C57/C3H) genetic background and non-Tg littermates hybrid (C57)/(C57/C3H) wild type (Wt) control mice of 7 months of age were used. The mice were obtained from the laboratory of Prof. P. St. George-Hyslop (CRND, Toronto, ON, Canada) and were bred in the Centre for Laboratory Animals, University of Florence, Italy. The animals were individually housed in macrolon cages until experiment with ad libitum food and water, and were maintained on a 12 h light–12 h dark cycle with light at 7:00 am. The room temperature was 23±1°C. All rats were kept for at least 1 week in the animal house facility of the University of Florence before experiment. All animal manipulations were carried out according to the European Community guidelines for animal care (DL 116/92, application of the European Communities Council Directive 86/609/EEC). Formal approval to conduct the experiments described has been obtained from the animal subjects review board of the University of Florence, and the Italian Ministry of Health. All efforts were made to minimize animal sufferings and to use only the number of animals necessary to produce reliable scientific data.

3.2 Drugs

Donepezil and rivastigmine were supplied by Novartis (Basel, Switzerland). (−)-N1phenethyl-norcymserine (PEC) was obtained from Dr. Nigel H. Greig, National

Institute on Aging, NIH, Baltimore MD, USA. Donepezil and rivastigmine were dissolved in saline and injected i.p. in a volume of 2 ml/kg of body weight. PEC was dissolved in saline containing 10% Tween 80-5% ethanol and injected i.p. in a volume of 2 ml/kg of body weight. NP-361 and NP-336 were supplied by Neuropharma (Madrid, Spain) and dissolved in N-methyl-2Pyrrolidone 5%, Solutol HS15 30%, Saline (10 ml/kg) for the enzymatic assays, in N-methyl-2Pyrrolidone 5%, Solutol HS15 30%, Saline (10 ml/kg) or Tween 80 2% diluted in Methylcellulose 0.5% (10 ml/kg) for behavioural experiments, in DMSO 400 μg/kg for microdyalisis experiments, and injected i.p. in a volume of 10 ml/kg of vehicle.

3.3 Microdialysis experiments

Rats were deeply anesthetized with 4% chloral hydrate and placed in a stereotaxic frame (Stellar, Stoelting Co.,Wood Dale, IL, USA) for surgery. At the end of surgery the rats were put back in their home cages (one rat per cage) to recover. Transversal microdialysis probes (AN 69 membrane, Hospal Dasco, Italy, molecular mass cut-off 15 kDA) covered with super epoxy glue except for the region corresponding to the length of frontal cortices (mm 8) were inserted in the frontal cortex according to the following coordinates: AP, 0.0 and H 1.7 mm from bregma (Paxinos and Watson, 1982). Transversal probes were preferred to vertical probes in order to increase the surface through which acetylcholine could diffuse from the extracellular space in the perfusing fluid and facilitate basal level determinations (Scali et al., 1997). On the following day, the inlets of the membranes were connected to a microperfusion pump (CMA/100) and were perfused with artificial cerebrospinal fluid (aCSF), of the following composition (in mM): 147 NaCl, 1.2 CaCl2, 3.0 KCl, 4 at a constant flow rate

(3 µl/min) with no cholinesterase inhibitors added. The dialysate was collected at 20-min intervals in minitubes containing 5 µl of 0.05 mM HCl to prevent hydrolysis of acetylcholine. After four samples had been collected under basal conditions, the rats were injected with the cholinesterase inhibitors or saline and samples were collected for 3 h after drug treatment. The samples were stored at −80 °C before assaying. At the end of the experiments the rats were sacrificed to check probe location visually and the brains were stored at −80 °C in case further analyses were necessary.

3.4 Assay of acetylcholine in the dialysates

Acetylcholine was assayed in the dialysate by HPLC with electrochemical detection (Damsma et al., 1987;Giovannini et al., 1994) using an acetylcholine/choline assay chromatographic kit purchased by ByoAnalytical System, Inc (Indiana, USA) consisting of an analytical column (BAS MF-6150, Bio Analytical Systems Inc., West Lafayette, Indiana, USA) and an acetylcholine/choline Immobilized Enzyme Reactor (IMER, BAS MF-6151, Bio Analytical Systems Inc., West Lafayette, Indiana, USA) containing acetylcholinesterase and choline oxidase. The mobile phase was 50 mM Tris/NaClO4 containing 0.05% ProClin (BAS CF-2150, Bio Analytical Systems Inc., West Lafayette, Indiana, USA), pH 8.5, at 1 ml/min flow rate. Acetylcholine and choline were separated in the analytical column, acetylcholine was hydrolized in the IMER by acetylcholinesterase to acetate and choline was then oxidized by choline oxidase to produce betaine and hydrogen peroxide.

Hydrogen peroxide was electrochemically detected by a platinum working electrode at +500 mV with a Ag/AgCl reference electrode. The sensitivity limit (s/n ratioN3/1) was 75–100 fmol/injection for acetylcholine. To evaluate the amount of acetylcholine in the

samples, a linear regression curve was made with acetylcholine standards and the peak heights of this compound in the samples were compared with those of the standards by means of an integrator (P.E. Nelson model 1020). Neurotransmitter levels in the dialysis samples were calculated as fmol/µl and then expressed as percent variation over basal levels, which in each group of experiments was the mean±S.E.M. of the 4 basal samples pre drug administration. Since increase in acetylcholine release always returned to basal levels after treatment, the evoked acetylcholine release was calculated evaluating the areas under the curve (in arbitrary units), between 100 and 200 min after treatment both in salineand in drug-treated animals. Statistical analysis among groups was performed comparing the areas under the curve.

3.5 Cholinesterase determination

Acetylcholinesterase and butyrylcholinesterase activity was measured in different groups of rats of the same strain and age, kept under the same housing conditions. At the time corresponding to the peak increase in acetylcholine levels after drug administration (55–60 min after administration), the rats were sacrificed by decapitation. Brains were quickly removed and placed in ice-cold saline to dissect out the parietal cortices, which were quickly weighted and frozen immediately on dry ice and kept at −80 °C until enzyme activity determination. Acetylcholinesterase and butyrylcholinesterase activities in the cerebral cortex were determined using three methods in different groups of rats:

1) Method of Ellman, (ELLMAN et al., 1961) as previously used by Scali et al. (2002), (Scali et al., 2002) with modifications by Chuiko et al. (2003) (Chuiko et al., 2003),

using the substrates acetylthiocholine and butyrylthiocholine iodide (5×10−4 M final concentration), for acetylcholinesterase and butyrylcholinesterase, respectively. Enzyme activity was expressed as μmol substrate hydrolyzed per minute per μg protein. Cortical samples of about 50–70 mg were homogenized in 50 mM Na-phosphate buffer, pH 7.2 (1:5, w:v) in a glass-teflon homogenizer on ice (15 strokes). For acetylcholinesterase determination, 25 μl of homogenate were added to 2875 μl of 5,5′-Dithiobis(2-nitrobenzoic acid) (DTNB) 0.3 mM in 50 mM Na-phosphate buffer, pH 7.2, containing 100 μl of 15 mM acetylthiocholine as the substrate. The reaction was developed for 2 min and read at 412 nm. Proper blanks were made up following the same procedure, with the exclusion of the homogenate.

For butyrylcholinesterase determination, the homogenate was added to the reaction mixture as above which contained 100 μl of 15 mM BuTCh as the substrate, and the sample was read at 412 nm at 2 min. In a few samples, the selective acetylcholinesterase inhibitor 1,5-bis(4 allyldimethylammo allyldimethylammoniumphenyl) pentan-3-one dibromide (BW 284-C51, Sigma- Aldrich) (10− 5 M) was added to the homogenate, reducing the volume of DTNB in order to maintain the total volume of 3 ml. Blanks were made up as above. No differences in butyrylcholinesterase activity were found between the samples with and without BW 284-C51. The enzyme activity was quantified using the following calculations taken from Ellman et al. (ELLMAN et al., 1961) as modified by Galli et al. (1984) (Galli et al., 1984):

[(OD_{412nm}/min)/136 x 100 (extinction coefficient of the yellow anion)] x [1/(μl sample/μl tot volume) x (μg/μl protein)] x 1000

which expresses acetylcholinesterase activity in pmol/min x μg protein.

2) Method of Ellman modified according to O. Lockridge for butyrylcholinesterase.

Cortical samples of about 50–70 mg were added to 10 volumes of 0.5% Tween-20 in 50 mM potassium phosphate buffer, pH 7.4. After homogenization in a glass homogenizer on ice (15 strokes), the samples were centrifuged in a microfuge for 10 min at 4 °C and 100 µl of the supernatant were added to 865 µl of 0.1 M potassium phosphate, pH 7.0 and 25 µl of 20 mM DTNB. The mixture

was incubated for 23 min to deplete free sulphydryls. The depletion of free sulphydryls was monitored at 412 nm. When the slope was constant (after 23 min), the activity of butyrylcholinesterase was monitored by starting the reaction with 10 µl of 0.1 M BuThCh to a total volume of 1 ml. The reaction was developed for 5 min and read at 412 nm. Blank samples were prepared as above, omitting the homogenate. The activity of the enzyme was calculated using the formula described by Ellman et al. (1961) (ELLMAN et al., 1961).

3) Radiometric method for acetylcholinesterase and butyrylcholinesterase: (Johnson and Russell, 1975;Thiermann et al., 2005). Cortical samples of about 50–70 mg were homogenized (1:5, w:v) on ice in 50 mM Tris–HCl buffer (pH 7.4) containing 1 M NaCl and 1% Triton X-100 (Lysis buffer). [3H-acetyl]acetylcholine working solution was made up with the specific activity of 1 mCi/mmol, 10 mM.

3a) Acetylcholinesterase activity determination. Thirty µl of cortex homogenates or of Lysis buffer (blanks) were added to 50 µl of 50 mM phosphate buffer (pH 6.8) in a plastic vial. Twenty µl of H]acetylcholine working solution were added, samples were vortexed for 15 s and incubated at 37 °C for 15 min in a water bath under slight agitation. The enzyme reaction was terminated by adding 100 µl of a stopping solution

consisting of 1 M monochloroacetic acid, 0.5 M NaOH and 2 M NaCl. The [3H] acetic acid formed by the reaction was extracted into 4 ml of a lipophilic scintillation cocktail (OptiScint HiSafe, Perkin Elmer Life Sciences, Inc., Boston, MA, USA), containing 10% isoamyl alcohol (v:v) by vigorous shaking for 1 min. After separation of the two phases, the radioactivity was counted with a Perkin Elmer Life Science scintillation counter. The radioactivity of the blanks (b0.5%) was subtracted from the values of the samples.

3b) Butyrylcholinesterase activity determination. Thirty ml of cortex homogenates or of Lysis buffer (blanks) were added to 25 µl of 100 µM phosphate buffer (pH 6.8) and to 25 µl of 40 µM BW 284-C51, a selective inhibitor of acetylcholinesterase, in a plastic vial and incubated for 30 min at 37 °C in a water bath under slight agitation. Twenty µl of [3H]acetylcholine working solution were added, samples were vortexed for 15 s and incubated at 37 °C for 30 min in a water bath under slight agitation. The same procedure described above was then followed. Enzymatic activity was quantified using the following formula taken from (Potter, 1967) as modified by (Johnson and Russell, 1975):

{{{[(sample$DPM_{average}$ - blank$DPM_{average}$)/1000]/2.22(converting factor)}

/µgprotein}/incubation time} x 1000

which gives as result acetylcholinesterase or butyrylcholinesterase activity expressed in pmol/min×µg protein.

3.6 Protein determination

Protein determination was performed in the homogenates using a Bio-Rad Protein Assay reagent (Bio-Rad, Hercules, CA) with bovine serum albumin as standard.

3.7 Step-down inhibitory avoidance task

In the step-down inhibitory avoidance task rodents, put on an elevated platform placed by one wall of an arena, learn to associate exploration of the adjacent compartment with a foot shock delivered through the floor grid. On a subsequent exposure to the same environment, the animal will avoid stepping down, or will increase the latency before "stepping down" onto the floor grid. We used a standard step-down apparatus placed in a soundproof room. Rats were handled and habituated to the experimenter and to the handling procedure the day before the test. Rats were positioned on an elevated platform placed in a dark compartment facing an open arena equipped with an electrified floor grid. We recorded the "Acquisition latency," i.e. the time spent before stepping down onto the grid where an aversive stimulus (10 electric shocks, 20 ms/0.5 mA/5 Hz) was delivered to the animal. Rats were immediately removed from the arena and placed in their home cage for consolidation ("Encoding"). Recall tests, given 60 min after the training test, were identical to training sessions, except that the footshock was omitted. At the recall test the time spent in the dark compartment before stepping down onto the arena was also recorded ("Recall latency"). All trained rats acquired the behavior. A 300 s ceiling was imposed on recall test latencies.

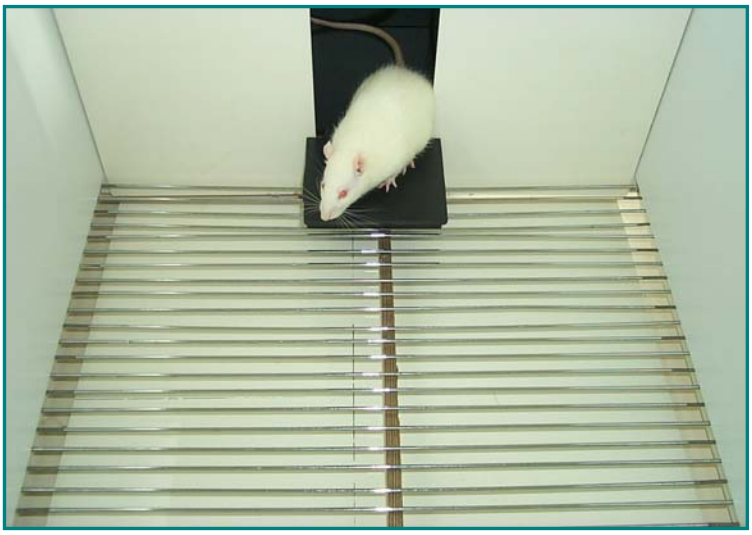

Fig. 7 Rat position on the platform of the step down inhibitory avoidance task.

3.8 Exploratory behaviour

The exploratory behaviour was investigated in an arena formed by a white-colored polyvinyl chloride box (70x60x30 cm) with a grid floor which could be easily cleaned. The arena was illumined by two 75-W lamps suspended 50 cm above the box. A microwave sensor was placed 70 cm above the arena to measure the rats' motor activity. Each animal was taken from it home cage and transferred in the adjacent arena, to which it had never been exposed before. To do this, the animal was manually picked up from it home cage, lifted approximately 50 cm and placed gently into the open field. This procedure lasted less than 5 s.

Total motor activity in the arena during exploration was recorded every 5 min by means of a microwave sensor placed 70 cm above he cage, in order to cover the entire arena. The impulses created by movements were recorded every 0.1 s by a counter, which added an expressed them in s/5min. No analysis of the movement type was made. Statistical analysis was performed on the mean ± SEM using a one way ANOVS followed by Newman-Keuls multiple comparison test.

3.9 Rota rod test

The motor performance was evaluated in the rotarod test for rats (Ugo Basile Rota-Rod). The day before the test, rats were trained twice in the rotarod treadmill, rotating at the speed of 8 rpm for 5 minutes. On the day of the test only the rats tat were able to stay balanced on the rotating rod between 70 and 120 s (cut-off time) were selected for the trial and randomly assigned to one of the experimental groups. Rats that fell off the rod before 70 sec were discarded. The test was then performed 60 min after i.p. injection of the compounds under investigation. The time rats spent in balance on the rod was measured in sec and statistical analysis was performed on the median ±

interquartile range using a non parametric test (Kruskall-wallis test followed by Dunn's multiple Comparison test).

The following groups were tested: saline, vehicles (N-methyl-2pyrrolidone 5%, Solutol HS15 30%, Saline), NP-361 (10 mg/kg and 20 mg/kg) or NP-336 (40 mg/kg and 80 mg/kg) dissolved in vehicle.

3.10 Fourth ventricle surgical procedure

Artificial cerebrospinal fluid (aCSF, n=20) or lipopolysaccharide (LPS, Sigma, E. coli, serotype 055:B5, TCA extraction, 1.0 µg/µl dissolved in aCSF, n=42) was chronically infused through a cannula implanted into the 4th ventricle of the brain that was attached (via Tygon tubing, 0.06 O.D.) to an osmotic minipump (Alzet model #2004, to deliver 0.25 µl/h) as previously described (Rosi et al., 2005). According to the manufacturer's specifications, the model #2004 will produce a continuous infusion for approximately 42 days (six weeks). The aCSF vehicle contained (in mM) 140 NaCl; 3.0 KCl; 2.5 $CaCl_2$; 1.0 $MgCl_2$; 1.2 Na_2HPO_4, adjusted to pH 7.4. Two weeks after the infusion began, some rats were anesthetized and had a second osmotic minipump implanted (model 2ML2, to deliver 2.5 ul/h) containing memantine (15 mg/kg/d); these rats were sacrificed two weeks later. Memantine was purchased from Tocris Bioscience (Ellisville, MO). Body weights were determined daily and general behavior was monitored for normal grooming behavior and seizures. Rats infused with aCSF were sacrificed one or eight weeks after surgery. Rats infused with LPS were sacrificed one, four or eight weeks after surgery. For rats that are sacrificed eight weeks after surgery, their exposure to either LPS or aCSF would have ended approximately six weeks after surgery. This group was included in order to determine whether microglial activation

was still present two weeks after the cessation of the infusion of LPS into the 4th ventricle. Serum samples were collected at sacrifice and levels of memantine were determined by gas chromatography (Misztal and Paw, 1996).

3.11 Immunohistochemistry

Antibodies.

The following antibodies were used: rabbit polyclonal anti-phospho (Thr202/Tyr204)-ERK1,2 antibody (1:750), anti-phospho-(Thr180/Tyr182)-p38MAPK antibody (1:250), antiphospho-(Thr183/Tyr185)-JNK antibody (1:1000) which detect the activated forms of ERK1,2, p38MAPK and JNK, respectively (all from Cell Signaling Technology, Inc., Danvers, MA, USA). Each antibody specifically recognizes the phosphorylated form of the respective kinase, with no cross-reaction with the two other ones. Activated microglia was evidenced using monoclonal OX-6 antibody (1:200; Pharmingen, BD Bioscience, Franklin Lakes, NJ, USA) against major histocompatibility (MHC) class II complex and polyclonal anti-glial fibrillary acidic protein (GFAP) (1:1000; DakoCytomation, Glostrup, Denmark) were used to detect activated microglial and astrocytes cells, respectively. CD200 was evidenced using monoclonal antibody (1:50; AbDserotec, Raleigh, NC), HMGB1 was evidenced using polyclonal antibody (1.500; AbCam, Cambridge, MA). Neuronal calcium was visualized using polyclonal antibody anti-calbindin (1:500; AbCam, Cambridge, MA). The inducible nitric oxide was visualized using the plyclonal antibody anti-iNOS (1:100; AbCam, Cambridge, MA). A monoclonal anti-neuronal nuclei (NeuN) antibody (1:200; Chemicon, Temecula, CA, USA) was used to detect neurons.

Rats were anesthetized with chloral hydrate (400 g/kg) and perfused transcardially with 500 ml of ice-cold paraformaldehyde (4% in phosphate-buffered saline (PBS), pH 7.4). The brains were postfixed for 4 h and cryoprotected in 18% sucrose/PBS solution for at least 48 h. Coronal sections (40 _m-thick) were cut with a cryostat, placed in 1 ml of anti-freeze solution and stored at -20 °C until immunohistochemistry.

Light microscopy immunohistochemistry.

Day 1. The antibodies were stained using the free-floating method (Giovannini et al., 2001b;Giovannini et al., 2003c). Coronal brain sections were placed in wells of 24-well plates and were rinsed for 10 min in phosphate buffered saline 0.3% Triton X-100 (PBS-TX), incubated for 15 min in PBS-TX containing 0.75% H2O2 and blocked with blocking buffer (BB) containing 1.5% normal goat serum and 0.05% NaN3 in PBS-TX for 1 h. Sections were then incubated overnight at 4 °C with the following primary antibodies: ERK1,2, JNK, p38MAPK, GFAP, OX6, iNOS.

Day 2. Slices were incubated in biotinylated goat anti-rabbit secondary antibody (Vectastain, Vector Laboratories, Burlingame, CA, USA), diluted 1:333 or anti-mouse diluted 1:1000 in BB for 2 h at RT, then for 1 h 30 min in AB solution (Vectastain ABC kit, Vector Laboratories) and staining was developed for 2–3 min using 3,3'-diaminobenzidine (DAB) staining kit (Vectastain, Vector Laboratories) with NiCl2 as an enhancer. DAB-stained slices were examined using an Olympus BX40 microscope equipped with an Olympus DP 50 (Olympus, Milan, Italy) digital camera.

For double staining, at the end of the second day, the sections underwent another cycle of immunohistochemistry with a polyclonal antibody raised against the β-amyloid(1–

42) (1:250, Biosource Europe, Nivelles, Belgium) peptide to label amyloid plaques or with monoclonal OX-6 antibody (1:200) (Pharmingen, BD Bioscience, San Jose, CA, USA) against MHC class II complex to visualize activated microglia. The staining was visualized by the use of a Vector NovaRed Kit (Vector Laboratories) and observed by means of a light microscopy, as above.

Laser confocal microscopy immunohistochemistry

Staining was performed with the free-floating method and slices were blocked 10% normal goat serum–10% normal horse serum in PBS-TX for 40 min (BB). Astrocytes were visualized using an anti– glial fibrillar acidic protein antibody incubated O/N at 4 °C and then for 2 h at RT with a Texas Red (TR) –conjugated anti-mouse (1:200) in BB. Colocalization of activated p38MAPK in neurons and astrocytes was visualized using double-labeling confocal microscopy with antibodies against phospho-p38MAPK, anti-NeuN for neurons, anti-MHC class II complex for activated microglia and anti-GFAP for astrocytes. After incubation with the two primary antibodies diluted in BB at the above concentrations, O/N at 4 °C under slight agitation, slices were incubated for 2 h at RT in the dark with fluorescein (FITC) -conjugated anti-rabbit antibody (1:200) and then for 2 h at RT in the dark with FITCconjugated anti-rabbit IgG plus TR-conjugated anti-mouse (1:200) in BB (Vectastain, Vector Laboratories). After extensive washings, slices were then mounted onto gelatin-coated slides for microscopic examination using Vectashield (Vectastain, Vector Laboratories) as mounting medium. TR single-labeled or FITC/TR double- labeled slices were observed under a BioRad 1024 confocal laser scanning microscope (Cambridge, MA, USA) with laser beam excitation at 488 and 568 nm wavelength. Optical z-sections were taken at 1 μm interval keeping all the

parameters (pinhole, contrast and brightness) constant. Image analyses were conducted on image z-stacks which contain the field of interest. Images were digitally converted to green (phospho-p38MAPK), or to red (OX-6 or GFAP) and digitally combined to obtain doublelabeled FITC/TR and then assembled into montages using Adobe Photoshop (Adobe Systems, Mountain View, CA, USA).

Immunofluiorescence staining for CD200, Calbindin, HMGB1

Free floating coronal sections (40 μm) were obtained using a vibratome, mounted on slides and air-dried. The tissues were then processed as described previously (Rosi et al., 2005). After washing in TBS solution the slides were incubated (4 °C) over night with either of the following primary antibody: HMGB1, CD200. Thereafter, the sections were incubated for 2h (22 °C) with the secondary antibody, followed by incubation with Avidin + Biotin amplification system (Vector) for 45 min. The staining was visualized using the TSA fluorescence system CY3 (Perkin-Elmer Life Sciences, Emeryville, CA). After washing in TBS solution, the tissues were quenched and blocked again and incubated with either of the following antibodies: OX6,NeuN, calbindin over night at 4 °C. Before applying the biotinylated secondary antibody rat absorbed antibody (Vector,) for 2h, the tissues were incubated with Avidin Biotin Blocking Kit (Vector,) for 30 min to block cross-reaction with the primary staining. Following treatment with an Avidin + Biotin amplification system (Vector), the staining was visualized with a TSA fluorescence system Cyanine 5 (CY5, Perkin-Elmer) and nuclei were counterstained with Sytox-Green (Molecular Probes, Eugene, OR). No staining was detected in the absence of the primary or secondary antibody.

3.12 Western Blot

Antibodies

The following antibodies were used: rabbit polyclonal anti-phospho (Thr202/Tyr204)-ERK1,2 antibody (1:1000), anti-phospho-(Thr180/Tyr182)-p38MAPK antibody (1:500), antiphospho-(Thr183/Tyr185)-JNK antibody (1:1000) which detect the activated forms of ERK1,2, p38MAPK and JNK, respectively (all from Cell Signaling Technology, Inc., Danvers, MA, USA). Total ERK was visualized using a rabbit polyclonal antibody raised against ERK1,2 protein (1:1000, Cell Signaling Technology, Inc., Danvers, MA, USA). HMGB1 was visualized using a polyclonal antibody (1:800; AbCam, Cambridge, MA). Actin was visualized with a rabbit polyclonal antibody (1:10,000; Sigma Chem Co., St. louis, MO, USA).

Western immunoblotting was carried out as previously described (Giovannini et al., 2001b). Rats were sacrificed and bilateral samples of hippocampus were dissected and transferred to ice-cold microcentrifuge tubes with lysis buffer, homogenized on ice (a Potter-Elvehjem homogenizer, 20 strokes, 1 stroke/s). The lysis buffer had the following composition (mM): 50 Tris–HCl, pH 7.5, 50 NaCl, 10 EGTA, 5 EDTA, 2 sodium pyrophosphate, 4-para-nitrophenylphosphate, 1-sodium orthovanadate, 1-phenylmethylsulfonyl fluoride, plus 20 μg/ml leupeptin and 30 ug/ml aprotinin and 0.1% SDS 10%. Immediately after homogenization protein concentration was determined (Bio-Rad, Hercules, CA). An appropriate volume of 2× loading buffer was added to the homogenates, and samples were boiled (@95 °C) for 5 min. Samples (65 μg of proteins per well) were loaded onto a 10% SDS-PAGE gel and resolved by standard electrophoresis. The proteins were then transferred electrophoretically onto nitrocellulose membrane (Hybond-C extra; Amersham, Arlington Heights, IL) using a

transfer tank kept at 4 °C, with typical parameters being O/N with a constant current of 12 mA. Membranes were blocked for 1 h at room temperature with blocking buffer (BB, 5% non-fat dry milk in TBS containing 0.05% Tween 20, TBS-T), then probed for 2 h at room temperature using the following primary antibodies: HMGB1, ERK1,2, JNK, p38MAPK. After washing in TBS-T (three washes, 15 min each), the membranes were incubated with horseradish peroxidase-conjugated anti-rabbit IgG for HMGB1 (Pierce, Rockford, Illinois, U.S.A, final dilution 1:7500) or with horseradish peroxidase-conjugated anti-mouse IgG (Pierce, Rockford, Illinois, U.S.A, final dilution 1:7500), or anti-rabbit IgG (Pierce, Rockford, Illinois, U.S.A, final dilution 1:7500) and proteins were visualized using chemiluminescence (Super vSignal West Pico Chemioluminescent Substrate, Pierce, Rockford, Illinois, U.S.A.). In order to normalize the values of the primary antibodies, we detected actin in the same analysis. Membranes were stripped by Restore Western Blot Stripping Buffer (Pierce) for 15 min at room temperature, blocked in blocking buffer for 1 h at room temperature and probed for 2 h at room temperature using antibodies for actin (Sigma Aldrich, final dilution 1:5000) and incubated in secondary antibody and developed as above. After development of the film, the bands were acquired as TIFF files, and the density of the bands was quantified by densitometric analysis performed using Un-Scan-It software for HMGB1 (Silk Scientific Corporation, Orem, UT). Or Scion Image for Windows (Scion Co., MD, USA) software for MAPKs. HMGB1 and phospho-MAPKs values were expressed as percentage of total actin run in the same Western blot analysis.

3.13 Slice preparation for *in vitro* carbachol (CCh) stimulation

CCh stimulated slices or control slices were used for Western blot analysis or for immunohistochemistry of phospho-ERK. Wt mice were anesthetized and decapitated and brains were rapidly removed and placed into oxygenated artificial cerebrospinal fluid (ACSF: D(+)-glucose monohydrate 9 mM, NaHCO3 24 mM, NaCl 125 mM, KCl 3,5 mM, NaH2PO4 1,25 mM, CaCl22H2O 1 mM, MgSO47H2O 1 mM), on ice. Brains were quickly glued to a vibratome block (Vibratome Series 1000, Sectioning System, Redding, CA, USA), placed in a chamber filled with ice-cold ACSF oxygenated with 95% O2/5%CO2 and 400 μm thick coronal slices were cut. Care was taken to maintain the temperature ACSF below 4 °C. Slices were incubated in a 24-well chamber, one per well, resting on a net submerged in oxygenated Krebs solution (NaCl 124 mM, KCl 3.3 mM, MgSO4 1.4 mM, CaCl2 2.5 mM, KH2PO4 1.25 mM, D(+)-glucose monohydrate 10 mM, NaHCO3 25 mM) and were allowed to equilibrate for at least 45 min at RT. After equilibration, control slices used for Western blot, were gently removed from the wells, placed on gelatin-coated slides, excess liquid aspirated and slices were quickly frozen on dry-ice. For immunohistochemistry, control slices were transferred in 24-wells plate, one per well, containing 1 ml of ice-cold 4% paraformaldehyde and fixed O/N.

The remaining slices (one per well) were placed in a bath at 35 °C in a solution containing 100 μM CCh and stimulated with the drug for 15 min. After incubation, slices were removed and frozen for WB or fixed for immunohistochemistry, as described above. Subsequently, slices used for Western blot, maintained on slides on dry ice, were dissected under a magnifying glass. The hippocampus was transferred into Eppendorff test tubes, kept at -80 °C until Western blot of phospho-ERK, as described. Slices used for immunohistochemistry were fixed in 4% paraformaldehyde overnight.

The day after, each slice was rinsed with PBS, glued on the Vibratome block and re sectioned into 40 μm-thick slices, which were then used for free-floating immunohistochemistry of phospho-ERK, as described. Quantitation of the effect was performed by counting the neurons blind in selected regions of the hippocampus. Care was taken to avoid thawing of the specimens.

3.14 Statistical analysis

Statistical comparison was performed using Student's t test, or one way ANOVA followed by Newman-Keuls multiple comparison test (if more than two groups were compared) or Dunnett multiple comparison test (when drug-treated groups were compared to the saline-treated group only). Significance was set at $P<0.05$.

4. RESULTS

4.1 STUDY OF NEURONAL CHANGES IN A MODEL OF LPS-INDUCED NEUROINFLAMMATION.

4.1.1 LPS induces activation of microglia.

Control rats, infused with aCSF, had few mildly activated microglia cells evenly scattered throughout the hippocampus including the DG (Fig. 8A,C), consistent with previous reports from our lab (Hauss-Wegrzyniak et al., 1998;Rosi et al., 2005;Rosi et al., 2006). Rats infused with LPS for only 1 week had only a few activated microglia cells (Fig. 8B) consistent with our previous findings that a full microglial response to LPS requires 10 to 14 days to develop (Willard et al., 1999; Marchalant et al., 2006). Infusion of LPS for 4 weeks significantly increased the number of activated microglia in the DG (Fig.8E,G, $P<0.05$) and CA3 (Fig. 8G, $P<0.05$), similar to previous reports from our lab (Hauss-Wegrzyniak et al., 1998;Rosi et al., 2005). Rats infused with LPS and then sacrificed 8 weeks after surgery, i.e. approximately 2 weeks after the cessation of the LPS infusion, also showed significantly (one way ANOVA Newman-Keuls post hoc test, $P<0.05$) increased number of activated microglia in the DG and CA3 regions of the hippocampus (Fig. 8D,G). The activated microglia showed bushy morphology with increased cell body size and contracted, and ramified processes, characteristic of cells in an activated state.

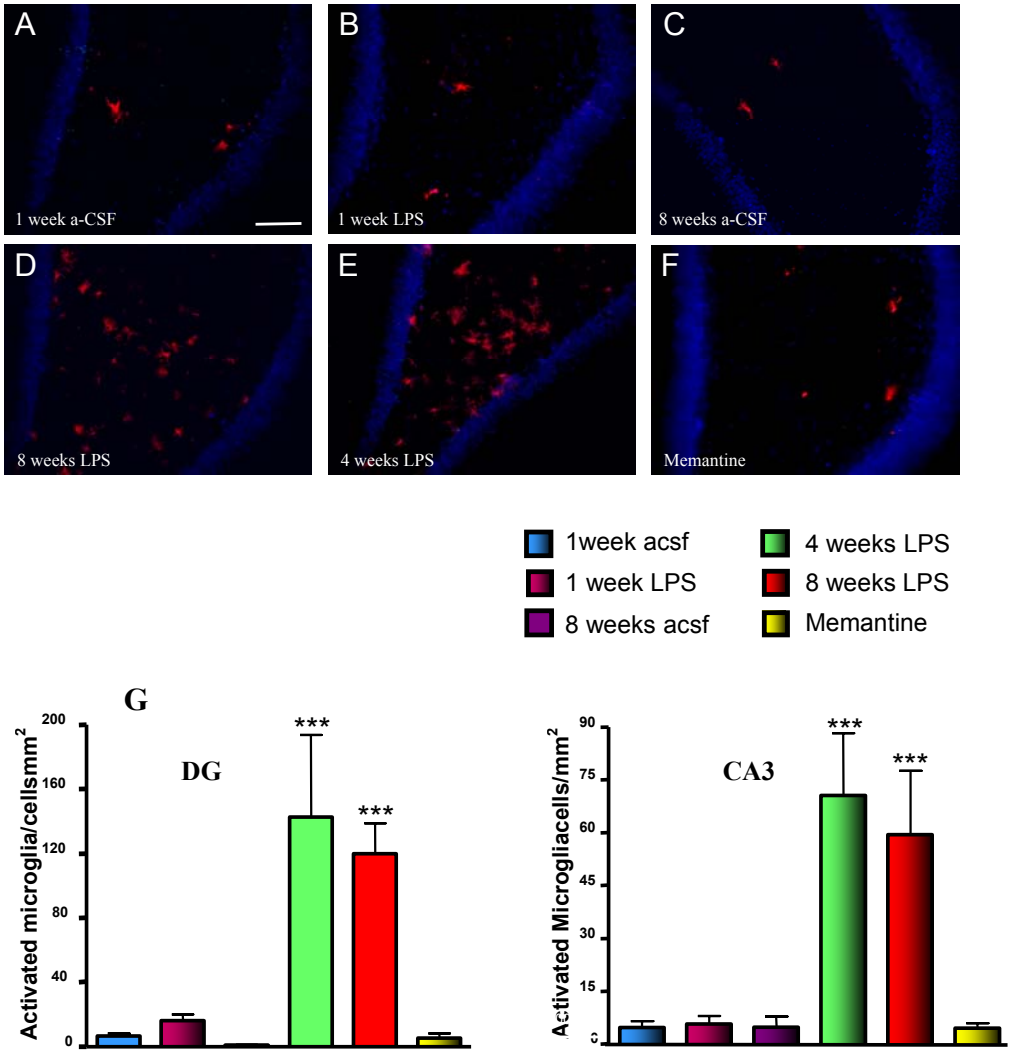

Fig.8 Immunoreactivity (IR) of activated microglia in the hippocampus. Note the increase of activated microglia cells (red) in the dentate gyrus of LPS infused animals. (A) OX6 IR (red) and nuclei (blue) of a 1 week a-CSF animal; (B) OX6 IR and nuceli of a 1 week LPS animal; (C) OX6 IR and nuclei of a 4 weeks LPS animal; (D) OX6 IR and nuclei of a 8 weeks a-CSF animal; (E) OX6 IR and nuclei of a 8 weeks LPS animal; (F) OX6 IR and nuclei of an LPS + memantine animal. Note the increase of activated microglia cells after 4 and 8 weeeks LPS treatment and their decrease to control values after 2 weeks of memantine (15mg/kg/d, s.c.) administration by osmotic minipump. Size bar=80µm. (G) Counts of OX-6 positive cells in the dentate gyrus (DG, *** $p<0.05$, one way ANOVA Newman-Keuls post hoc test) and CA3 of the hippocampus (*** $p<0.05$, one way ANOVA Newman-Keuls post hoc test); Means ± SD.

4.1.2 Memantine attenuates ongoing microglial activation

Chronic administration of the NMDA receptor antagonist memantine under the conditions used in the current study typically produces a serum concentration of ~1 μM within 3 days, an extracellular fluid concentration of 0.5-0.7 μM and a brain tissue concentration of 12-15 μM; free drug plasma levels are probably about 20-50% lower than this value due to protein binding, similar to the levels reached in humans at therapeutic doses of memantine (Rogawski and Wenk, 2003). In our experiments, the 2 weeks administration of memantine via an osmotic minipump produced a serum level of the drug of 0.77 ± 0.18 μM (n=7).

Rats that received memantine treatment for 2 weeks, initiated 2 weeks after the commencement of the LPS infusion, showed a significant reduction in the number of activated microglia cells within the DG (Fig 8F,G, $P<0.05$) and CA3 area. The activated microglia still present in the LPS-infused animals treated with memantine presented a morphology characteristic of a less advanced activation state.

4.1.3 LPS reduces CD200 expression

CD200 is a membrane glycoprotein, expressed by neurons, that binds to a structurally similar receptor that is expressed by microglia. The intercommunication between neurons and microglia through CD200 binding to its microglia receptor is believed to maintain microglia in a quiescent state (Hoek et al., 2000;Lyons et al., 2007;Frank et al., 2007).

Four weeks of LPS infusion (Fig. 9D,F) significantly reduced the number of cells expressing CD200 protein in the CA3 region of the hippocampus (one way ANOVA Newman-Keuls post hoc test, $P<0.05$). The number of cells with CD200 immunoreactivity

remained significantly reduced in the hippocampus of rats that were infused with LPS and sacrificed 8 weeks after surgery (Fig. 9B,F). No changes in the number of CD200-immunoreactive cells in the CA3 were found after only 1 week of LPS infusion (Fig. 9C,F) or after 1 or 8 weeks of aCSF infusion (Fig. 9A,B,F) into the 4^{th} ventricle. Administration of memantine for 2 weeks restored the number of CD200-immunoreactive cells to a level similar to that of aCSF treated control rats (Fig. 9E, F). The Western blot analysis of CD200 expression did not reveal a statistically significant (One way ANOVA, Newman-Keuls post hoc test, p=0.06) change in CD200 protein expression between groups (data not shown); the absence of statistical significance may be related to the fact that the entire hippocampus was used for this analysis, thus diluting and masking the effect that was present in the CA3 area only, according to the immunohistochemical results..

4.1.4 Persistent microglia activation depends on Ca^{2+} entry through NMDA receptors

We hypothesized that neuron-to-microglia communication influences microglia activation through NMDA receptors. Thus, neuronal NMDA receptor activation and the ensuing Ca^{2+} influx may be a key link in the ongoing maintenance of an inflammatory environment. We thus predicted that the LPS inflammatory response might increase Ca2+ influx through NMDA receptors and blocking this receptor channel, and thus reducing Ca^{2+} entry, would alter the intercommunication between neurons and microglia, therefore reducing the number of activated microglia cells caused by LPS infusion. Calbindin was used as an indicator of Ca^{2+} entry. Indeed, in rats infused with LPS for 4 weeks, CA3 hippocampal neurons showed increased immunoreactive

expression of cytoplasmic calbindin as compared to rats infused with aCSF (Fig. 10A,D). Blockade of NMDA receptors with memantine restored calbindin immunoreactivity to levels similar to those seen in rats infused with aCSF (Fig. 10G).

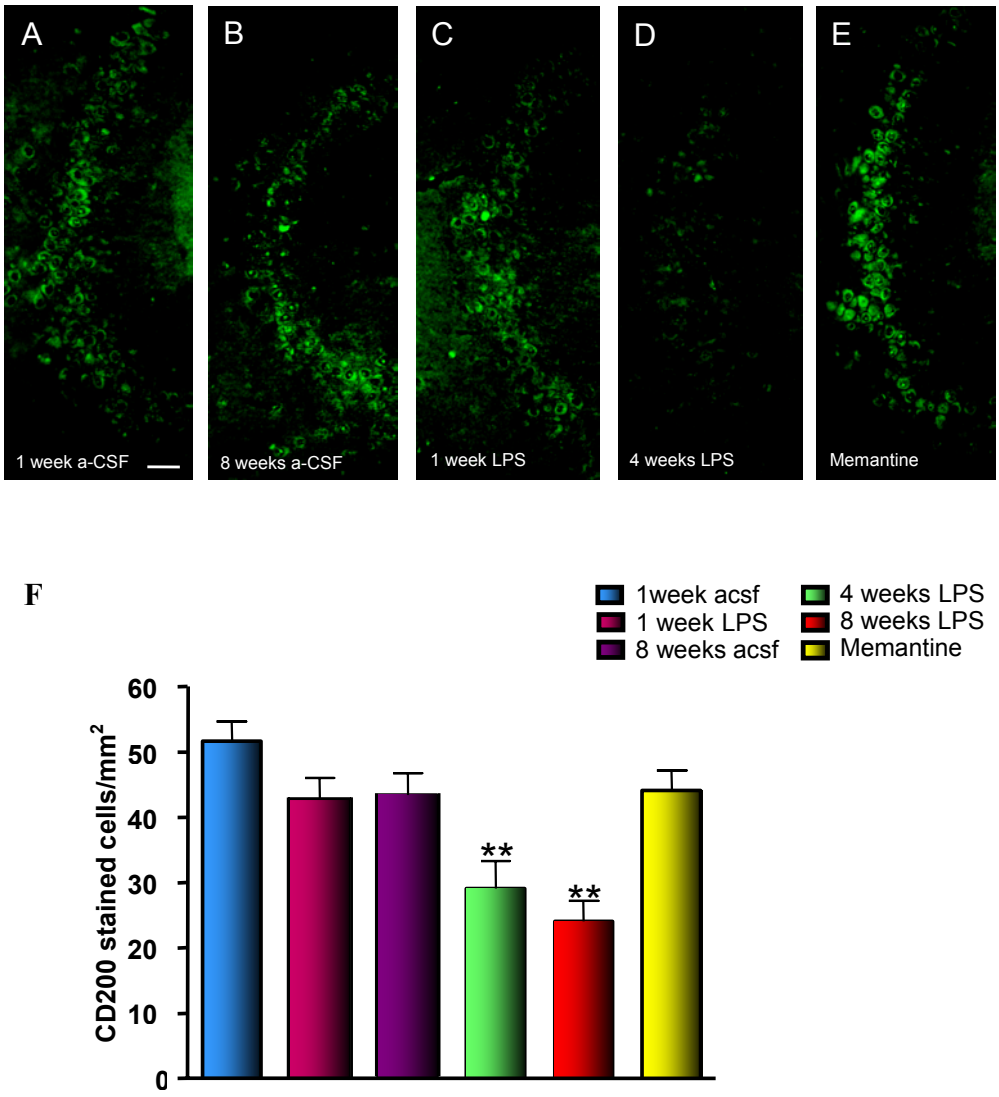

Fig. 9 Immunoreactivity (IR) of CD200 in the CA3 region of the hippocampus. Note the diminution of CD200 immunoreactive cells after 4 weeks of LPS exposure (D), and that memantine administration (15mg/kg/d, s.c.) (E) restored the number of CD200 immunoreactive cells to the same levels observed in a-CSF infused rats (A,B). No differences in CD200 immunoreactive cells were found in the 1-week LPS rats (C) as compared to a-CSF rats (A,B). Size bar=40μm. (F) Counts of the number of CD200 immunoreactive cells in the CA3 region defined by the region of hippocampus defined by the box in the diagram (**P<0.05, one way ANOVA Newman-Keuls post hoc test); Mean ± SD

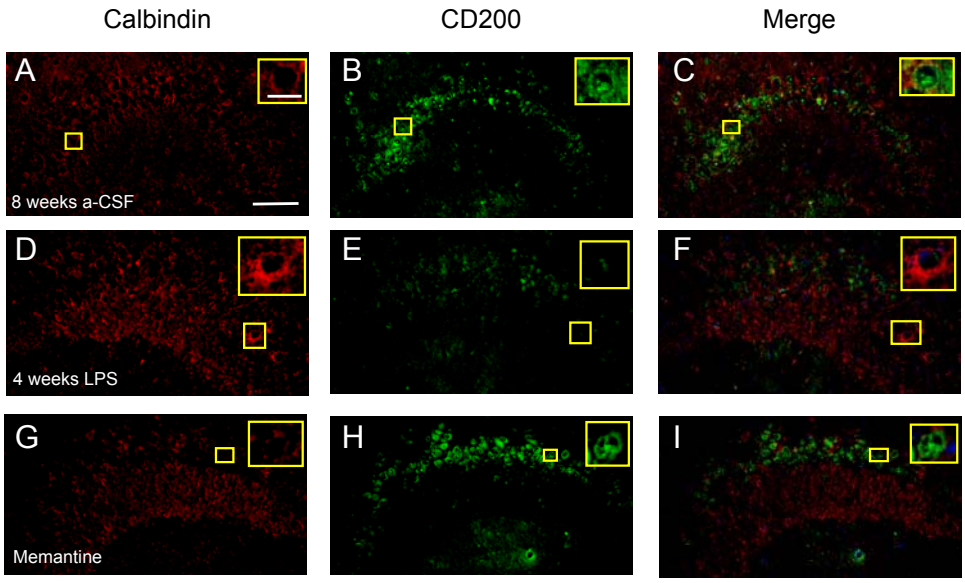

Fig. 10 Double immunofluorescence of CD200 and calbindin in the CA3 of the hippocampus. Calbindin distribution in the CA3 from an 8 weeks a-CSF rat (A), 4 weeks LPS rat (D) and LPS+memantine rat (G). The inserts show single calbindin immunoreactive neurons (size bar 13μm). Note the increased immunoreactivity in the 4 weeks LPS rat as compared to the 8 weeks a-CSF rat and LPS+memantine rat. For comparison, the images of CD 200 distribution from an 8 weeks a-CSF rat (B), 4 weeks LPS rat (E) and LPS+memantine rat (H) are merged (C,F,I) merged from the same rats. In the 4 weeks LPS rat neurons that have more calbindin have less CD200 staining as compared to the other two groups. Size bar=80μm

4.1.5 Expression of microglial quiescence signalling molecule CD200 is modulated by Ca^{2+}-dependent processes

Double-immunofluorescence studies revealed that cytoplasmic calbindin levels were inversely related to CD200 expression within the same neurons. Rats infused with LPS for 4 weeks exhibited elevated calbindin expression and greatly reduced CD200 expression (Fig. 10 D,E,F), as compared to control rats infused with aCSF (Fig. 10 A,B,C). Blockade of NMDA receptors by memantine in rats infused with LPS restored cytoplasmic calbindin and CD200 immunoreactivity to control levels (Fig 10 G,H,I).

4.1.6 HMGB1 expression is unaltered by chronic neuroinflammation

HMGB1 is a non-histone DNA-binding protein that has a pro-inflammatory cytokine-like function that may influence the activation of microglia following injury or insult (Kim et al., 2006). It has been demonstrated that HMGB1 levels are low in resting glia but are increased in the brains of patients with Alzheimer's disease (Takata et al., 2004). Extracellular HMGB1 has also been described as a mediator of lipopolysaccharide (LPS) toxicity (Ulloa & Messmer, 2006).

We investigated whether extracellular HMGB1 mediates LPS toxicity or whether its expression paralleled changes in CD200 expression or microglial activation within the hippocampus. Double-immunofluorescence staining for HMGB1 (Fig. 11A) confirmed previous reports that HMGB1 is contained within the nucleus of neurons (Guazzi et al. 2003; Scaffidi et al., 2002); we observed no evidence for extracellular HMGB1 in the presence of chronic brain inflammation produced by 4 weeks LPS. Histological and Western blot analyses found no significant differences in hippocampal HMGB1 protein levels among treatments (Fig. 11B).

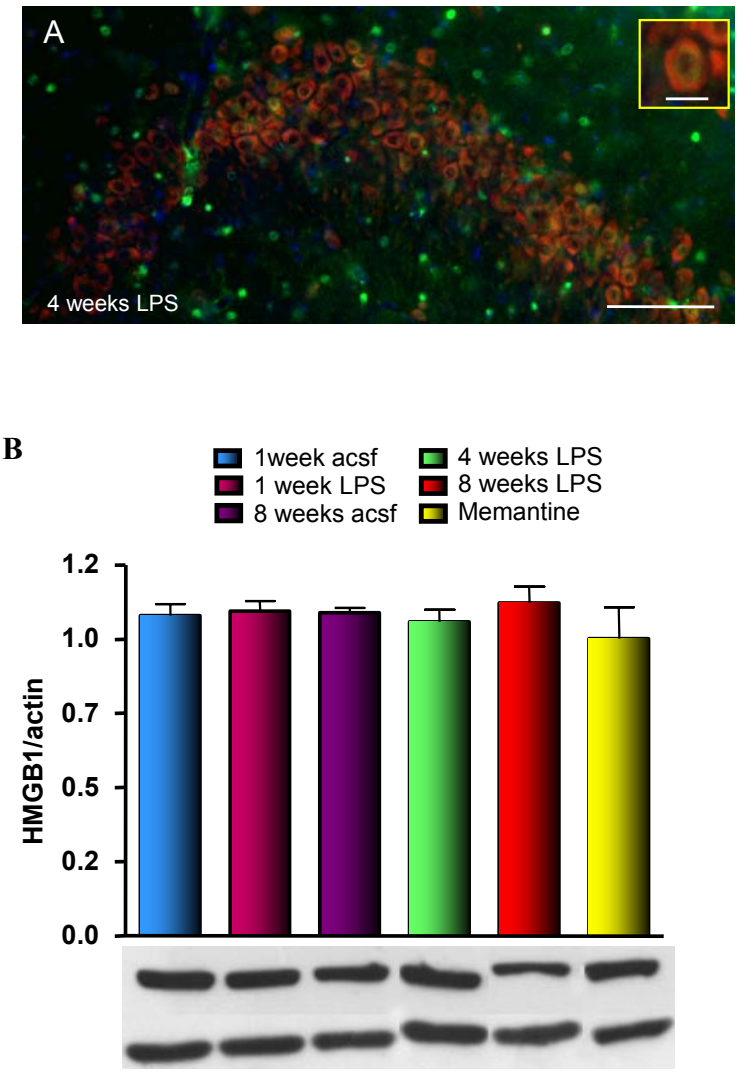

Fig. 11 HMGB1 colocalizes with neurons but its expression does not change among the different treatment groups. (A) Double immunofluorescence of HMGB1 (green) and NeuN (red), nuclei are counterstained in blue (magnification 200X). Size bar=80μm. The insert shows single HMGB1 immunoreactive neurons (size bar 13μm). (B) Densitometric ratio of HMGB1 and actin ± SD of the immunoblotting of HMGB1. No differences of HMGB1 expression among groups.

4.2 STUDY OF CELLULAR CHANGES IN AGED RATS COMPARED TO YOUNG RATS.

4.2.1 Latencies in the step down inhibitory avoidance task

In order to evaluate memory deficits in a model of natural aging, we performed the step down inhibitory avoidance in old rats (24 months) compared to young rats (3 months).

As shown in Fig. 13, recall latencies in a step down inhibitory avoidance are decreased in old rats compared to young rats (one way ANOVA and Newman-Keuls multiple comparison test, **P<0.01).

4.2.2 ERK activation in hippocampal slices of old rats

In a previous paper published by our laboratory in 2005 (Giovannini et al., 2005), we demonstrated that the treatment of young rats with the MEK1 inhibitors PD98059 and U0126, 30 min before the step down inhibitory avoidance acquisition task, brings about impairments in memory encoding, as demonstrated by the decrease of recall latency. This result correlates with an involvement of ERK pathway in memory encoding. Moreover, in the paper we demonstrated that ACh, acting through muscarinic receptors, activated the cascade that leads to ERK phosphorylation (Fig. 12).

In order to evaluate activation of ERK in hippocampal slices of old rats, we performed immunhistochemistry with a selective anti-phospho-ERK antibody in hippocampal slices from old rats compared to young rats. Phospho-ERK–positive neurons were counted in the CA1 area of aged and young rats. As shown in Fig. 14, while a significant increase of activated ERK was present in CA1 of young rats 10 min after acquisition, no difference was observed in the aged animals. (one way ANOVA and

Newman-Keuls multiple comparison test, *P<0.05). This results indicates that in aged animals that do not acquire the step down inhibitory avoidance task, no activation of ERK is visible in the CA1 region of the hippocampus, thus posing further basis to the hypothesis of the involvement of ERK in this type of memory.

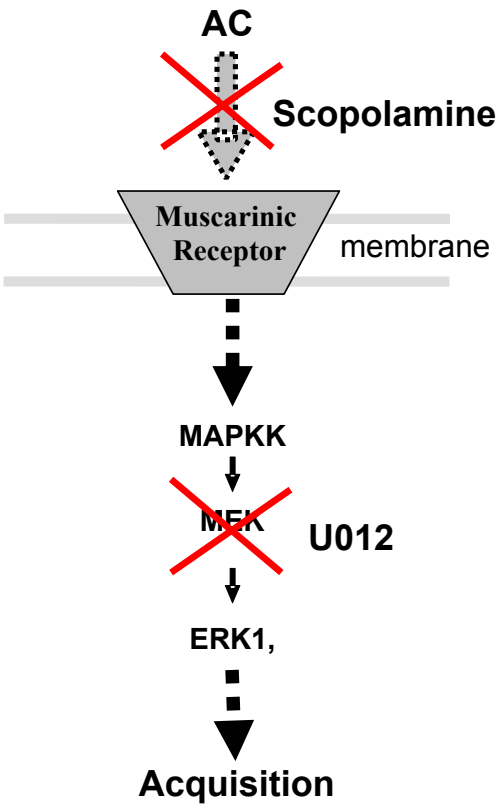

Fig. 12 Schematic representation of the proposed mechanism fo encoding of the step-down inhibitory avoidance memory.

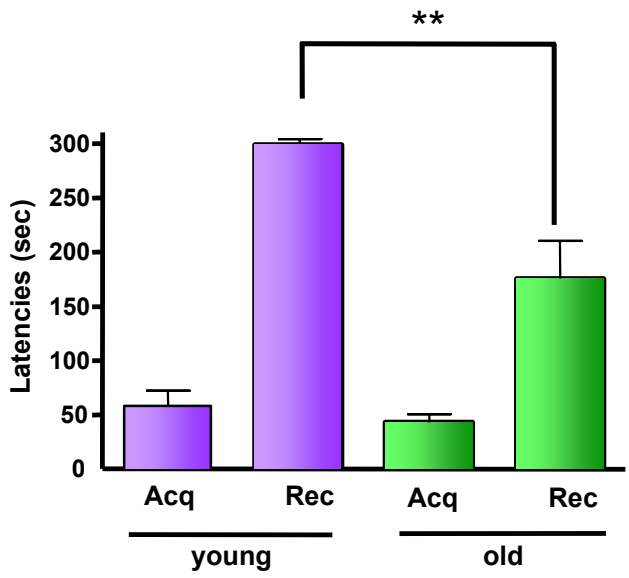

Fig. 13 Latencies in a step down inhibitory avoidance task. Note the decreased recall latencies in a step down inhibitory avoidance of old rats compared to young rats (**P< 0.01, one way ANOVA and Newman-Keuls post hoc test).

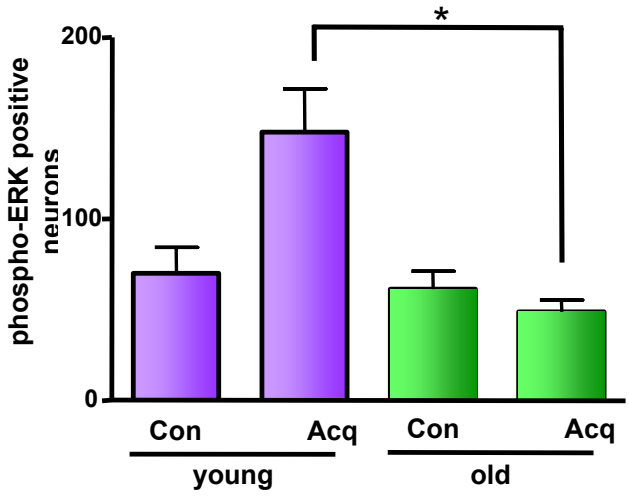

Fig. 14 ERK activation in old and young rats after acquisition in a step down inhibitory avoidance task. While in young rats, 10 min after acquisition, we found a significant increase of activated ERK in pyramidal neurons of CA1 region, in old rats no difference of phospho ERK positive neuronsin CA1 was found. Indee, the number of phospho-ERK positive neurons in the CA1 region of the aged rats 10 min after acquisition were significantly lower than in young rats(*P<0.05, one way ANOVA Newman-Keuls post hoc test).

4.2.3 JNK and p38MAPK activation in hippocampal slices of old rats

We investigated the activation of the other MAPKs, JNK and p38MAPK in the hippocampus of aged rats, in comparison to young animals using selective antibodies for the phosphorylated form of the enzymes. As shown in Fig. 15, no differences of JNK activation in the three regions of the hippocampus between old (Fig. 15B) and young rats (Fig. 15A) were observed. On the contrary, marked differencesof p38MAPK activation in CA3, CA1 and DG of old rats compared to young rats were found. As shown qualitatively by immunohistochemistry in Fig. 16, old rats (Fig. 16B) presented an increased number of phospho p38MAPK positive cells in all three regions of the hippocampus compared to the young rats (Fig.16A). The bar graphs of Fig. 16 show the quantitative analysis of phospho p38MAPK positive neurons in CA3 (Fig. 16 panel A), CA1 (Fig. 16 panel B) and DG (Fig. 16 panel C) of old and young rats. As shown in the figure, we found statistically significant differences in the number of phospho p38MAPK positive neurons in the three region of the old rats hippocampus, as compared to the young rats hippocampus (Student's t-test, *P<0.05; **P<0,01, ***P<0,001).

4.2.4 Evaluation of neuroinflammatory markers in the hippocampus of old and young rats

As previously shown in the model of LPS-induced neuroinflammation, young rats infused with LPS show an increase of the number of activated microglia, particularly in CA3 and DG of the hippocampus. Thus, we looked at activated microglia and other neuroinflammatory markers in old rats to verify whether a form of neuroinflammation might also be present in the old rats model. Fig. 17 shows representative images of

iNOS immunohistochemistry in CA3 of young (Fig. 17A) and old rats (Fig. 17B) hippocampus. It appears in the images that old rats have more iNOS positive cells as compared to young rats. And indeed, quantitative analysis in Fig. 17C shows that iNOS positive cells are significantly more numerous in CA3 area of old rats, compared to young rats (Student's t-test, **P<0.01).

Since astrocytes and microglia are part of CNS immune system, and are thus involved in neuroinflammatory mechanisms, we looked at their activation using GFAP and OX6 antibodies, respectively.

GFAP (Glial Fibrillary Acidic Protein) is a protein specifically expressed by astrocytes, GFAP immunostaining of astrocytes is shown in Fig. 18A-H. A difference in the number and morphology of GFAP positive cells between young and old rats is evident in DG (Fig. 18C,F) CA3 (Fig. 18D,G) and CA1 (Fig. 18E,H) regions of the hippocampus. Indeed, in the three regions of the hippocampus of old rats we found that the number of GFAP immunopositive cells was significantly less (Fig 18F,G,H) as compared to young rats (Fig. 18C,D,E). In Fig. 10I the quantitative counting of GFAP positive cells in the three regions of the hippocampus is presented. The bar graph shows a statistically significant decrease of GFAP positive cells in CA3, DG and CA1 of old rats compared to youg rats (** p<0.001, two way ANOVA and Bonferroni post hoc test). Furthermore, images taken at higher magnification (20X) show that old rats astrocytes have a smaller cell body and shorter and thinner branchings, compared to young rats astrocytes that have densely arborized cell bodies, a phenotype typical of activated astrocytes (Fig. 19A,B).

OX6 antibody is a selective antibody that binds to the MHCII complex expressed by activate microglia and it is thus used tovisualize activated microglia. Fig. 20 shows the immunohistochemistry of activated microglia in the DG of young (Fig. 20A) and old

(Fig. 20B) rats. As shown in the figure, old rats present an increased number of activated microglia in DG as compared to young rats. The quantitative counting of OX6 positive cells (Fig. 20C) indicate a statistically significant increment of activated microglia in CA3, DG and CA1 of old rats compared to young rats (One way ANOVA and Bonferroni post hoc test, **P<0.001). As shown in the graph, the number of activated microglia cells in CA1 is lower compared to CA3 and DG, as previously shown in the LPS-induced neuroinflammation model.

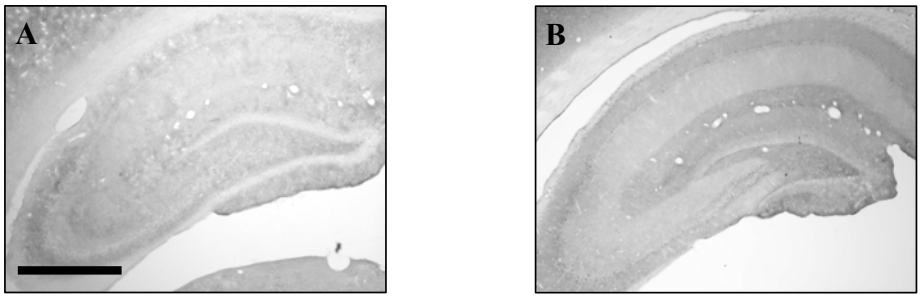

Fig. 15 Immunoreactivity of phospho JNK in the hippocampus of young rats (A) and old rats (B). No differences between the two groups were observed. Size bar=500µm

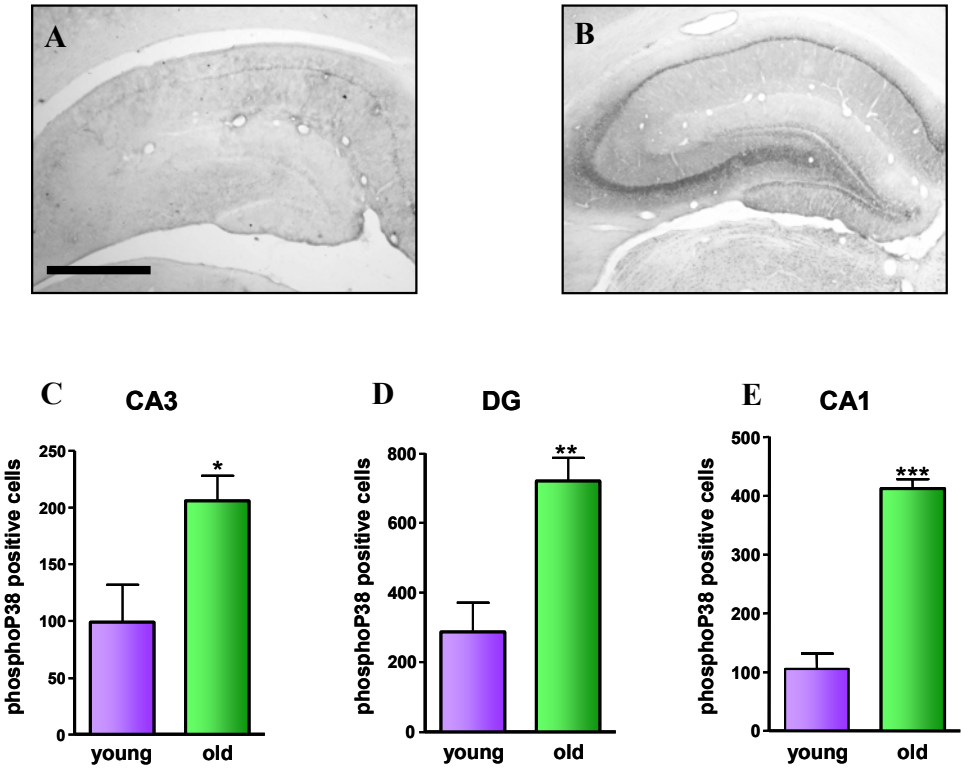

Fig. 16 Immunoreactivity of phospho p38MAPK in hippocampal slices of young (A) and old (B) rats. Note the increased number of phospho p38MAPK positive cells in old rats as compared to young rats in the three regions of the hippocampus.Size bar=500µm. (C,D,E) Phospho p38MAPK positive cells in CA3 (C,*P< 0,05, Student's t-test), DG (D,** p<0.001 Student's t-tes) and CA1 of the hippocampus of old and young rats, Mean ± SEM. The number of p38MAPK positive cells is significantly increased in the three region of the hippocampus of old rats as compared to the same areas of the young rats (E, *** p<0.001, Student's t-test).

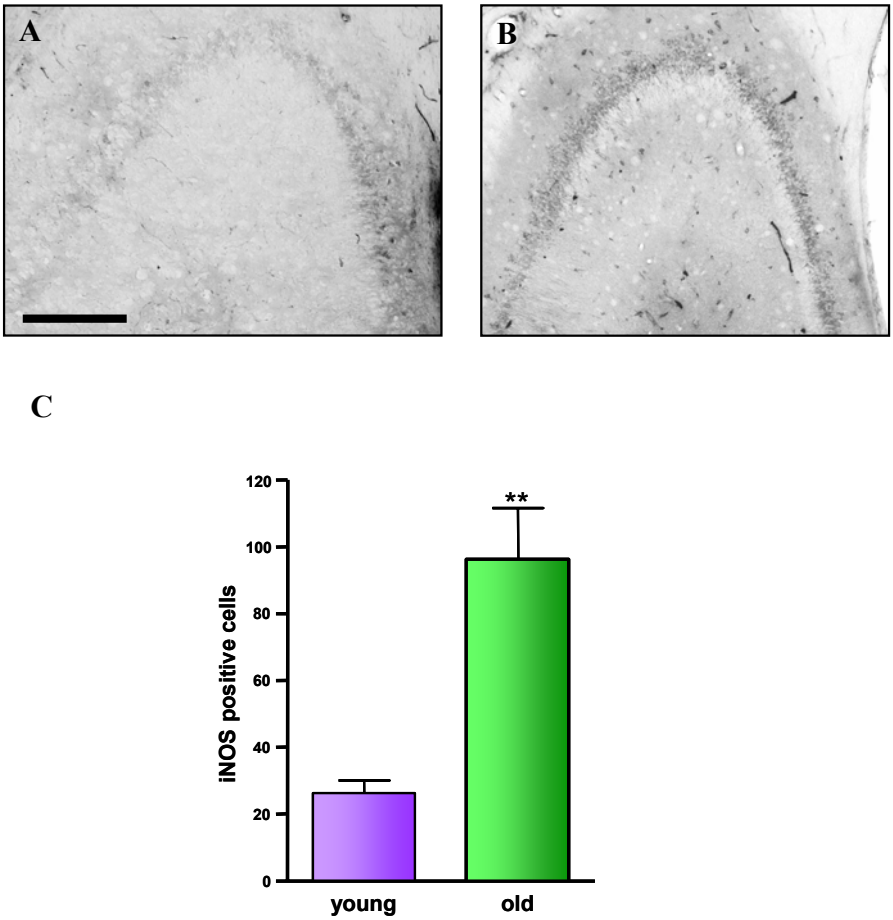

Fig. 17 Immunoreactivity of iNOS in hippocampal slices of young (A) and old (B) rats. Note the increased number of iNOS positive cells in the CA3 of the old rats hippocampus as compared to the young rats. Size bar=400μm. (C) Counting of iNOS positive cells in CA3 of the hippocampus of old and young rats (** $p<0.01$, Student's t-test); Mean ± SEM

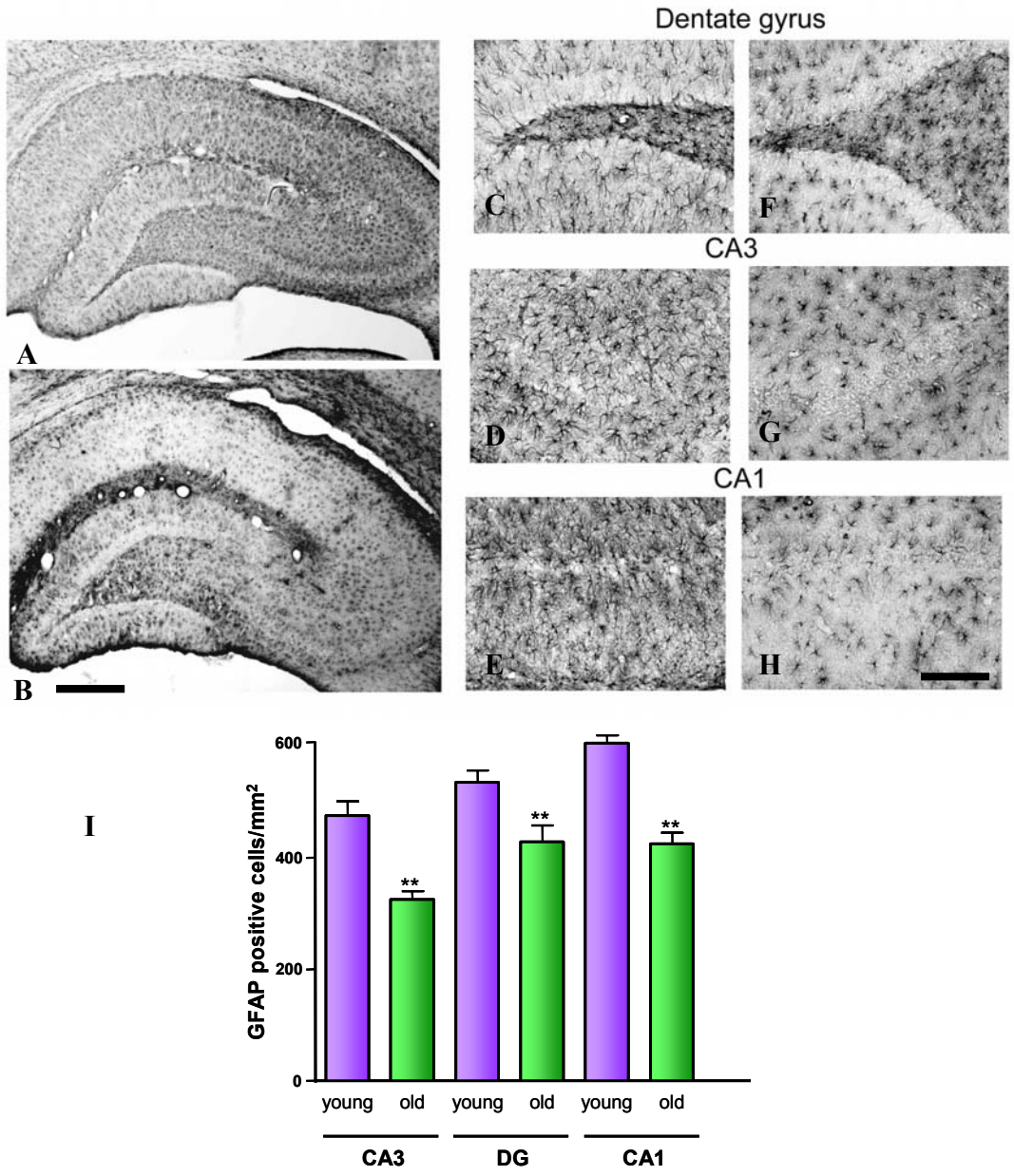

Fig. 18 Immunoreactivity of GFAP in hippocampal slices of young (A) and old (B) rats. Note the different density and morphology of GFAP positive cells in dentate gyrus (DG), CA3 and CA1 (F, G, H) of the old rats as compared to the same areas of young rats (C, D, E). Size bar=500µm for A,B; size bar=125µm for C, D, E, F, G, H,. (I) Counting of GFAP positive cells in CA3, DG and CA1 of the hippocampus of old and young rats, Mean ± SEM. The density of GFAP positive cells in the three areas of the hippocampus of old rats is significantly decreased as compared to the same areas of young rats (** $p<0.001$,two way ANOVA and Bonferroni post hoc test).

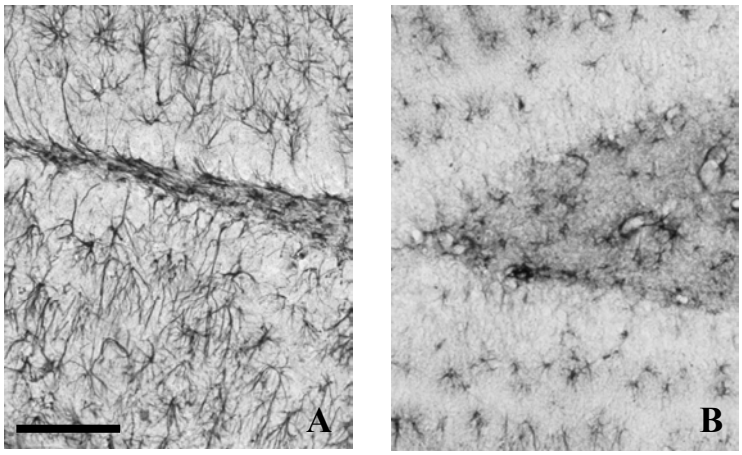

Fig. 19 Immunoreactivity of GFAP in hippocampal slices of young (A) and old (B) rats. Note the different density and morphology of GFAP positive cells in dentate gyrus of the old rats (B) compared to the same area of young rats (A). Size bar=100μm.

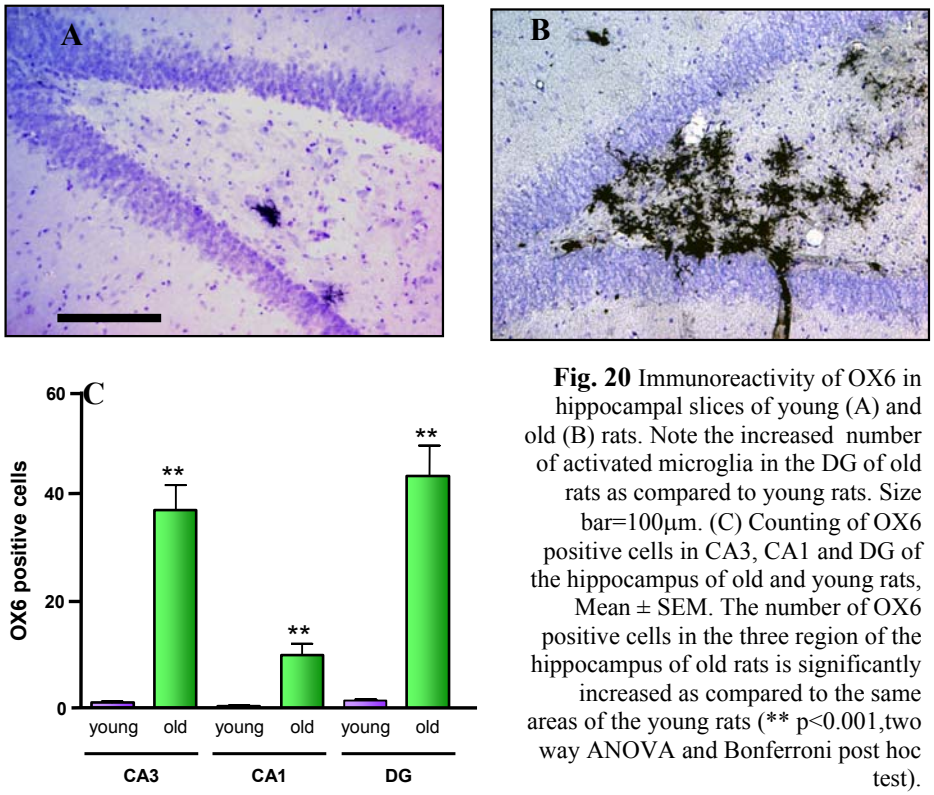

Fig. 20 Immunoreactivity of OX6 in hippocampal slices of young (A) and old (B) rats. Note the increased number of activated microglia in the DG of old rats as compared to young rats. Size bar=100μm. (C) Counting of OX6 positive cells in CA3, CA1 and DG of the hippocampus of old and young rats, Mean ± SEM. The number of OX6 positive cells in the three region of the hippocampus of old rats is significantly increased as compared to the same areas of the young rats (** $p<0.001$,two way ANOVA and Bonferroni post hoc test).

4.3 DIFFERENT ACTIVATION OF MITOGEN-ACTIVATED PROTEIN KINASE PATHWAY IN THE TgCRND8 TRANSEGNIC MOUSE MODEL OF ALZHEIMER DISEASE.

4.3.1 Activation of p38MAPK in the hippocampus of TgCRND8 mice

As reported in previous paper (Bellucci et al., 2006, 2007), TgCRND8 mice at 7 months of age show the presence of numerous β-amyloid deposit in the hippocampus and other brain areas, as well as astrocytes and microglia activation, inflammatory markers, nitrosative stress, neuronal damage hyperphosphorylated tau, cholinergic dysfunction and impairment in learning and memory functions. Therefore, we decided to look at the intracellular pathways that might be switched on/off in the hippocampus of the Tg mouse compared to wild type (Wt) littermates. Three major protein kinase pathways have been demonstrated to be responsive to environmental stress, inflammatory stimuli or other insults: ERK1,2, p38MAPK and JNK.

Immunohistochemistry showed higher activation of P38MAPK in cells distributed in the hippocampus of the Tg (Fig. 21A,C) than of Wt mouse (Fig. 21B,D). In particular, phospho-p38MAPK immunopositive cells were located mainly in the pyramidal layer of the CA1, in the stratus radiatum, in the stratum lacunosum molecularis and to a less extent in the dentate gyrus (DG) (Fig. 21C).

Quantification of p38MAPK activation was performed by Western blot (WB) analysis of homogenates of the entire hippocampus. In Fig. 21E WB analysis of the hippocampus of Tg and Wt mice shows one single major band at an apparent molecular weight of 38 kDa. The quantitative analysis was performed comparing the immunopositive bands of phospho-p38MAPK with that of actin run on the same gel and

the results are shown in Fig 21F. Data presented in Fig 21F show that the levels of phospho-p38MAPK in Tg mouse hippocampus were two fold higher than in Wt littermates and the increase was statistically significant (*P<0.05, Student's t-test).

Images taken at higher magnification show that activated p38MAPK was present in different cell types in the hippocampus of Tg mice. Both neurons and glia were positive for phospho-p38MAPK. Indeed, phospho-p38MAPK immunoreactivity was present in the nuclei of CA1 pyramidal cells (Fig. 22A-E, open arrows) as shown by DAB staining (A,B) and fluorescence staining revealed by double labelling confocal microscopy (C-E, z-stacks reconstructed images of a single cell by confocal laser microscopy; red labelling NeuN; green labelling phospho-p38MAPK). Fig 22A and B shows that phospho-p38MAPK immunopositive CA1 pyramidal neurons were localized in the vicinity of amyloid plaques (evidenced by the asterisks). Furthermore, the parenchyma surrounding the amyloid plaques was also characterized by infiltration of numerous, hypertrophic phospho-p38MAPK immunopositive cells (Fig. 22A, B, F black arrows) with densely arborized cell bodies with a phenotype typical of activated astrocytes. Amyloid plaques induced massive activation of astrocytes (Fig. 22G, white arrows), visualized by the immunoreactivity for the specific marker GFAP (red), as well as transformation of astrocytes from a resting to an activated state, highlighted by phenotypic changes characterized by cell hypertrophy and long, thick branchings (Fig 22G, I, white arrows). From their shape and position in the surroundings of the amyloid plaques, it appeared that these phospho-p38MAPK immunopositive cells in the hippocampus of Tg mice were activated astrocytes, as also demonstrated by colocalization of phospho-p38MAPK immunoreactivity in GFAP-positive cells by confocal laser microscopy (green labelling phospho-p38MAPK, red labelling GFAP).

Activated microglia cells immunopositive for the MHC type II, with round-shape appearance (Fig. 23A, black staining, arrows), infiltrated the amyloid plaques, (evidenced in Fig. 23A by staining with an antibody raised against β-amyloid(1-42), brown-red staining, red arrows). Furthermore, phospho-p38MAPK positive cells with round cell bodies and intensely stained short processes and "bushy" appearance were present in the stratum radiatum of Tg mice, not only infiltrating the Aβ plaques (Fig. 23B, white arrows) but also in the parenchyma distant from the plaques (Fig. 23C, E, black arrow). Phospho-p38MAPK positive cells were also present in the stratum radiatum of Wt mice but had smaller cell bodies and thinner processes (Fig 23D, I), indicative of lower state of activation From their shape the phospho-p38MAPK positive cells present in Tg mice hippocampus resembled activated microglia. Indeed, double-labeled confocal microscopy for phospho-p38MAPK (Fig. 23F) and MHCII complex (Fig. 23G) showed colocalization of the staining (Fig. 23H, z-stacks reconstructed images of a single cell by confocal laser microscopy; the yellow-orange colour is indicative for colocalization), demonstrating that the phospho-p38MAPK positive cells are microglial cells in an activated state.

4.3.2 JNK activation in the hippocampus of TgCRND8 mice.

As shown in Fig. 24B no staining for phospho-JNK was found in the hippocampus of Wt mice at the age of 7 months. However, several phospho-JNK immunopositive, round-shaped cells surrounded the plaques in the hippocampus of Tg mice, as shown in the insert of Fig 24A. Double-labeled immunohistochemistry for phospho-JNK (Fig. 24C, blue-gray) and MHC class II complex (Fig. 24C, brown-red) showed

colocalization of phospho-JNK in most, but not all, activated microglial cells around plaques.

Quantitation of JNK activation was performed by Western blot analysis in homogenates of the hippocampus. As shown in Fig 24D, a typical WB analysis of the hippocampus of Tg and Wt mice with the primary antibody raised against phopsho-JNK, shows only two major bands at an apparent molecular weight of 46 kDa and 54 kDa. The quantitative analysis was performed separated on the two bands of phospho-JNK which were compared with actin run on the same gel. The results are shown in Fig. 24E. Data presented in the figure show that in the homogenates of Tg mouse hippocampus the activation of phospho-JNK significantly increased in comparison to Wt littermates (*$P<0.05$, Student's t-test).

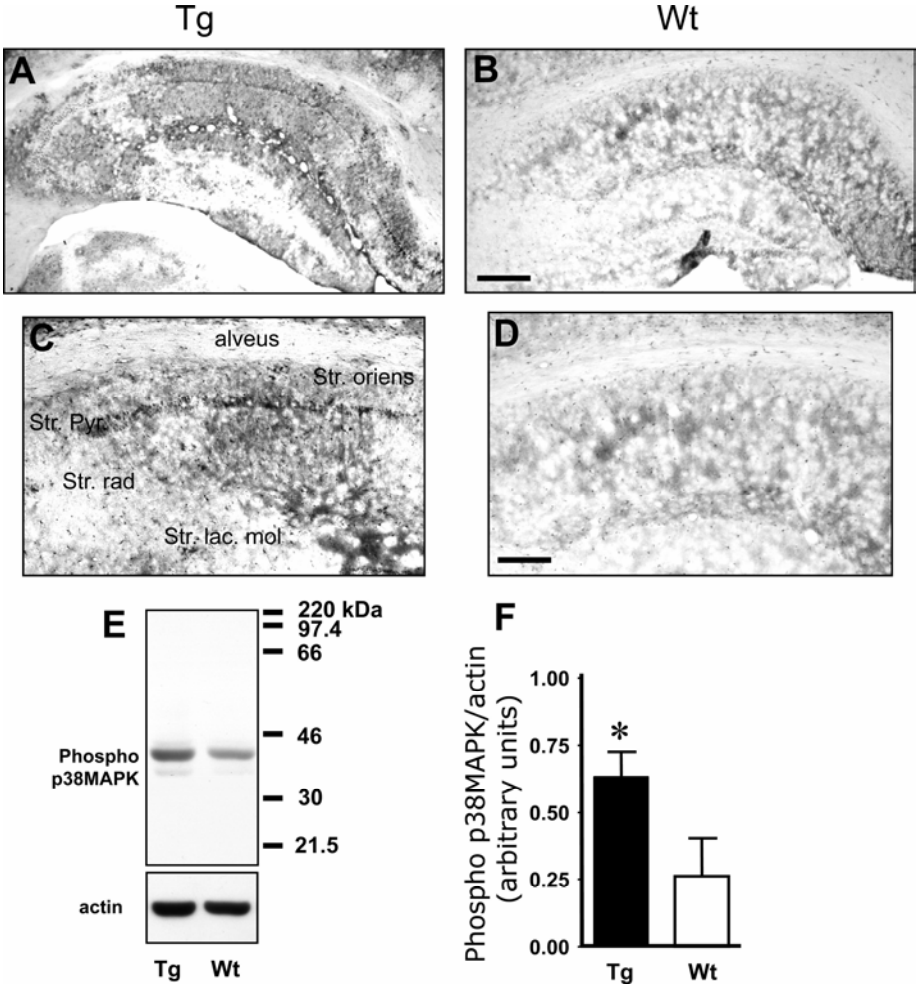

Fig. 21 Activation of p38MAPK in the hippocampus of TgCRND8 and Wt mice. Activation of p38MAPK was visualized using a specific antibody for its phosphorylated form and DAB staining followed by light microscopy. (A–C) Immunohistochemical staining of activated p38MAPK in the hippocampus of TgCRND8 (A, C) and Wt (B, D) mice. Note the phospho p38MAPK-positive cells in all the subregions of the hippocampus. Selected photographs (A, C and B, D) were shot from stained slices taken from different mice. The figure shows representative photomicrographs obtained from three to six independent experiments. Scale bars=250 μm A, B; C, D: 125 μm. (E) Representative Western blot analysis of phospho-p38MAPK on homogenates of the entire hippocampus of Tg and Wt mice. One major band at an apparent molecular weight of 38 kDa is present. Western blot analysis of actin, performed on the same gel, is shown for comparison. (F) Quantitative analysis of activated p38MAPK performed comparing the immunopositive band of phospho-p38MAPK with that of actin run on the same gel. The levels of phospho-p38MAPK in TgCRND8 hippocampus were significantly higher than in Wt (* $P<0.05$, Student's *t*-test). Tg: $n=8$; Wt: $n=6$.

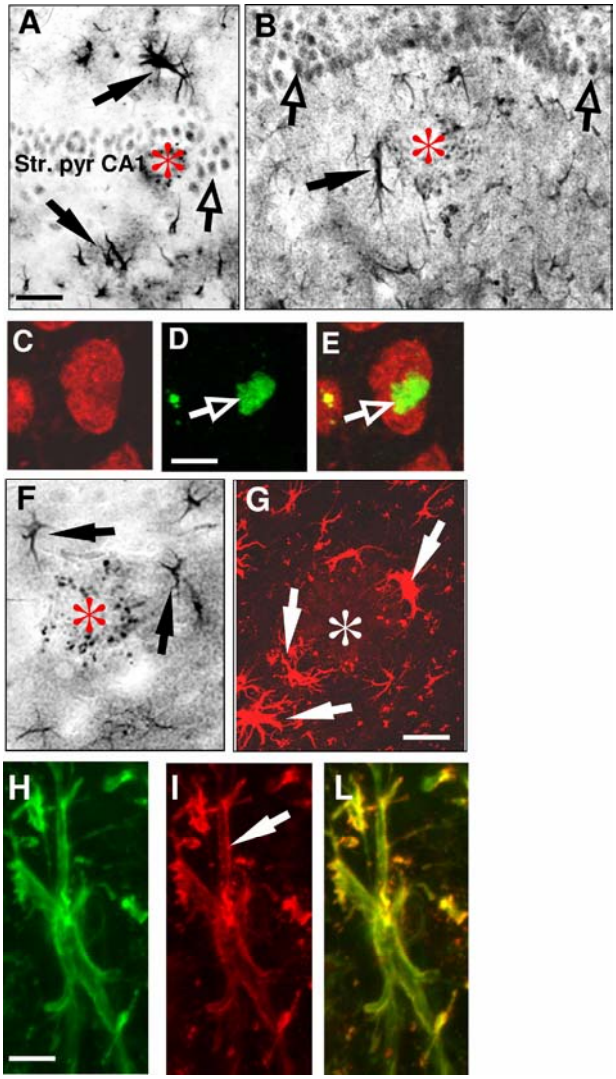

Fig. 22 Phospho-p38MAPK colocalizes in neurons and astrocytes in the hippocampus of TgCRND8 mice. All images were obtained from 40 μm-thick coronal slices of the hippocampus of Tg mice and show representative photomicrographs obtained from three independent experiments. (A, B, F) Immunohistochemical staining of activated p38MAPK in the hippocampus of Tg mouse visualized using a specific antibody for its phosphorylated form and DAB staining followed by light microscopy. Scale bar=50 μm. (C–E) Double-labeled confocal microscopy images obtained from CA1 pyramidal cell layer of TgCRND8 mouse labeled using antibodies anti-phospho-p38MAPK and anti-NeuN for neurons. NeuN labeling is indicated by red (C, E), phospho-p38MAPK labeling is indicated by green (D, E), and combined labeling is indicated by yellow–orange (E). The images were obtained stacking 15 z-step scans (1.5 μm depth each) acquired using a ×60 objective. Images were then flattened on one plane, and

converted into false colors. Scale bar=10 μm. The digitally combined image (E) shows that phospho-p38MAPK is localized in CA1 pyramidal cells and translocates to the nuclear region. G: astrocytes, labeled using the anti-GFAP antibody, in the surroundings of an amyoloid plaque (asterisk) in the hippocampus of TgCRND8 mice. Scale bar=50 μm. (H, I, L) Double-labeled confocal microscopy images obtained from hippocampal slices of TgCRND8 mice labeled using antibodies specific for phospho-p38MAPK and astrocytes. Activated astrocytes labeling is indicated by red (I, L), phospho-p38MAPK labeling is indicated by green (H, L), and combined labeling is indicated by yellow–orange (L). The images were obtained stacking 15 z-step scans (1.5 μm depth each) acquired using a ×60 objective. Images were then flattened on one plane, and converted into false colors. Scale bar=10 μm. The digitally combined image (L) shows that phospho-p38MAPK colocalizes in astrocytes where it is not localized solely to the nucleus.

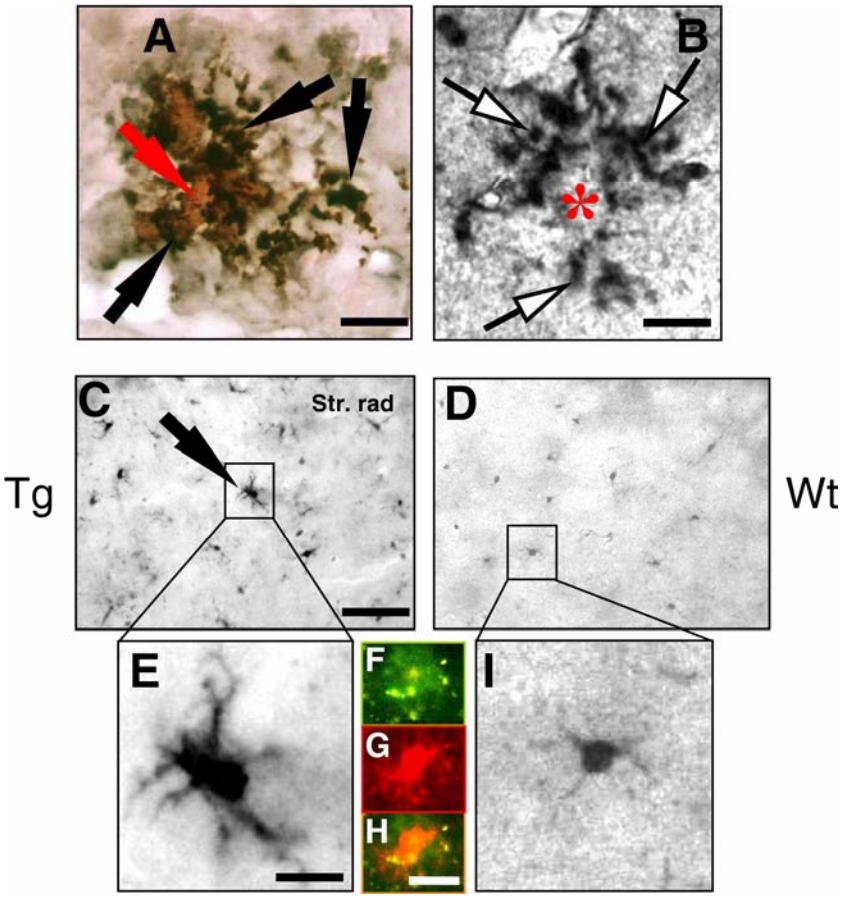

Fig. 23 Phospho-p38MAPK colocalizes in activated microglia in the hippocampus of TgCRND8 mice. All images were obtained from 40 μm-thick coronal slices of the stratum radiatum of Tg mice and show representative photomicrographs obtained from three independent experiments. (A) Double staining of activated microglia cells (labeled with antibodies against the MHC type II, black staining, arrows), and amyloid plaques (labeled with an antibody raised against β-amyloid(1–42), brown–red staining, red arrow). Activated

microglia cells infiltrated the amyloid plaques. Scale bar=25 μm. (B–E, I) Immunostaining of phospho-p38MAPK positive cells (B, white arrows) infiltrating the Abeta plaque (B, asterisk), and in the parenchyma distant from the plaques (C, E, black arrow). Phospho-p38MAPK positive cells were also present in the stratum radiatum of Wt mice (D) but were smaller and had thinner processes (I). Scale bars=25 μm B; C, D, 50 μm; E, I: 10 μm. (F–H) Double labeling confocal microscopy immunohistochemistry of phospho-p38MAPK (F, green labeling) and MHC type II (G, red labeling); z-stacks reconstructed images of a single cell in the hippocampus of TgCRND8 mice; combined labeling is indicated by yellow–orange (H). The images were obtained stacking 15 z-step scans (1.5 μm depth each) acquired using a ×60 objective. Images were then flattened on one plane, and converted into false colors. Scale bar=10 μm. The digitally combined image (H) shows that phospho-p38MAPK colocalizes in activated microglial cells where it is not localized solely to the nucleus.

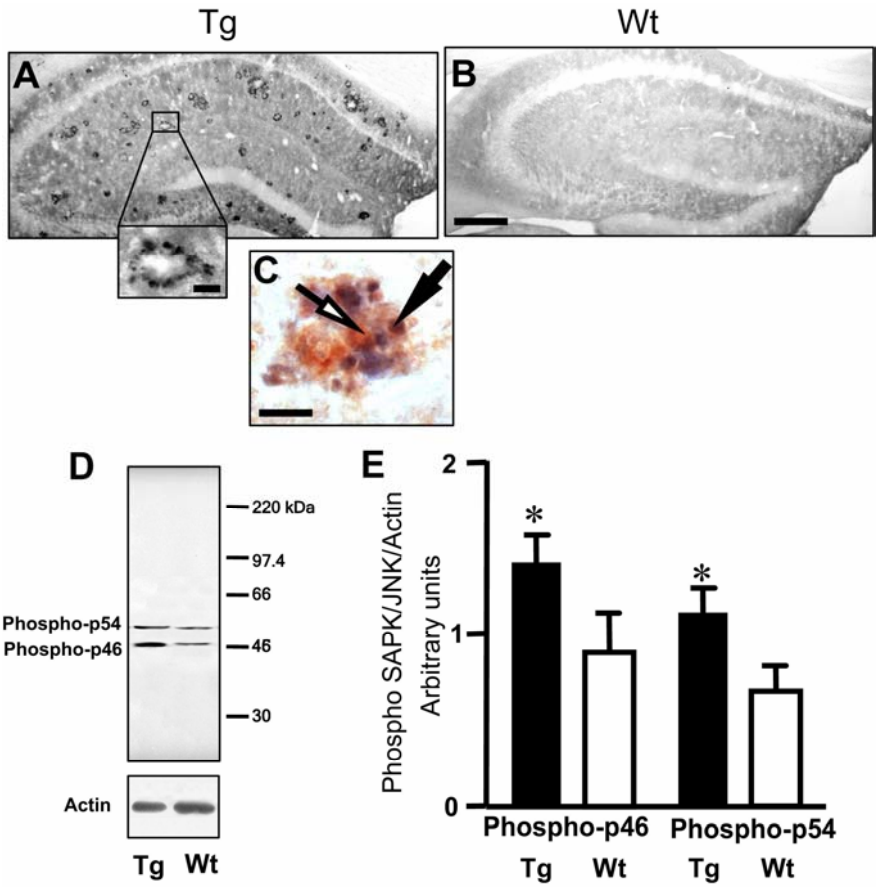

Fig. 24 Activation of JNK in the hippocampus of TgCRND8 and Wt mice. Activation of JNK was visualized using a specific antibody for its phosphorylated form and DAB staining followed by light microscopy. (A, B) Immunohistochemical staining of activated JNK in the hippocampus of Tg (A, inset) and Wt (B) mice. Note the complete lack of phospho-JNK-positive cells in the hippocampus of Wt mice, and the presence of phospho-JNK-positive cells around the plaques in Tg mice. The figure shows representative photomicrographs obtained from three to six independent experiments. Scale bars=400 μm A, B; inset: 30 μm. (C) Double

staining of phospho-JNK (labeled with an antibody raised against β-amyloid(1–42), blue–gray staining, white arrow) and of activated microglia cells (labeled with antibodies against the MHC type II, brown–red staining, black arrow). Scale bar=25 μm. (D) Representative Western blot analysis of phospho-JNK on homogenates of the entire hippocampus of Tg and Wt mice. Two major bands at an apparent molecular weight of 46 and 54 kDa are present. Western blot analysis of actin, performed on the same gel, is shown for comparison. (D) Quantitative analysis of activated JNK performed comparing the immunopositive band of phospho-JNK with that of actin run on the same gel. Each band density was calculated separately. The levels of phospho-JNK in TgCRND8 hippocampus were significantly higher than in Wt (* $P<0.05$, Student's *t*-test). Tg: $n=3$; Wt: $n=3$.

4.3.3 ERK activation in the hippocampus of TgCRND8 mice in basal and stimulated condition.

We evaluated whether ERK activation was modified in the hippocampus of TgCRND8 mice in comparison to Wt littermates, both in basal and cholinergic-stimulated conditions.

In basal conditions, very few phospho-ERK immunopositive neurons were present in the hippocampus of Wt mice, and localized mainly in the DG, where scattered phospho-ERK positive granule cells were stained (Fig. 25B, D), but not in CA1 and CA3. In the DG of TgCRND8 mouse hippocampus, phospho-ERK positive neurons were significantly less numerous than in Wt mice, as shown in Fig. 25A and C. Some immunopositive staining was also present in the mossy fibres of Wt mice (Fig 25D). Quantitative analysis of ERK activation was performed by means of Western blot on homogenates of the entire hippocampus, shown in Fig 25E.

We used a primary polyclonal antibody raised against phospho-(Thr202/Tyr204)-ERK, selective for the two isoforms of the enzyme, not showing any further bands than those corresponding to phospho-ERK1 and phospho- ERK2 (at an apparent molecular weight of 44 kDa and 42 kDa, respectively, see Fig. 25E). However, as also shown by others (Berman et al., 1998; Patterson et al., 2001), activated ERK1 appeared to be less

conspicuous than activated ERK2 in both mice strains, as evidenced by the very faint phospho-ERK1 band in Western immunoblots (Fig. 25E), notwithstanding the presence of total ERK1 protein both in Wt and in Tg mice hippocampus (Fig. 25G), Thus, we took into consideration only the variations of the activation of the ERK2, and not of the ERK1, isoform that might ensue in the two mouse strains. Quantitative data, reported in Fig. 25F, indicate that in basal conditions ERK2 was significantly less activated in the hippocampus of Tg mice in comparison to Wt mice (-45%, ** $P<0.02$, Student's *t*-test). In order to verify whether the differential activation of ERK2 in Tg mouse hippocampus might be due to lower expression of the ERK protein, we analyzed total ERK protein in mouse hippocampus by means of WB, using antibodies against the non-phosphorylated form of ERK1,2. A typical WB analysis is shown in Fig. 25G, where the two bands corresponding to ERK1 (44 kDa) and ERK2 (42 kDa) are present. Quantitative analysis of ERK2, performed comparing the density of the corresponding band to that of actin run in the same gel is shown in Fig. 25H. No significant difference in the level of total ERK was found between Tg and Wt mice hippocampus (n.s., Student's *t*-test). Furthermore, immunohistochemistry revealed that total ERK was expressed homogeneously in the entire hippocampus of Tg and WT mice (not shown).

Since it has been demonstrated in different systems that ERK activation is downstream of cholinergic stimulation, via both muscarinic (Rosenblum et al., 2000) and nicotinic receptors (Dineley et al., 2001), we verified whether cholinergic stimulation might activate ERK in a comparable manner in the hippocampus of Wt and Tg mice *ex vivo*. Slices (400 μM) of fresh mouse brain containing the hippocampus were cut and stimulated *in vitro* using the non-selective cholinergic agonist CCh (100 μM). In order to verify whether ERK is activated by cholinergic stimulation and in which subregion(s)

of the hippocampus phospho-ERK immunopositive neurons are located, activation of ERK was first studied by immunohistochemistry in Wt mice hippocampus after stimulation with CCh (Fig. 26B, B1, B2). Cholinergic stimulation with CCh strongly increased ERK activation in the cell bodies of CA1 pyramidal neurons and of DG granule cells (Fig. 26B1 and B2) of Wt mice. No activation of ERK was found in the cell bodies of CA3 pyramidal neurons (Fig. 26B, arrow). Quantitation of the effect was performed by counting the neurons blind in selected areas of the CA1 and DG (framed areas in Fig. 25A and B, shown at higher magnification in the insets A1, A2 and B1, B2). Stimulation of Wt mouse hippocampus with CCh induced significant activation of ERK in the cell bodies of DG and CA1 (Fig. 25C, D; ** P<0.02 vs. respective non-treated controls, Student's t-test). Stimulation of ERK activation by CCh in the hippocampus of Tg mice was visualized in CA1 pyramidal cell layer and DG by immunohistochemistry (Fig. 27A1 and A2). Activation of ERK by CCh was present both in CA1 and DG of Tg mice, which however appeared less intense than in Wt mouse hippocampus, as confirmed by quantitative analysis performed on homogenates of the entire hippocampus of Wt and Tg mice, with and without CCh stimulation, by WB analysis. A typical WB analysis of homogenates of the hippocampus of Tg and Wt mice after stimulation with CCh is shown in Fig. 26B, in comparison with actin run in the same gel. Statistical evaluation of the differences among the four experimental groups (Wt and Tg, no drug; Wt and Tg stimulated with CCh) was performed by two-way ANOVA followed by Bonferroni post hoc test and shown in Fig. 27C. Two-way ANOVA revealed that higher activation of ERK in Wt mice in comparison to Tg mice was present in all experimental conditions (Strain: $F_{1,20}$=33.57, P=0.0014; * P<0.05, vs. Wt No drug, Bonferroni post hoc test) and that CCh stimulation significantly activated ERK (Treatment: $F_{1,20}$=23.32, P=0.0059, # P<0.05 vs. all other groups, Bonferroni post

hoc test, Fig. 27C). It is interesting to note that cholinergic stimulation by CCh caused an increase of ERK activation in both mouse strains, as indicated by the not significant interaction between Strain and Treatment (interaction: $F_{1,18}$=6.36, P=6.36, not significant), indicating that the pathway is still functioning in the hippocampus of Tg mice. However, ERK activation evoked by CCh was significantly increased in Wt hippocampus (# P<0.05 vs. all other groups, Bonferroni post hoc test), while a non-significant trend toward an increase was found in Tg mouse hippocampus (Tg CCh vs. Tg No drug, not significant, Bonferroni post hoc test). These results show that activation of ERK in CA1 pyramidal neurons and in the granule cells of the DG is downstream of cholinergic activation. However, this effect is significantly less conspicuous in the hippocampus of Tg mice, indicating a possible mechanism responsible for the memory deficits present in TgCRND8 mice (Bellucci et al., 2006), possibly due to the strong connections between the cholinergic system and the ERK pathway in the mechanisms of memory (Giovannini, 2006).

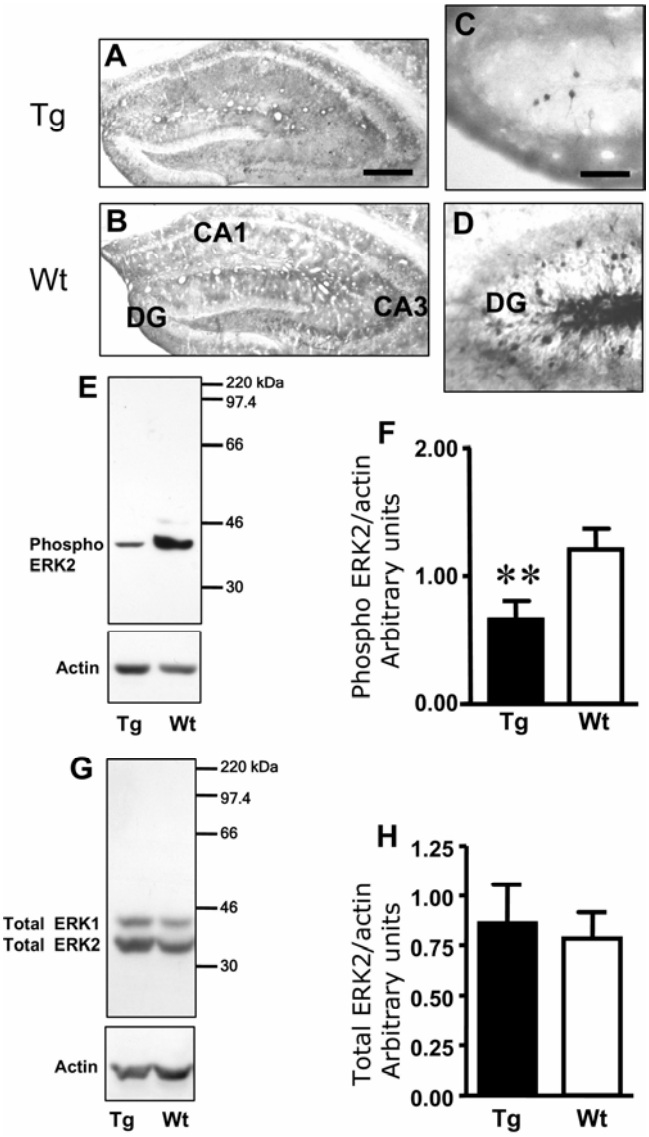

Fig. 25 ERK2 is less activated in the hippocampus of TgCRND8 than in Wt mice. (A–D) Immunohistochemical staining of activated ERK in the hippocampus of Tg (A, C) and Wt (B, D) mice. Note the phospho-ERK-positive granule cells in the DG of the hippocampus. Selected photographs (A, C and B, D) were shot from stained slices taken from different mice. The figure shows representative photomicrographs obtained from three to six independent experiments. Scale bars=250 μm A, B; C, D: 50 μm. (E) Representative Western blot analysis of phospho-ERK1,2 on homogenates of the entire hippocampus of Tg and Wt mice. The two typical bands at apparent molecular weights of 42 (phospho-ERK2) and 44 (phospho-ERK1) kDa are present. Phospho-ERK2 is more abundant than phospho-ERK1. Western blot analysis of actin, performed on the same gel, is shown for comparison. (F) Quantitative analysis of activated ERK2 performed comparing the immunopositive band of phospho-ERK2 with that of actin run

on the same gel. The levels of phospho-ERK2 in TgCRND8 hippocampus were significantly lower than in Wt hippocampus (** $P<0.02$, Student's *t*-test). Tg: $n=7$; Wt: $n=8$. (G) Representative Western blot analysis of total-ERK1,2 on homogenates of the entire hippocampus of Tg and Wt mice. The two typical bands at apparent molecular weights of 42 (total-ERK2) and 44 (total-ERK1) kDa are present. Western blot analysis of actin, performed on the same gel, is shown for comparison. (H) Quantitative analysis of total ERK2 performed comparing the immunopositive band of total ERK2 with that of actin run on the same gel. The levels of total ERK2 in TgCRND8 hippocampus were not significantly different to those in Wt hippocampus (not significant, Student's *t*-test). Tg: $n=7$; Wt: $n=7$.

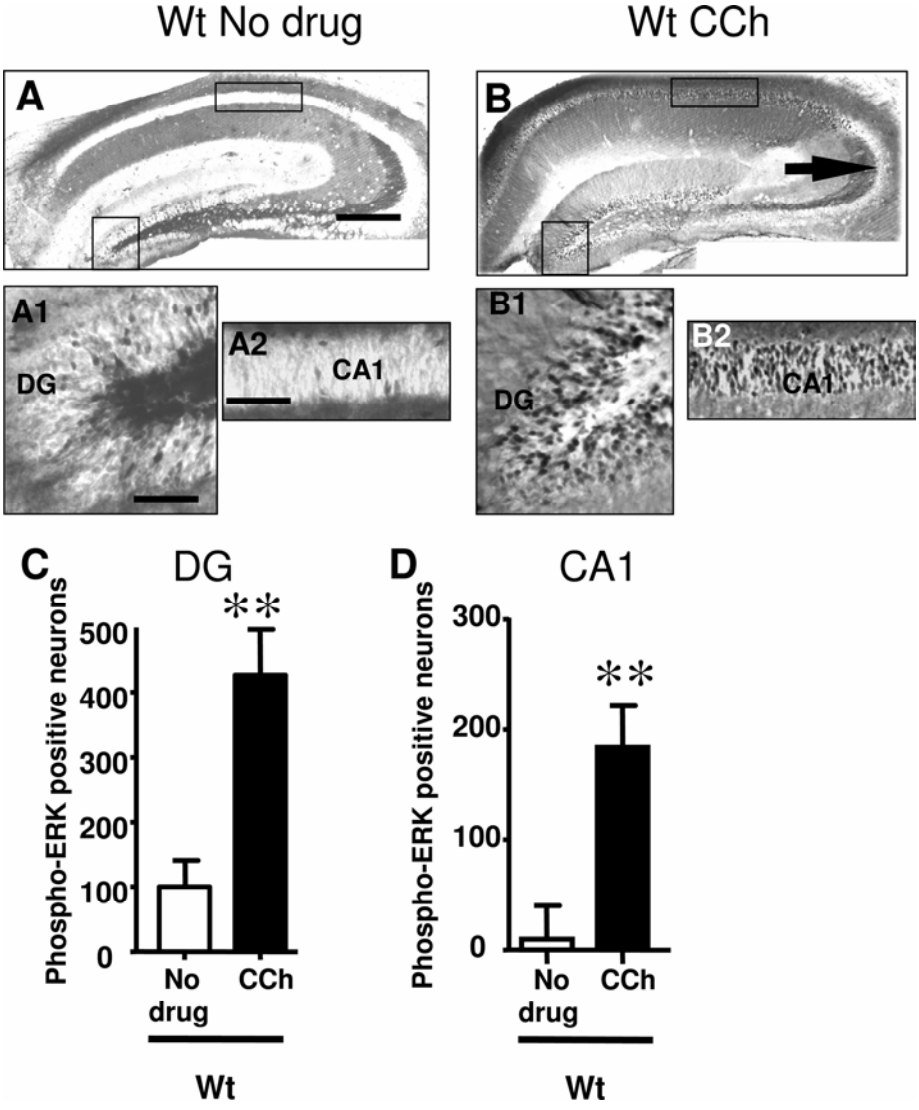

Fig. 26 Activation of ERK in the hippocampus of Wt mice by cholinergic stimulation ex vivo. Immunohistochemical staining of phospho-ERK in slices of fresh mouse hippocampus of Wt mice in control conditions (Wt no drug) and after stimulation with CCh (100 μM, 15 min, Wt

CCh). (A, B) Activation of ERK studied by immunohistochemistry; A1, A2 and B1, B2 show enlarged photographs of framed areas in A and B, respectively. CCh-activated ERK in neurons of CA1 and DG (B1 and B2), but not of CA3 (B, arrow). Scale bars=250 μm A, B. A1–B2: 50 μm. (C, D) Counts of phospho-ERK positive neurons in areas corresponding to the framed areas in A and B (each experimental group n=3). Counts of phospho-ERK positive neurons in the DG (C) and in CA1 (D). ** P<0.02 vs. respective No drug slices, Student's t-test.

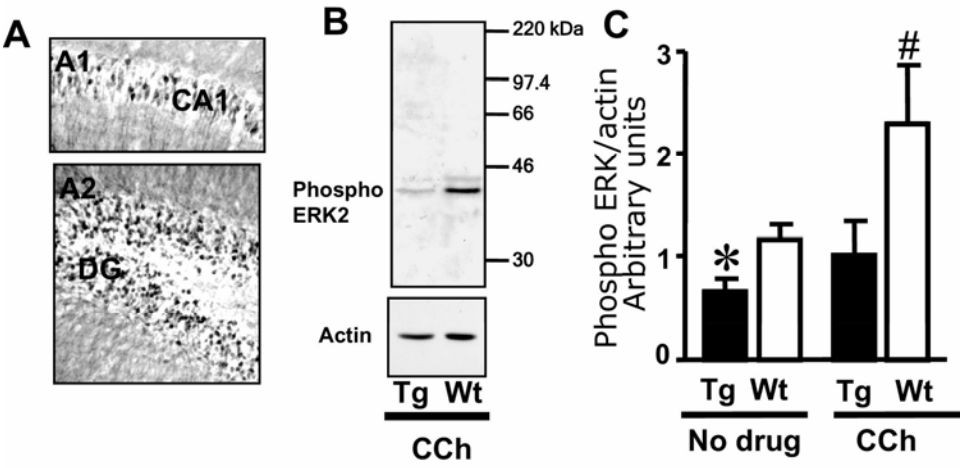

Fig. 27 Activation of ERK in the hippocampus of TgCRND8 mice by cholinergic stimulation ex vivo. (A) Immunohistochemical staining of phospho-ERK in slices of fresh mouse hippocampus of Tg mice after stimulation with CCh (100 μM, 15 min). Scale bar=50 μm. (B) Representative Western blot analysis of phospho-ERK1,2 on homogenates of the entire hippocampus of Tg and Wt mice. The two typical bands at apparent molecular weights of 42 (phospho-ERK2) and 44 (phospho-ERK1) kDa are present. Phospho-ERK2 is more abundant than phospho-ERK1. Western blot analysis of actin, performed on the same gel, is shown for comparison. (C) Quantitative analysis of ERK activation in homogenates of hippocampi of Wt and Tg mice in control conditions (No drug) and after 100 μm CCh stimulation, performed comparing the immunopositive band of phospho-ERK2 with that of actin run on the same gel. Statistical analysis was performed by two-way ANOVA followed by Bonferroni post hoc test. Strain: $F_{1,20}$=33.57, P=0.0014; * P<0.05, vs. Wt, Bonferroni post hoc test; Treatment: $F_{1,20}$=23.32, P=0.0059, $^{\#}$ P<0.05 vs. all other groups, Bonferroni post hoc test. Cholinergic stimulation by CCh activated ERK in both mouse strains (Strain and Treatment interaction: $F_{1,18}$=6.36, P=6.36, not significant). ERK activation by CCh was highly significant in Wt hippocampus (+96%; Wt CCh vs. Wt No drug, $^{\#}$ P<0.05 vs. all other groups, Bonferroni post hoc test), while it did not reach significance in Tg mouse hippocampus (+53%; Tg CCh vs. Tg No drug, not significant, Bonferroni post hoc test). Wt CCh: n=4; Wt No drug: n=7; Tg CCh: n=4; Tg No drug: n=7.

4.4 EFFECT OF PEC ON ACh RELEASE FROM THE CEREBRAL CORTEX AND CHOLINESTERASE ACTIVITY

4.4.1 Determination of inhibitory doses of PEC on AChE and BuChE

In order to measure the activity of AChE and BuChE, we used the colorimetric method first developed by Ellman et al. (1961). However, using this method, the measurements of BuChE activity *ex vivo* did not give reproducible and reliable results in the crude brain homogenate preparation. In such a tissue, indeed, BuChE activity is more than ten times lower than that of AChE. Such a low level of activity may give too little variations of the OD read at 412 nm, resulting in high variability of the determinations which may confound the results. For this reasons, in order to obtain reliable data on BuChE inhibition, BuChE activity was determined both using a modification of the Ellman method, by Dr. O. Lockridge (O. Lockridge, personal communication), in which Tween 20 was added to the homogenate (Li et al., 2000), and using a radiometric method (Thiermann et al., 2005). The radiometric method was also used to validate the results AChE activity obtained with the Ellman method. The enzymatic activities of AChE and BuChE in cerebral cortex homogenates of control rats are shown in Table 1. The results shown were obtained with the radiometric method, with the method of Ellman et al. (1961) for AChE activity, and with Lockridge's modification of Ellman's method for BuChE activity. It is noteworthy that the results obtained for AChE (Table 1, first column) and BuChE (Table 1, second column) using the Ellman methods were comparable with those obtained with the radiometric methods. Furthermore, the different quantification methods show that the activity of BuChE in the cortex of control

rats is much lower than that of AChE, ranging between 5% (Lockridge's modification of Ellman) and 9% (radiometric method), of AChE activity (Table 1, third column). Fig. 28 shows the inhibition of brain AChE activity 55–60 min after administration of the drugs, the time point corresponding to the peak increase in extracellular ACh levels found in the microdialysis experiments. The results obtained with Ellman method are shown in panel A. A statistically significant inhibition of AChE activity was found after rivastigmine (0.6 mg/kg,–40% vs saline, one way ANOVA and Newman–Keuls multiple comparison test, **P<0.001) and donepezil (1.0 mg/kg,–22% vs saline, one way ANOVA and Newman–Keuls multiple comparison test, *P<0.05). PEC (5.0 mg/kg) administration was followed by a 5% inhibition of AChE activity, which was statistically not significant (one way ANOVA and Newman–Keuls multiple comparison test, P>0.05). Comparable results on AChE inhibition were obtained with the radiometric method, as shown in Fig. 28, panel B. Rivastigmine caused a 37% AChE inhibition (one way ANOVA and Newman–Keuls multiple comparison test, **P<0.02 vs saline), a 26% inhibition was found after donepezil (one way ANOVA and Newman–Keuls multiple comparison test, *P<0.05 vs saline) while PEC decreased by a non significant 12% AChE activity (one way ANOVA and Newman–Keuls multiple comparison test , P>0.05).

The determinations of BuChE activity were carried out using both a radiometric method with [^{3}H]ACh as a substrate, and the Lockridge's modification of Ellman method. As shown in Fig. 29A, using the radiometric method, PEC administration resulted in a significant 39% inhibition of BuChE activity (one way ANOVA and Newman–Keuls multiple comparison test, **P<0.01 vs saline). Rivastigmine and donepezil inhibited BuChE activity by 18% and 8%, respectively (one way ANOVA and Newman–Keuls multiple comparison test, both not statistically different vs saline). As shown in Fig.

29B, using the Lockridge's modification of the Ellman colorimetric method, with butyrylthiocholine as the substrate, both PEC and rivastigmine caused a statistically significant 25% inhibition of BuChE activity (one way ANOVA and Newman–Keuls multiple comparison test, *P<0.01 vs saline), while donepezil induced a 10%, not significant, inhibition (one way ANOVA and Newman–Keuls multiple comparison test, P>0.05 vs saline).

	AChE	**BuChE**	**%**
Ellman Method	**1.06 ± 0.1**[a]	**0.058 ± 0.004**[b]	**5.5**
Radiometric Method	**0.97 ± 0.1**	**0.084 ± 0.008**	**9**

Table 1. AChE and BuChE activity in the cerebral cortex of control rats.
Values are expressed as pmol substrate hydrolized per µg protein per min (mean ± S.E.M.).
[a] AChE activity calculated with the method of Ellman.

[b] BuChE activity calculated with the method of Ellman modified according to O. Lockridge.

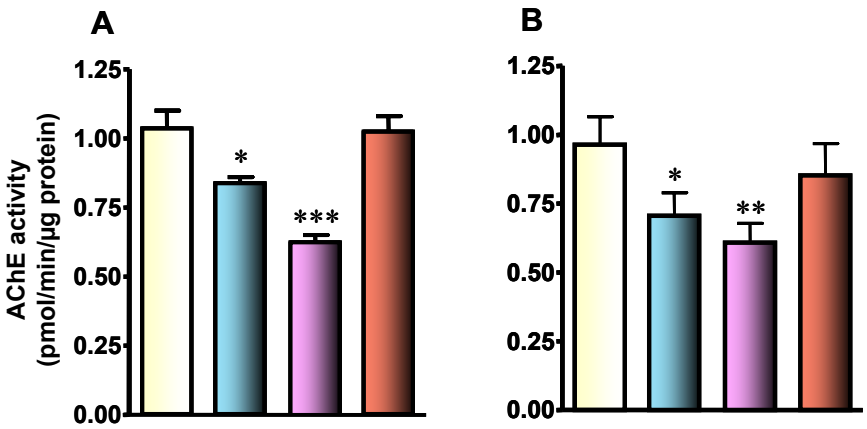

Fig. 28. A: Inhibition of acetylcholinesterase activity in the cerebral cortex of the rat 60 min after drug administration, determined *ex vivo* with the method of Ellman et al. (1961). Drugs were administered i.p. The columns indicate the pmol of acetylthiocholine hydrolyzed per min per µg protein. Saline (i.p. injection of 2 ml/kg of saline solution; yellow bar, n=9); Donepezil, 1 mg/kg (light blue bar, n=8); Rivastigmine, 0.6 mg/kg (pink bar, n=9); PEC, 5.0 mg/kg (orange bar, n=11). *P<0.05 and ***P<0.001 vs saline; AChE activity in the cerebral cortex of the rat 60 min after drug administration, determined *ex vivo* with the radiometric method. The columns indicate the pmol of acetylthiocholine hydrolyzed per min per µg protein. Saline (i.p. injection of 2 ml/kg body weight of saline; yellow bar, n=6); Donepezil, 1 mg/kg (light blue bar, n=8); Rivastigmine, 0.6 mg/kg (pink bar, n=6); PEC, 5.0 mg/kg (orange bar, n=8). *P<0.05 and **P<0.02 vs saline; one-way ANOVA followed by Newman–Keuls multiple comparison test.

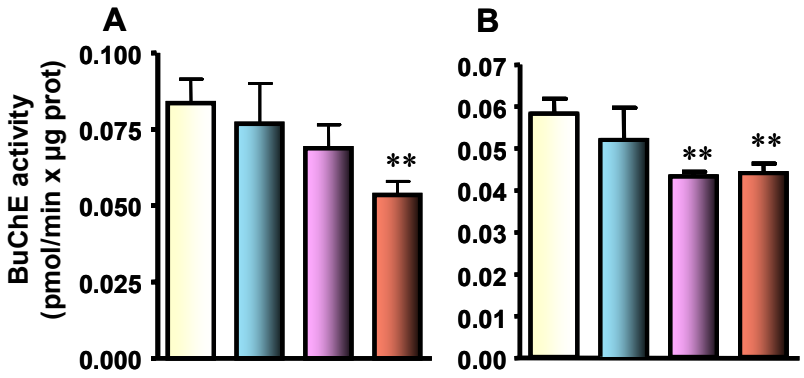

Fig. 29 A: Inhibition of BuChE activity in the rat cerebral cortex 60 min after drug administration, determined *ex vivo* with the radiometric method after the addition of a selective AChE inhibitor. The columns indicate the pmol of acetylthiocholine hydrolyzed per min per µg protein. Saline (i.p. injection 2 ml/kg body weight of saline; yellow bar, n=15); Donepezil, 1 mg/kg (light blue bar, n=4); Rivastigmine, 0.6 mg/kg (pink bar, n=9); PEC, 5.0 mg/kg (orange bar, n=11). **P<0.01 vs saline; one-way ANOVA followed by Newman–Keuls multiple comparison test. B: Inhibition ofBuChE activity in the rat cerebral cortex 60 min after drug administration, determined *ex vivo* with the Lockridge's modification of the Ellman method. The columns indicate the pmol of butyrylthiocholine hydrolyzed per min per µg protein. Saline (i.p. injection 2 ml/kg body weight of saline; yellow bar, n=6); Donepezil, 1 mg/kg (light blue bar, n=3); Rivastigmine, 0.6 mg/kg (pink bar, n=8); PEC, 5.0 mg/kg (orange bar, n=8). **P<0.01 vs saline; one-way ANOVA followed by Newman–Keuls multiple comparison test. Please note the different scale of the y axes.

4.4.2 Effect of PEC on cortical ACh extracellular levels

The extracellular level of ACh in the rat cerebral cortex before the administration of the cholinesterase inhibitors was 2.90 ± 0.28 fmol/µl (n=28). The value is similar to those previously reported (Scali et al., 1997). In saline-treated rats, ACh extracellular level remained practically constant for the entire duration of the experiment (±10% vs basal values, variation not significant, Fig. 30). The time course of the increase in ACh release from the cortex of rats after drug administration is shown in Fig. 30A. Both donepezil (1.0 mg/kg) and rivastigmine (0.6 mg/kg) brought about a 4-fold increase in ACh levels within 40 min after administration. PEC (5 mg/kg) administration was followed by a 2.5 fold increase in ACh release within 40 min which was slightly smaller than those evoked by donepezil or rivastigmine. The increase in ACh extracellular levels brought about by the three drugs faded gradually within 2 h. Quantitative analysis of the effect of the three drugs in comparison to saline was performed by calculating the areas under the curve between 100 and 200 min after treatment (shown in Fig. 30B). The areas under the curve after donepezil and rivastigmine administration were about 3 times larger than that of the saline-treated rats. The area under the curve after PEC administration showed a 2-fold increase over the saline-treated rats. Statistical analysis performed on the areas under the curves indicated that the three treatments increased significantly cortical ACh extracellular levels, in comparison to saline-treated rats (one way ANOVA and Newman–Keuls multiple comparison test; *$P<0.05$ vs saline). However, no significant difference was found among the increases evoked by the three drugs (one way ANOVA and Newman–Keuls multiple comparison test; n.s.).

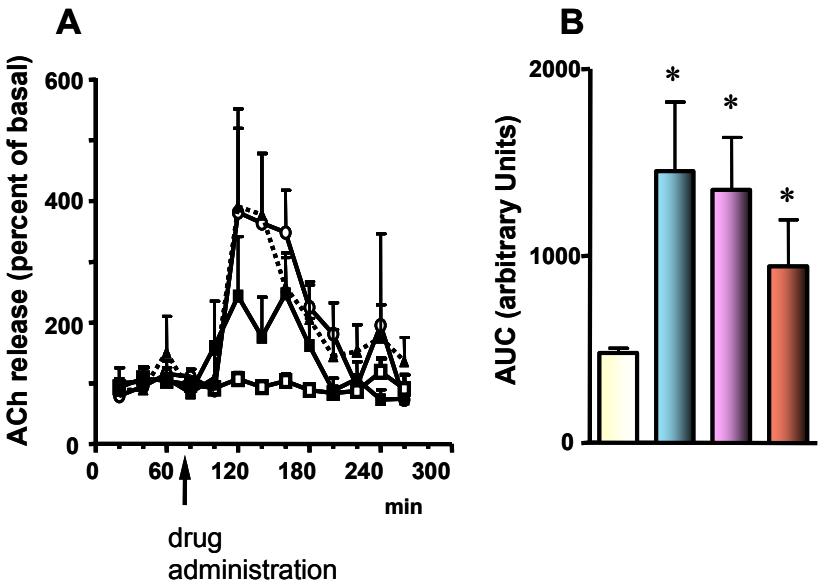

Fig. 30 Effect of cholinesterase inhibition on rat cortical extracellular levels of ACh. A: Time course of the effect of donepezil, rivastigmine or PEC administration on ACh levels in the dialysate. The drugs were administered i.p. after collecting four basal samples (administration time shown by the arrow). ACh release is expressed as percent changes over the mean of all pre-drug determinations (basal levels). Control rats received i.p. injection of 2 ml/kg of saline solution (open square; n=6); Donepezil, 1 mg/kg (open circle; n=7); Rivastigmine, 0.6 mg/kg (black triangle; n=7); PEC, 5 mg/kg (black square; n=6). B: Areas under the curve were calculated between time 100 min and time 200 min. *P<0.05 vs saline; one way ANOVA followed by Newman-Keuls multiple comparison test.

4.4.3 Determination of cholinesterase inhibitors concentrations in the brain

The concentrations of two of the three cholinesterase inhibitors (donepezil and rivastigmine) in the brain are shown in Table 2. At the time point at which a peak effect of ACh release was found (55-60 min after drug administration) the concentration of donepezil in the rat brain was 177 nM while that of rivastigmine amounted to 14 nM. Due to the mechanism of AChE inhibition by rivastigmine (carbamate interaction with the catalytic centre) the concentration of the catalytically generated metabolite NAP

226-90 was added to that of native compound. The total concentration of the two drugs adds up to 72 mM.

Drug	Dose mg/kg i.p.	Time after drug	N° rats	Concentration nM ± S.D.
Donepezil	1.0	60 min	3	177.1 ± 40.6
Rivastigmine	0.6	60 min	4	14.1 ± 21.9
NAP 226-90				58.5 ± 11.9
Sum of Riva+NAP				72[a]

Table 2. Concentrations of the cholinesterase inhibitors in the rat cortex
[a] including the rivastigmine metabolite NAP 226-90

4.5 EFFECT OF NP-0361 AND NP-0336 ON ACh RELEASE AND CHOLINESTERASE ACTIVITY IN THE CEREBRAL CORTEX OF YOUNG RATS

4.5.1 Rotarod test

As shown in Figure 31A and B, treatment with NP-0361 at 20 mg/kg or NP-0336 at 80 mg/kg significantly impaired the rat's ability to perform on a rotarod test. Both drugs at the lower doses tested showed a non significant tendency to decrease the rat ability to balance on the rotarod test. The vehicle used (N-methyl-2pyrrolidone 5%, Solutol HS15

30%, Saline) inhibited motor activity in the rotarod test in 3/7 rats tested (effect not significant).

4.5.2 Exploratory behaviour

The experiments on the effect of the two drugs on exploratory activity were started at the lower dose of the two drugs, both dissolved in MP/solutol/saline. The results are shown in Figure 32A. It is evident that the vehicle MP/solutol/Saline used to dissolve the drugs (10 ml/kg) has an impairing effect on the spontaneous motor activity of the animals, significantly inhibiting the exploration of the arena in comparison to saline treated rats. We therefore decided to use a different vehicle to dissolve the two drugs (Tween 80 2% diluted in Methylcellulose 0.5%). The results obtained is shown in Figure 32B. The new vehicle used significantly decreased motor activity in comparison to saline treated rats, although by a lesser extent than MP/solutol/saline. Treatment with NP-0336 at 40 mg/kg did not vary motor activity in comparison to vehicle treated rats (MC 0.5%/Tween 80 2%). On the other hand, NP-0361 at the doe of 10 mg/kg further decreased rat motor activity in the arena ($P<0.001$ vs vehicle treated rats).

Following these results we explored the possibility to use DMSO as a vehicle to dissolve the two drugs for the microdialysis experiments. Since the two drugs are both very insoluble, we decided to dissolve them in pure DMSO in order to inject small quantities of the pure solvent. The effect of DMSO on the rat behaviour was defined in the open field arena test. Indeed, administration of DMSO (400 µl/kg) did not modify the rat behaviour in the spontaneous rat mobility test, as shown in Figure 33. Therefore we decided to use DMSO as the solvent to dissolve the drugs for the microdialysis experiments.

A

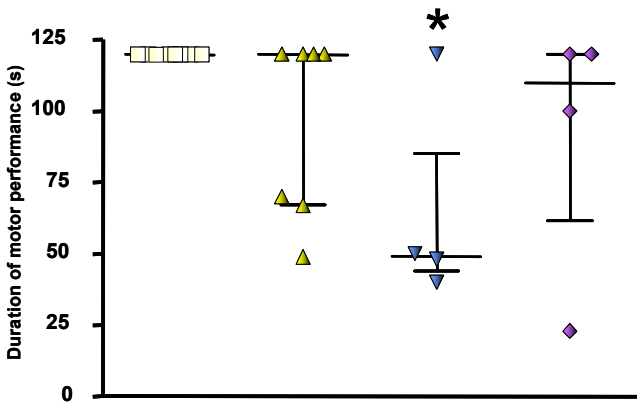

B

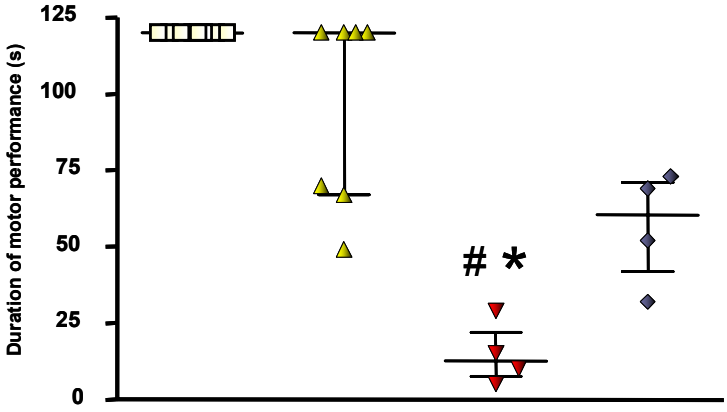

Fig. 31 Effect of treatment with NP-0361 ad NP-0336 on rotarod test. (A) treatment with 10 mg/kg NP-0361 (purple diamonds) does not show a significant tendency to decrease the rat's ability to balance on the rotarod test, while treatment with 20 mg/kg NP-0361 (blue triangles) shows a significantly tendency to impair the rat's ability to balance on the rotarod test versus saline (yellow squares) (Krusal-Wallis and Dunn's post comparison test, *P<0.05), treatment with vehicle (yellow triangles) inhibits motor activity in the rotarod test in 3/7 rats tested (not significant). (B) treatment with NP-0336 at 40 mg/kg (grey diamonds) does not show a significant tendency to decrease the rat's ability to balance on the rotarod test, while treatment with NP-0336 at 80 mg/kg (red triangles) shows a significant tendency to impair the rat's ability to balance on the rotarod test (yellow squares) (Krusal-Wallis and Dunn's post comparison test, *P<0.001 vs saline; #P<0.05 vs vehicle)Treatment with vehicle (yellow triangles) inhibits motor activity in the rotarod test in 3/7 rats tested (not significant).

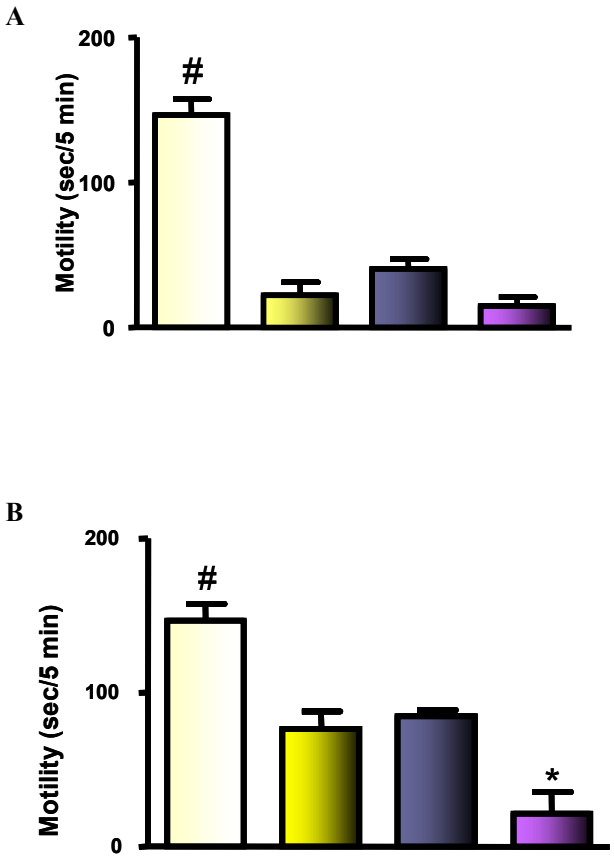

Fig. 32 Effect of treatment with NP-0336 and NP-0361 on spontaneous rat mobility in an open field arena. (A) treatment with the lowest doses of either drug (NP-0361 at 10 mg/kg, purple bar, and NP-0336 at 40 mg/kg, grey bar) dissolved in the vehicle MP/solutol/saline (yellow bar) has an impairing effect on the spontaneous motor activity of the animals as compared to saline-treated rats (light yellow bar) (one way ANOVA, $F_{3,16} = 44.22$, $P<0.0001$, #<0.01 versus all other groups, Newman-Keuls post hoc test). (B) treatment with the lowest doses of either drug (NP-0361 at 10 mg/kg, purple bar, and NP-0336 at 40 mg/kg, grey bar) dissolved in the vehicle Tween 80 2%diluted in Methylcellulose 0.5% (yellow bar) has an impairing effect on the spontaneous motor activity of the animals as compared to saline-treated rats (light yellow bar), although by a lesser extent than MP/solutol/saline (one way ANOVA, $F_{3,14} = 20.80$, $P<0.0001$, #P<0.01 vs all other groups, *P<0.05 vs vehicle and NP-0336, Newman-Keuls post hoc test).

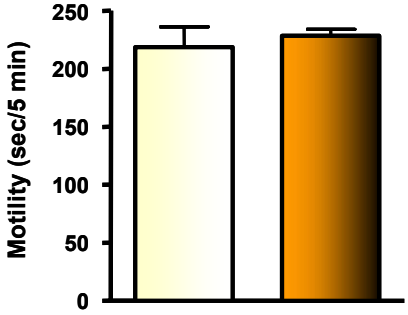

Fig. 33 Effect of treatment with DMSO on spontaneous rat mobility in an open field arena. Administration of DMSO (400ml/kg) did not modify the rat behaviour in the spontaneous rat mobility test.

4.5.3 Determination of inhibitory doses of NP-0361 and NP-0336 on AChE and BuChE activity

The effect of two novel compounds, NP-0361 and NP-0336, was tested *ex vivo* on AChE and BuChE activity in the cerebral cortex of the young rat. Initially, a dose of 10 mg/kg of NP-0361 and 40 mg/kg of NP-0336 was tested on 6 rats in order to verify whether inhibition of AChE and/or BuChE activity could be detected.

As shown in Fig. 34 and 35, at the doses of 10 mg/kg of NP-0361 and 40 mg/kg of NP-0336, no significant inhibition of AChE or BuChE activity was found. Therefore, we decided to increase the dose of the two drugs to 20 mg/kg for NP-0361 and 80 mg/kg for NP-0 d336. AChE activity in rats treated with vehicle used to dissolve the two drugs did not significantly differ from enzyme activity in naïve rats (vehicle alone -12% vs naïve, P=0.3637, two-tailed Student's t test).

The results obtained after treatment with NP-0361 at the doses of 10 and 20 mg on AChE activity are shown in Fig. 34A. A statistically significant inhibition of AChE

activity was found after administration of NP-0361 20 mg/kg (-39% vs vehicle; one way ANOVA: $F_{2,16}$= 6.72; P<0.01, and Newman-Keuls post hoc test, **P<0.01 vs all others group). No inhibition of AChE activity was found after treatment with NP-0361 10 mg/kg (+5% vs vehicle, not significant).

Fig. 34B shows the results obtained after administration of NP-0336 at the doses of 40 and 80 mg/kg on AChE activity. NP-0336 80 mg/kg caused an inhibition of 22% of AChE activity, not statistically different from vehicle, while no effect was observed after treatment with 40 mg/kg NP-0336 (+5% vs vehicle, not statistically different, one-way ANOVA: $F_{2,16}$= 2.212; P=0.1419).

The effect of rivastigmine at the dose of 1.0 mg/kg, as positive control, is shown in panel C. As expected, we found a statistically significant inhibition of AChE activity after rivastigmine administration (-50% vs vehicle, **P<0.01, two-tailed Student's t test). Fig. 35 shows that in rats treated with vehicle alone BuChE activity did not significantly differ from enzyme activity in naïve rats (vehicle alone -4% vs naïve; P=0.5903, two-tailed Student's t test).

The results obtained after treatment with NP-0361 and NP-0336 on BuChE activity are shown in Fig. 35. The results obtained after treatment with NP-0361 at the doses of 10 and 20 mg/kg are shown in panel A. No effect on BuChE activity was observed with NP-0361 10 mg/kg (+13% vs vehicle, not significant), whereas an inhibition of 13.6% (not statistically significant) was observed with NP-0361 20 mg/kg (one way ANOVA, $F_{2.15}$= 9.239, P<0.05, and Newman-Keuls post hoc test, +P<0.05). The results obtained after treatment with NP-0336 at the doses of 40 and 80 mg/kg are reported in panel B. No effect was observed with 40 mg/kg NP-0336 (+10%vs vehicle, not statistically significant), while treatment with 80 mg/kg NP-0336 caused an inhibition of 15% on

BuChE activity, statistically significant, both versus vehicle and 40 mg/kg NP-0336 (one way ANOVA $F_{2,15}$=9.239, P<0.05, and Newman-Keuls post hoc test, +P<0.05).

The effect of rivastigmine at the dose of 1.0 mg/kg on BuChE activity is shown in panel C. We found that rivastigmine at this dose caused a significant 15% inhibition of BuChE activity (P<0.05, two-tailed Student's t test).

4.5.4 Effect of NP-0361 and NP-0336 on cortical ACh extracellular levels

The extracellular levels of ACh before the administration of cholinesterase inhibitors were 2.82 ± 0.27 fmol/µl (n=25). This basal value is similar to that reported in previous papers from our laboratory (Scali et al., 1997).

The doses of the cholinesterase inhibitors (80 mg/kg NP-0336 and 20 mg/kg NP-0361) chosen to study variations of cortical ACh extracellular levels by microdialysis were selected on the basis of AChE and BuChE inhibition described above.

The results are shown in fig 36A. In rats treated with vehicle alone ACh extracellular levels remained practically constant throughout the experiment (4 h, yellow line). Both NP-0336 at the dose of 80 mg/kg (red line) and NP-0361 at the dose of 20 mg/kg (blue line) brought about a significant increase of cortical ACh extracellular levels. The effect of 80 mg/kg NP-0336 (maximum +73% vs basal) was observed between 120 and 140 min after administration. The effect disappeared gradually and levels returned to basal within 1 h. Rivastigmine at the dose of 1.0 mg/kg (green line) increased ACh extracellular levels by about 600% with a maximum 80 min after administration and a gradual decrease of the effect to basal levels within the following 2 h. Significativity of the effect was defined using the areas under the curve (AUC) at the maximum peak

effect (between 100 and 160 min after administration of NP-0.361, Figure 36C and between 160 and 220 min after administration of NP-0336, Figure 36B). The corresponding AUC were also calculated for the control groups, and used as controls in the statistical analysis. The AUC of rivastigmine was calculated between 100 and 160 min (Figure 36D). Comparing the AUCs, the effect of the two drugs on ACh extracellular levels was statistically different from vehicle treated rats and controls (NP-0336: *P< 0.05 vs controls; NP-0361 **P< 0.02 vs controls, Student's t test). Furthermore, the effect of NP-0336 was similar to that of NP-0361 (not statistically different with the Student's t test, P= 0.95). However, both drugs evoked a much smaller increase of ACh extracellular levels than that of rivastigmine (AUC of the two drugs P< 0.001 vs rivastigmine, one way ANOVA and Newman Keuls multiple comparison test).

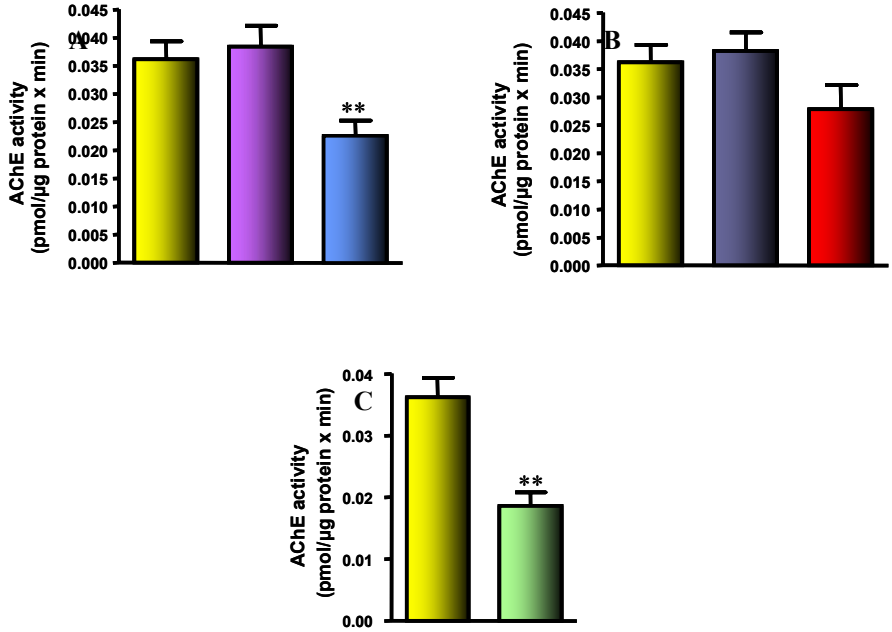

Fig. 34 Acetylcholinesterase (AChE) activity in young rats. Panel A: treatment with 10 mg/kg NP-0361 (purple bar) does not significantly inhibit AChE activity versus vehicle (yellow bar), while treatment with 20 mg/kg NP-0361 (blue bar) causes an inhibition of 39% on AChE

activity, statistically significant versus vehicle and NP-0361 (one way ANOVA, $F_{2,16} = 6.725$, $P<0.05$, and Newman-Keuls post hoc test, $^{**}P<0.01$). Panel B: treatment with 40 mg/kg NP-0336 (grey bar) and with 80 mg/kg NP-336 (red bar) does not significantly inhibit AChE activity versus vehicle (yellow bar). Panel C: treatment with 1.0 mg/kg rivastigmine (green bar) causes an inhibition of 50% on AChE activity, statistically significant versus vehicle (yellow bar).

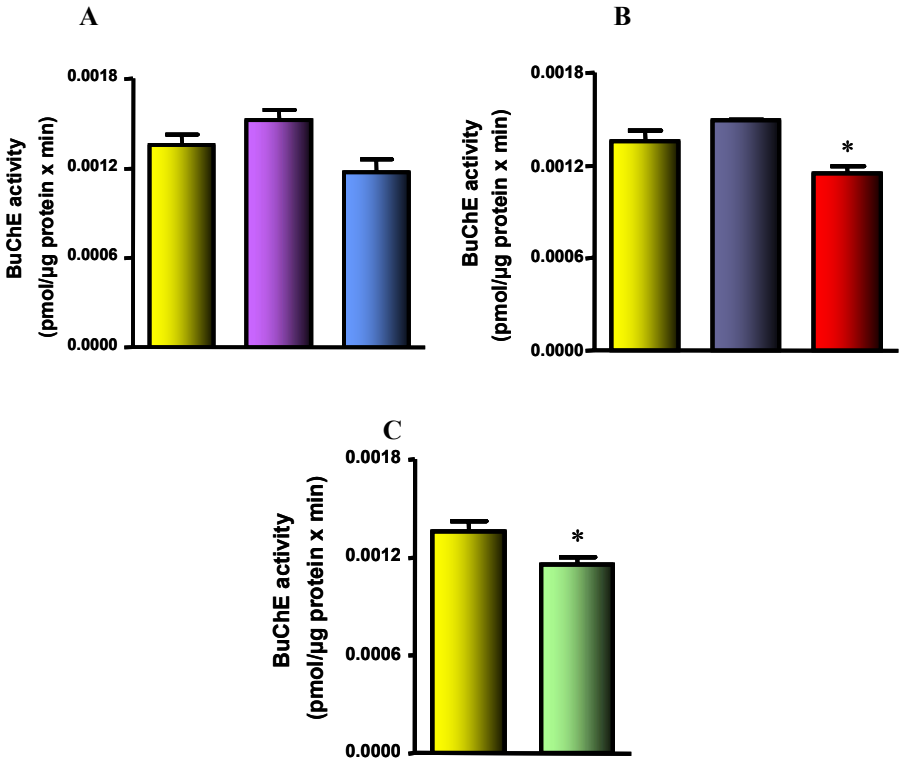

Fig. 35 Butirylcholinesterase (BuChE) activity in young rats. Panel A: treatment with 10 mg/kg NP-0361 (purple bar) and with 20 mg/kg NP-0361 (blue bar), does not change BuChE activity compared to vehicle(yellow bar). Panel B: treatment with 40 mg/kg NP-0336 (grey bar) does not change BuChE activity while treatment with 80 mg/kg NP-0336 (red bar) causes an inhibition of 15% on BuChE activity, statistically significant versus vehicle (yellow bar) and 40 mg/kg NP-0336 (one way ANOVA, $F_{2,15} = 9.239$, $P<0.05$, and Newman-Keuls post hoc test, $^{*}P<0.05$). Panel C: treatment with 1.0 mg/kg rivastigmine (green bar) causes an inhibition of 15% on BuChE activity, statistically significant versus vehicle (yellow bar).

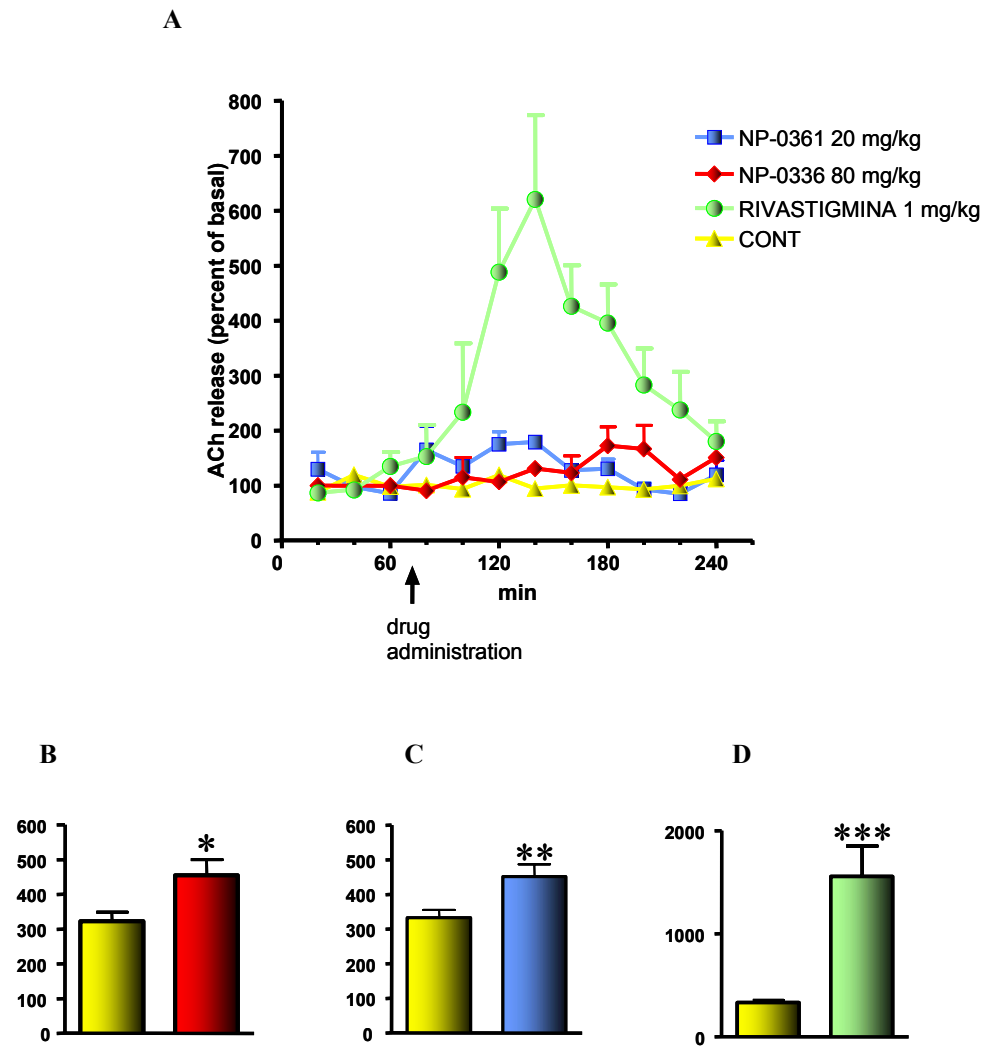

Fig. 36 Effect of AChEI or BuChEI administration on cortical ACh release. (A) treatment with vehicle does not change ACh extracellular levels throughout the experiment (4h, yellow line); treatment with 80 mg/kg NP-0336 (red line) and 20 mg/kg NP-0361 (blue line), causes a significant increase of ACh extracellular levels, of 80% and 73% versus basal respectively.; treatment with 1.0 mg/kg rivastigmine (green line) causes a significant increase of ACh extracellular levels. ACh release is expressed as percent changes over the mean of all pre-drug determinations (basal levels). . (B) area under the curve (AUC) at the maximum peak effect of 80 mg/kg NP-0336 (red bar), calculated between 160 and 220 min, *P<0.05 versus vehicle (yellow bar), (Student's t-test). (C) AUC at the maximum peak effect of 20 mg/kg NP-0361 (blue bar), calculated between 100 and 160 min; **P<0.02, versus vehicle (yellow bar) (Student's t-test). (D) AUC) at the maximum peak effect of 1.0 mg/kg rivastigmine (green bar), calculated between 100 and 160 min; ***P<0.005, versus vehicle (yellow bar) (Student's t-test).The effect of both NP-0361 and NP-0336 on the increase of ACh extracellular levels is much smaller than the effect of rivastigmine.

5. DISCUSSION

Aim of the research was to valuate the modification of different intracellular transduction pathways and extracellular intercommunicating proteins as well as activation/deactivation of microglia and astrocytes in animal models of neuroinflammation, normal aging and AD-related neurodegeneration that lead to memory deficits. To this aim different animal models were used. In particular, the molecular mechanisms involved in neuron-glia intercommunication during inflammation in the hippocampus were studied using the model of LPS-induced neuroinflammation in the rat. The differential activation of MAPKs intracellular transduction pathways as well as the cellular modifications in the hippocampus during aging and AD related neurodegeneration were studied in normal aged rats and in TgCRND8 transgenic mice, respectively. In the last part of this research it was evaluated the efficacy of treatment with novel compounds on differential inhibition of AChE/BuChE activity in the brain and on cortical ACh release. These latter experiments were aimed at obtaining a proof of concept for the development of these novel compounds as possible drugs for the treatment of memory impairments in neurodegenerative diseases.

Commento [n1]:

5.1 MODEL OF LPS-INDUCED NEUROINFLAMMATION

The animal model of chronic neuroinflammation used in this thesis is produced by a slow long-term infusion of the pro-inflammogen LPS. LPS selectively binds to a signal-transduction receptor complex (CD14/Toll-like receptor 4) that is expressed only by microglia (Lehnardt et al., 2003). By activating microglia through LPS infusion, young rats can show pathological, biochemical and behavioral changes that are similar to those

observed in several neurodegenerative diseases associated with neuroinflammation. These include impaired spatial memory, reduction of NMDA-R1 receptors, astrocytosis, elevated cytokines and proinflammatory transcription factors (Hauss-Wegrzyniak et al., 1998, 2000; Rosi et al., 2004, 2005, 2006). The results obtained in this thesis using this model demonstrate an important regulatory intercommunication that involves glutamate and neuronal NMDA receptor-dependent influx of Ca^{2+} in the control of the release of CD200, a molecular messenger that maintains the response of microglia to ongoing brain inflammation.

Because chronic neuroinflammation results in increased levels of glutamate, it is possible that a significant proportion of NMDA channels may thus be relieved from the Mg^{2+} block by the high glutamate, thus allowing elevated Ca^{2+} entry into postsynaptic neurons (Brown and Bal-Price, 2003). Therefore, further increases in glutamatergic activity induced by behavior could lead to excessive influx of Ca^{2+} ions (Albin and Greenamyre, 1992).

In these experiments we have shown that chronic infusion of LPS into the 4^{th} ventricle increased the number of activated microglia in the hippocampus, mainly within the DG and CA3 regions, in accordance to our previous report (Rosi et al, 2006) in which we also showed that activation of microglia within the hippocampus can be significantly reduced by memantine, a low to moderate-affinity non competitive NMDA receptor antagonist (Rosi et al, 2006). NMDA receptors have an important physiological role in learning and memory, but receptor overactivation owing to increased glutamate release leads to excessive Ca^{2+} entry, triggering neuronal death, a phenomenon termed 'excitotoxicity'. Memantine is postulated to exert its therapeutic effect through its action as a low to moderate affinity uncompetitive (open-channel) NMDA receptor antagonist which binds preferentially to the NMDA receptor-operated cation channels, (Ferris SH.

Evaluation of memantine for the treatment of Alzheimer's disease. Expert Opin Pharmacother. 2003 Dec;4(12):2305-13), thus blocking pathological, but not physiological, activation of the NMDA receptor. The current study extended the discovery by Rosi et al. (2006) that showed that blockade of the NMDA receptor by memantine can reduce microglia activation even if the inflammatory processes were fully initiated prior to the beginning of drug therapy. This finding is consistent with the hypothesis that the maintenance of microglial activation in the presence of an inflammogen requires continuing activation of NMDA receptors. Thus, because of its unique biophysical and pharmacological properties, memantine, given at low doses, can selectively block the pathological influx of Ca^{2+} through NMDA receptors without affecting the voltage-dependence of NMDA receptor transmission, which is critical for learning and memory (Rogawski and Wenk, 2003). In addition, it has been demonstrated that during LPS infusions elevated levels of glutamate activate phospholipase A_2 which increases the release of arachidonic acid from neurons and thus the formation of prostaglandins that act on microglia to augment a vicious cycle of cell inflammation (Lee et al., 2004). By restoring normal Ca^{2+} entry through the NMDA receptor channels, memantine also prevents the release of arachidonic acid and the consequent elevation of prostaglandins, resulting in lowered activation of microglial cells.

The results of the current study lead us to hypothesize that the following series of events are set in motion under the conditions of a pro-inflammatory environment that is initiated by the slow long term infusion of LPS: increased release of cytokines by resident microglia that express the TLR4/CD14 receptor complex (Quan et al., 1994); cytokines in turn induce the production of other proinflammatory mediators including prostaglandins (Katsuura et al., 1989); prostaglandins induce the release of glutamate by

astrocytes (Bezzi et al., 1998); increased extracellular levels of glutamate activate its receptors leading to the unblocking of the NMDA receptor channel, thus allowing the entry of Ca^{2+} ions into neurons with increased synaptic activity (Viviani et al., 2003).

It has been demonstrated that chronic neuroinflammation significantly increases the behaviourally-induced expression of the immediately early gene *Arc* (Rosi et al., 2005) in hippocampal cell fields containing the highest numbers of activated microglia induced by LPS infusion (Rosi et al., 2005). Given that *Arc* mRNA transcription is induced by NMDA receptor activation (Steward and Worley, 2001) and Ca^{2+}-mediated activation of cAMP (Waltereit et al., 2001), it was speculated that the overexpression of *Arc* was due to excess Ca^{2+} influx through postsynaptic NMDA receptors (Rosi et al., 2005). Furthermore, this disruption in glutamate-dependent Ca^{2+} regulation is associated with impaired learning and memory abilities (Rosi et al., 2006). NMDA receptor current is also potentiated by increased levels of arachidonic acid that also characterize the pro-inflammatory environment (Miller et a., 1992). In the current study, the elevated entry of Ca^{2+} ions, as confirmed by increased cytoplasmic levels of immunoreactive calbindin, initiated a cascade of molecular processes, possibly involving activation of a mitogen-activated protein kinase (MAPK) signaling pathway (Haddad, 2005), that leads to reduced expression of CD200 (Hoek et al., 2000; Lyons et al., 2007; Stamenkovic et al., 1991; Frank et al., 2006). CD200 is a membrane glycoprotein, expressed by neurons, that binds to a receptor expressed by microglia. The intercommunication between neurons and microglia through CD200 binding to its microglia receptor is believed to maintain microglia in a quiescent state (Hoek et al., 2000; Lyons et al., 2007; Stamenkovic et al., 1991; Frank et al., 2006).

Indeed we have demonstrated in these experiments that chronic LPS infusion significantly reduced the number of CD200 positive cells in the CA3 region of the

hippocampus. We speculate that the decrease of CD200 may create a permissive environment which will last not only during active inflammation, but also after the levels of LPS have decreased, thus permitting persistent activation of microglia, as evidenced in the 8-weeks rats that presented OX-6 immunoreactive microglia even after the end of LPS treatment..

The fact that memantine administration restored CD200 expression to normal levels suggests that the increased influx of Ca^{2+} ions through open NMDA channels is necessary for maintenance of a pro-inflammatory environment. Consistent with this hypothesis, we found that the reduced Ca^{2+} ions entry into CA3 neurons in memantine-treated rats infused with LPS was associated with reduced cytoplasmic calbindin immunoreactivity. Taken together, our results indicate that in the presence of memantine, neurons are able to produce and release CD200 in order to communicate with microglia to reduce its expression of MHCII and become quiescent. Consistent with our hypothesis, a recent report demonstrated that enhanced expression of CD200 in an animal model of experimental autoimmune encephalomyelitis is associated with neuroprotection from LPS-induced microglia-mediated toxicity, while treatment with anti-CD200 antibodies increase neurotoxicity (Chitnis et al., 2007).

HMGB1 is a non-histone DNA-binding protein that has a pro-inflammatory cytokine-like function that may influence the activation of microglia following injury or insult (Kim et al., 2006). It has been demonstrated that HMGB1 levels are low in resting glia but are increased in the brains of patients with Alzheimer's disease (Takata et al., 2004). Extracellular HMGB1 has also been described as a mediator of lipopolysaccharide (LPS) toxicity (Ulloa & Messmer, 2006). These experiments demonstrate that hippocampal HMGB1 expression did not differ across groups when examined by immunofluorescence and western blot analyses. As reported by others, the protein was

expressed in the nucleus of hippocampal neurons within the CA3 regions (Lo Coco et al., 2007). HMGB1 can be released by neurons undergoing necrosis and retained in the nucleus by cells undergoing apoptosis (Scaffidi at al., 2002). Taken together with the current findings, the long term, low dose infusion of LPS or low dose administration of memantine, does not induce necrosis or apoptosis, a conclusion that is consistent with our previous reports (Rosi et al., 2005, 2006), thus demonstrating that this protein is not involved in LPS-induced neuroinflammation.

Our results offer a novel molecular mechanism to explain how inflammation can disturb the intercommunication between neurons and glia.

Which comes first in the process of reduction of neuroinflammation, the signal from neurons or the signal from microglia? Our results are consistent with the hypothesis that under resting conditions, the neuron continually informs the resident microglia that activation is not necessary. This communication ceases when the neuron experiences an injury that leads to the activation of the surrounding microglia. Many neurodegenerative diseases that involve diffuse brain inflammation occur in aged humans and the number of activated microglia increase with aging. A decline in CD200 mRNA levels with aging may underlie these changes (Frank et al., 2006; Lyons et al., 2007). Therefore, therapeutically relevant doses of memantine delivered at any stage in the progression of age-associated neuroinflammation-influenced diseases may confer neuroprotection by partially restoring normal communication between neurons and microglia.

5.2 CELLULAR CHANGES IN AGED RATS COMPARED TO YOUNG RATS.

Since LPS-induced neuroinflammation is a model that reproduces a condition present in patients with neurodegenerative disorders, such as AD, we arose the question about the possible differences on inflammatory markers activation in old rats compared to young rats. In order to verify the activation status of neuroinflammatory markers, activated microglia, astrocytes and iNOS were studied in old and young rats.

Consistent with the results of the LPS–induced neuroinflammation model, in the hippocampus of old rats, a natural model of neuroinflammation, we found an increase of activated microglial cells in comparison to the same brain region of young rats. As already reported for the LPS-induced neuroinflammation model, the activation of microglial cells was mainly observed in the CA1 and the hilus of the dentate gyrus of the hippocampus. These results are consistent with the hypothesis that there are aging-related neuronal changes in the brain. Several studies have reported significant age-related changes in microglial expression of MHC class II antigens in rats (Ogura et al., 1994; Perry et al., 1993), and changes in microglial morphology (Conde et al., 2005; Streit et al., 2005).

The reasons that determine the regional gradient of microglia activation are actually unknown. However, it is interesting to consider the topographic overlap of the architecture of hippocampal vascularisation and distribution of activated microglial cells observed in aged hippocampus. The hilar and CA3 region displayed a higher capillary density compared to CA1 (Cavaglia et al., 2001) Thus, it is possible to conseive the existence of aged-related structural and functional alterations in the blood-brain barrier (BBB) leading to an increase in permeability, with serum leakage and leukocyte

infiltration into the neuronal parenchyma, all supported by the increased expression of the mRNA coding for interferon-gamma, synthesized by T-cells observed in aged rats hippocampus (Gavilàn et al., 2007).

Other studies report also an aged-related increment of astrogliosis (Duffy et al., 1980; Anderson et al., 1983). On the contrary our results show a decrease of astrocytes in the regions of the hippocampus (CA3, CA1 and DG) of old rats. Furthermore, hippocampal astrocytes of old rats show an apparent morphology, as stained using GFAP antibodies, that is different from that seen in young rat hippocampus. Indeed, old rats astrocytes have smaller cell bodies and shorter and thinner branchings, compared to young rats astrocytes that, on the contrary, have stellate morphology, hyperthrophic body and dense, long arborizations departing from cell bodies. These results are at variance with what one might be expecting, since this latter phenotype is usually typical of activated astrocytes. It is also evident from the images taken that a dysregulation not only of astrocytes morphology, but also of their distribution in the hippocampal parenkyma is present in aged rats. Contrary to the original belief that astrocytes mainly represent support elements in the CNS, (Peuchen, S., Bolanos, J.P., Heales Jr., S., Almeida, A., Duchen, M.R., Clark, J.B., 1997.. Prog. Neurobiol.52, 261–281.), in recent years it has started to emerge the crucial roles that astrrrocytes may play in maintaining normal brain physiology, such as production of neurotrophic factors, conservation of glycogen as energy reserve, regulation of extracellular ionic composition, and uptake and degradation of neurotransmitters (Takuma, K., Baba, A., Matsuda, T., 2004.. Prog. Neurobiol. 72, 111–127.). It has recently been demonstrated (Lü et al, Neurochemistry International 52 (2008) 282–289) that an oxidative stress leads to inadequate peroxide detoxification by astrocytes in colture. This is followed by astrocytes death, and possibly by damage to the neurons. These effect may play a role in aging of the central

nervous system, since the production of reactive oxygen species increases with age. Thus, the results obtained in the present work may be explained hypothesizing that in aged rat hippocampus astrocytes decrease in number because of increased oxidative stress thus loosing their normal trophic activity towards hippocampal pyramidal neurons and granule cells. However, these findings need to be further investigated to better understand the mechanisms underlying the decrease in astrocytes present in the hippocampus of aged rats and the functional meaning of the morphological changes.

Finally, we studied the expression of iNOS, another inflammatory marker, commonly overexpressed in different cell types during inflammation. Our results show an increased iNOS expression in the CA3 of the hippocampus of old rats in comparison to young rats, mainly in pyramidal neurons. These results are consistent with published studies where an increased iNOS expression was mainly found in the CA3 of the hippocampus, the same area where there is the highest activation of microglial cells (Gavilàn et al., 2007).

In conclusion we can say that age-related differences in the structure of the BBB, in the changes of inflammatory markers, together with other genetics and environmental factors, could constitute summatory risk factors of multifactorial disease such as AD, for which aging represents the most important risk factor.

5.2.1 The ERK1/2, p38MAPK, and JNK pathways

Three main mammalian MAPK subfamilies have been described: ERK1,2, JNK, and p38MAPK kinase (Pearson et al., 2001). MAPKs are implicated in various cellular processes (Raman et al., 2007), and dysfunction of specific MAPKs is associated with diseases such as cancer and immunological disorders. In the nervous system, as well as in other tissues, activation of JNK and p38MAPK has often been correlated with death

in various cell types, including neurons (Xia et al., 1995; Kummer et al., 1997; Willaime- Morawek et al., 2003), while it is widely accepted that activation of neuronal ERK1,2 has protective effects and leads to memory formation (Sweatt, 2001, 2004). Nevertheless, the genuine *in vivo* physiological functions of MAPK still remain to be fully unraveled. We have demonstrated that the three main MAPK pathways are differentially activated in cells of the hippocampus of old rats in comparison to young rats and in the hippocampus of transgenic TgCRND8 mice in comparison to Wt littermates. Indeed we found that the ERK pathway, both in basal and stimulated conditions is less activated in the hippocampus of old rats and of TgCRND8 mice in comparison to young rats and Wt littermates, respectively. On the contrary the p38MAPK pathway is more activated in the hippocampus of old rats and of TgCRND8 mice in comparison to young rats and Wt littermates, respectively. The third MAPK under investigation, the JNK pathway was highly activated in the surroundings of the amyloid plaques in the hippocampus of TgCRND8 mice, but was not activated in the hippocampus of aged rats.

5.3 DIFFERENTIAL ACTIVATION OF MAPK PATHWAYS IN THE HIPPOCAMPUS OF AGED RATS.

Old rats showed high levels of phospho-p38MAPK in neurons of the entire hippocampus. The distribution of activated p38MPAK is mainly in pyramidal neurons of CA3, CA1 and DG. On the contrary, in our experiments no differences on JNK activation in the hippocampus of old animals compared to young animals were observed, in contrast with other results reported in the literature in which it was found

an 3.5 fold increment of phospho-JNK in old animals compared to young animals (Yousin, 2001).

As known, JNKs and p38MAPKs are collectively termed the stress-activated protein kinases (SAPKs) because they are activated by similar stress-related stimuli (Karin, 1995; Paul et al., 1997). Activation of SAPKs has been associated wit stress responses that promote either cell recovery and cell survival or apoptotic death after cellular damage (Paul, 1997; Ono and Han, 2000). Studies have demonstrated that activation of microglia by adenovirus vector induces activation of p38MAPK pathways (Narayan and Fan Fan, 2002).Thus, in our study, activation of microglia by normal aging, leads to activation of p38MAPK.

Aged rats have memory impairment in a step down inhibitory avoidance test, as demonstrated by the significantly shorter time spent to step down from the platform during the recall test, in comparison to young animals. Activation of the ERK pathway was studied 10 min after the acquisition of the step down inhibitory avoidance test in old and young rats. Our results show no activation of ERK in the hippocampus of old rats 10 min after the acquisition, in comparison with young rats.

The components of the Extracellular signal Regulated Kinases-1 and -2 (ERK1/2) signal transduction pathways are ubiquitous and well conserved protein kinases involved in relaying extracellular signals into intracellular responses, and are involved in the mechanisms of synaptic plasticity, learning and memory. ERK activation is required for the full expression of LTP (English and Sweatt, 1997, Giovannini et al., 2001), the principal cellular mechanism thought to underlie neuronal plasticity. Furthermore, ERK is activated in and is necessary for the development of several forms of memory, such as fear conditioning (Atkins et al., 1998), conditioned taste aversion memory (Berman et al., 1998), spatial memory (Blum et al., 1999; Selcher et al. 1999), step-down inhibitory

avoidance (Walz et al., 2000; Cammarota et al., 2000) and object recognition memory (Kelly et al., 2003). In a previous paper published by our laboratory in 2005 (Giovannini et al., 2005), we demonstrated that ERK activation is secondary to neurotransmitter release and activation of the forebrain cholinergic neurons during and immediately after acquisition of an inhibitory avoidance response, revealed by increased release of ACh, which in turn activates ERK in neurons located in the CA1 of the hippocampus. Increased release of ACh and ERK activation are events mechanistically related to each other, as demonstrated by the use of scopolamine, a muscarinic receptor antagonist, and by inhibitors of ERK activation, which all blocked memory encoding and ERK activation. A critical function of activated ERK downstream of the increased ACh release occurring during learning is to promote cellular integration of divergent downstream effectors which may trigger different responses, depending upon which subsets of scaffolding anchors, target proteins and regulatory phosphatases are involved. In the present study, the results obtained demonstrate that in old rats, after the acquisition of a inhibitory avoidance memory task, there is a lower activation of ERK as compared to young rats in CA1, and this low activation is correlated to a worse performance of the task as compared to young rats, as shown by the graph of the latencies. Taken together these results demonstrate a correlation between memory deficit of the rats, and low activation of ERK pathway. The hope is that by studying how ERK is activated by different neurotransmitter systems and the ensuing downstream cellular modifications, the molecular basis of memory encoding and memory impairment will be better understood.

5.4 DIFFERENTIAL ACTIVATION OF MAPK PATHWAYS IN TRANSGENIC TgCRND8 MICE, MODEL OF AD.

5.4.1 The p38MAPK and JNK pathways

Our results show that in the hippocampus of 7-month-old TgCRND8 mice a significant activation of p38MAPK and JNK was present in comparison to Wt littermates. High levels of phospho-p38MAPK were present not only in activated microglia and astrocytes localized in the parenchyma surrounding amyloid plaques, but also in neurons of the CA1 hippocampal region. On the contrary, activated JNK was localized only in round-shaped cells surrounding the amyloid plaques. Similar distribution of activated p38MAPK and JNK around the plaques was also found in other brain areas outside the hippocampus (data not shown). The presence of phospho-p38MAPK in astrocytes and activated microglia not only surrounding and infiltrating the plaques, but also localized in the more distant parenchyma of the hippocampus of TgCRND8 mice, support the idea that this transduction pathway may contribute to the neurodegenerative process. We found that phospho-p38MAPK was localized diffusely in the cell body of activated astrocytes and microglia thus implicating that downstream targets may be intracellular enzymes and cytosolic proteins (Xia et al., 1995). Indeed, given that activated p38MAPK is both upstream and downstream of proinflammatory agents, it appears that conditions exist in the AD brain for a self-propagating cycle of stimulation (Hull et al., 2002; Sun et al., 2003), in which p38MAPK plays a prominent role through the production of pro-inflammatory cytokines, IL-1β and others, cyclooxygenase-2, iNOS (Gonzalez- Scarano and Baltuch, 1999; Harris et al., 1995; Markesbery, 1999; Kaminska, 2005). We also demonstrated the presence of activated p38MAPK in the

pyramidal neurons of CA1. Phospho-p38MAPK may render these neurons more susceptible to neurodegenerative damage through activation of further intracellular signaling pathways. It is interesting to note that in the CA1 pyramidal neurons phospho-p38MAPK presented solely a nuclear localization, implying downstream activation of transcription factors such as ATF-2 (Kaminska, 2005) and increased expression of proteins, among which TNF-α (Takeda and Ichijo, 2002).

Three genes encoding for JNKs have been identified (JNK1, JNK2 and JNK3). Neurons from JNK3_/_ mice are more resistant than normal mice neurons to β-amyloidinduced apoptosis (Morishima et al., 2001) and to glutamate- induced excitotoxicity. In human postmortem brains from AD patients, JNK phosphorylation is markedly increased and there is pronounced redistribution of JNK compared with age-matched controls. JNK2 and JNK3 are associated with neurofibrillary pathology, and JNK upregulation has a complete overlap with phosphorylated tau (Zhu et al., 2001b). Indeed, increased activation of JNK and p38MAPK has been found in brain homogenates in all the tauopathies (Ferrer et al., 2005) and aberrantly activated p38MAPKs and JNK have been reported to be associated with cells that contain filamentous tau in AD (Atzori et al., 2001; Ferrer et al., 2001), suggesting that β-amyloid triggers activation of stress kinases which may phosphorylate tau in neurites surrounding β-amyloid deposits and form tau fibrils (Churcher, 2006). Moreover, activated JNK and p38MAPK phosphorylate c-Jun, AP1 and their target genes in AD (Ferrer et al., 2005). Unfortunately, it was not possible to confirm that phosphop38MAPK and phospho-JNK are colocalized in the same cellular species in TgCRND8 mice. Our results showing the presence of activated JNK in cells surrounding the amyloid plaques, are in agreement with other studies which demonstrate that in a different model of AD, namely

Tg2576/PS1 mice, APP is an excellent substrate for JNK3, and phosphorylation of this peptide is thought to be one of the factors mediating its cleavage by secretases (Savage et al., 2002). JNK activation is associated with amyloid deposits and phospho-tau staining (Savage et al., 2002; Bellucci et al., 2007). An overlap between activated JNK and p38MAPK in severe AD cases has been reported, implying that JNK and p38MAPK are both activated by the same signal and seem to work synergistically *in vivo* (Zhu et al., 2001a). Comparing these results with those obtained in the aged animals it appears that highly stressful conditions might be necessary for JNK to be activated within cells. These conditions can evidently be found in the surroundings of amyloid plaques but not in a normal aging brain.

5.4.2 The ERK pathway

Our findings demonstrate for the first time that the ERK2 isoform of the ERK pathway was less activated in the hippocampus of TgCRND8 mice both in basal conditions and after cholinergic stimulation, suggesting a mechanism responsible for the memory deficits typical of AD, possibly due to the interplay between the cholinergic system and the ERK pathway in the mechanisms of memory (Giovannini, 2006). We found that in basal conditions very sparse phospho-ERK immunopositive neurons were present in the hippocampus of the two mouse strains, mainly localized in the DG. However, ERK was more activated in the DG of Wt than Tg mice. Immunopositive staining was also present in the mossy fibers of Wt mice only. ERK is likely to participate in diverse forms of neuronal plasticity by virtue of its ability to regulate both transcription, once it is rapidly translocated into the nucleus (Impey et al., 1998), and translation at the dendritic level (Kim et al., 1998; Chen et al., 1998). The effects of ERK activation are

somehow controversial, since, while activation of ERK is widely believed to confer survival advantage to cells (Xia et al., 1995; Guyton et al., 1996), there are conditions in which ERK activation may result in cell death (Murray et al., 1998). However, it has been shown that in AD ERK seems to be highly activated (Webster et al., 2006; Swatton et al., 2004). Thus, the hypothesis as to whether ERK activation might exert beneficial or detrimental effects on neuronal activity, depending on the cellular context, the duration of activation, the presence of scaffolding proteins (Pouyssegur et al., 2002) should be taken into consideration. Indeed, differential durations of ERK activation/disactivation are regulated by different molecular/cellular components and can elicit unique gene expression profiles (York et al., 1998; Corbit et al., 1999), which result in different cellular functions (Marshall, 1995), and final cellular outcomes. For instance, transient activation of ERK triggers cell differentiation in PC12 cells, whereas prolonged activation results in cell proliferation (Traverse et al., 1992). In accordance with our data, the basal levels of phospho-ERK1,2, measured in cell lines from AD patients and age-matched controls, were lower in AD cell lines suggesting that the intrinsic phosphorylation of ERK was dysfunctional in AD patients (Khan and Alkon, 2006). Similarly, it has been demonstrated that β-amyloid generates oxidative species that can activate p38MAPK and JNK and decrease ERK activity (Troy et al., 2001), possibly leading to cell death (Daniels et al., 2001). Furthermore, lower activation of ERK in hippocampal neurons may lead to memory deficits (Kelleher et al., 2004; Atkins et al., 1998; Selcher et al., 1999). It should also be pointed out that in the brains of double Tg mice, expressing both the mutant APPsw and PS1, it was found that ERK1,2 was not significantly activated while activation of JNK-1 and p38MAPK were

increased (Hwang et al., 2005) indicating that JNK and p38MAPK activation may be required for β-amyloid –induced cell death, while ERK is not involved (Hwang et al., 2005). The rationale for a signaling pathway being responsible at the same time for survival/plasticity/memory and/or neuronal degeneration is not clear. However it appears (Pouyssegur et al., 2002) that the kinetics and duration of ERK activation may play an important role in influencing its effect on cell fate. Obviously, differential durations of ERK activation are regulated by different molecular players (York et al., 1998; Corbit et al., 1999), and can elicit unique gene expression profiles, which consequently result in different cellular function (Marshall, 1995). The possibility that sustained ERK can activate death programs independent of caspases in neurons (Subramaniam et al., 2004) suggests that ERK activation appears to be involved in non-apoptotic modes of neuronal death. On the contrary, activation of ERK and Akt has been found to confer neuroprotection in several models of apoptosis (Hetman et al., 1999). Similarly, both Akt and ERK have been reported to play a role in regulating hippocampal neurogenesis (Aberg et al., 2003). Most interestingly, our experiments demonstrated that *ex vivo* incubation with the non-selective cholinergic agonist CCh, mimicking a cholinergic stimulation, induced much lower activation of ERK in Tg mice hippocampus than in Wt littermates. This effect was not ascribable to lower levels of the ERK protein, similar in the two mouse strains, but possibly to modifications upstream of ERK, among which a decrease in the number of muscarinic receptors, significantly less numerous in TgCRND8 mice (Bellucci et al., 2006), might play a role. The "cholinergic hypothesis" of AD (Bartus et al., 1982) posits degeneration of cholinergic neurons and loss of cholinergic transmission as the principal cause of cognitive dysfunction in patients with AD (Perry et al., 1978; Bartus et al., 1982). Studies in

animal models of AD (Hsiao et al., 1996; Calhoun et al., 1998; Bondolfi et al., 2002; Giovannini et al., 2002; Geula et al., 1998; Bellucci et al., 2006), reinforce the notion that overexpression of β-amyloid may induce subcellular alterations and cholinergic loss in specific brain regions such as the basal forebrain. The ERK pathway has been demonstrated to be activated in neurons i*n vitro* by several G-protein-coupled receptors, among which the M1 muscarinic receptors in rat (Rosenblum t al., 2000) and mouse (Berkeley et al., 2001) brain as well as by nicotinic receptors (Dineley et al., 2001), indicating strong connections between these two systems whose dysregulation is involved in AD pathogenesis. Indeed, activation of the cholinergic system and of the ERK pathway is necessary for memory formation (Giovannini, 2006). Thus, the loss of basal forebrain cholinergic neurons in the Tg mouse (Bellucci et al., 2006) may lead to decreased tonic cholinergic input to the hippocampus which, together with the decrease of muscarinic receptors (Bellucci et al., 2006), might be responsible for the lower activation of ERK, thus causing the memory deficits observed in this mouse strain, which resemble the memory deficits typical of AD (Bellucci et al., 2006). Thus, our findings may pose a molecular basis for the memory disruption of AD, since memory function requires proper functioning of the basal forebrain cholinergic neurons (Pepeu, 1983; Sarter and Bruno, 1997) and ERK2 activation (Adams and Sweatt, 2002; Atkins et al., 1998; Kaminska et al., 1999; Blum et al., 1999; Walz et al., 2000; Cammarota et al., 2000). Since all MAPK pathways transduce intracellular signalling to increase expression of different proteins, dysregulation of MAPK-dependent pathways suggests a systematic disorder of protein translation regulation in AD brains. Thus, the exact knowledge of the MAPK role and of the complex molecular interactions between MAPKs and proteins associated with the evolution of neurodegeneration, among which

a role might be played by CD200, may be a cornerstone in the burgeoning field of AD, and the outcome of basic research aimed at understanding the role of MAPKs in neurodegeneration is also of significant interest to find new therapies for AD.

5.5 EFFECT OF PEC, NP-0361 AND NP-0336 ON ACh RELEASE AND CHOLINESTERASE ACTIVITY IN THE CEREBRAL CORTEX OF YOUNG RATS

Colinergic neurons of the basal forebrain are known to be involved in cognitive and behavioral functions that are widely disturbed in Alzheimer's disease (AD). In particular, AD is characterized by a forebrain cholinergic neuron loss and a progressive decline in ACh (Perry, E., Perry, R., Blessed, G. & Tomlinson, B. (1978) *Neuropathol. Appl. Neurobiol.* **4,** 273–277.; Geula, C. & Mesulam, M. M. (1995) *Alz. Dis. Assoc. Dis.* **9,** Suppl. 2, 23–28.). Activity of ACh in the brain is terminated by the hydrolytic action of ChEs. Inhibitors of these enzymes have been developed to augment the availability of synaptic ACh in patients with AD. All ChEIs currently available for AD inhibit AChE, and, to a varying extent, BuChE,, a second ChE in brain (Lahiri, D., Farlow, M., Sambamurti, K., Greig, N., Giacobini, E. & Schneider, L.(2003) *Curr. Drug Targets* **4,** 97–112.). AChE and BuChE have numerous physiological functions depending on their localization and time of expression (Soreq, H. & Seidman, S. (2001) *Nat. Rev. Neurosci.* **2,** 294–302). In healthy human brain, AChE predominates over BuChE activity (Giacobini, E. (2003) *Int. J. Geriatr. Psychiatry* **18,** S1–S5.), but the latter likely has been previously underestimated (Li, B., Stribley, J., Ticu, A., Xie. W., Schopfer, L., Hammond, P., Brimijoin, S., Hinrichs, S. & Lockridge, O. (2000) *J. Neurochem.* **75,** 1320–1331.).

While AChE is localized mainly to neurons, BuChEis associated primarily with glial cells, as well as to endothelial cells and neurons (Darvesh, S., Hopkins, D. & Geula, C. (2003) *Nat. Rev. Neurosci.* **4,** 131–138.). The close spatial relationship of glial BChE would allow synergistic BuChE-mediated hydrolysis to assist in the regulation of local ACh levels to permit the maintenance of normal cholinergic function. The survival of AChE knockout mice (Li, B., Stribley, J., Ticu, A., Xie. W., Schopfer, L., Hammond, P., Brimijoin, S., Hinrichs, S. & Lockridge, O. (2000) *J. Neurochem.* **75,** 1320–1331.) with normal levels and localization of BuChE (Mesulam, M., Guillozet, A., Shaw, P., Levey, A., Duysen, E. & Lockridge, O. (2002) *Neuroscience* **110,** 627–639) supports the concept that BuChE has a key role that can partly compensate for the action of AChE. In the AD brain, increasing levels of BChE correlate positively with the development of hallmark cortical and neocortical amyloid rich neuritic plaques and neurofibrillary tangles (Geula, C. & Mesulam, M. M. (1995) *Alz. Dis. Assoc. Dis.* **9,** Suppl. 2, 23–28., Guillozet, A., Smiley, J., Mash, D. & Mesulam, M. (1997) *Ann. Neurol.* **42,** 909–918). In light of the suggested role of BChE in central cholinergic transmission, its altered expression in AD brain, and probable association with the development of neuropathologic changes, inhibiting this enzyme would be of clinical value. We tested novel BuChE inhibitors on cortical ACh release and AChE/BuChE activity.

Our results show that donepezil (1 mg/kg) and rivastigmine (0.6 mg/kg) administration is followed by 4 fold, while PEC administration (5 mg/kg) by 2.5 fold increase in cortical ACh release. At the doses used, when peak ACh levels were reached in the rat cerebral cortex, donepezil inhibited significantly only AChE activity, PEC inhibited only BuChE activity, while rivastigmine inhibited both AChE and BuChE. The different inhibitory profiles of the three drugs “in vivo” correspond to their “in vitro” affinity for

AChE and BuChE. Donepezil is a selective AChE inhibitor (Giacobini, 2000), rivastigmine is a dual inhibitor exerting a comparable inhibition on both AChE and BuChE (Giacobini, 2000), while PEC is a selective BuChE inhibitor with a BuChE/AChE ratio of 0.0002 (Giacobini, 2003). We also demonstrated that the brain concentration of donepezil measured at peak effect (1 h) is about 180 nM which is in good agreement with earlier measurements by Kosasa et al. (2000). The experimentally-determined concentration of donepezil in the rat brain after administration of 1 mg/kg is 10 to 20 times higher than the reported in vitro IC50 ranging from 5 to 11 nM according to Rogers et al. (1991) and Enz (unpublished data), respectively. The brain rivastigmine concentration, measured after administration of 0.6 mg/kg, at peak ACh releasing effect (1 h after administration), was lower than that of donepezil, but still in the nM range (14 nM). Given that rivastigmine is rapidly metabolized by AChE and BuChE to the metabolite NAP 226-90 (Bar-On et al., 2002), we added up the concentration of both the parent drug and its metabolite, resulting in a total drug concentration of 72 nM. It is difficult to perform a direct comparison of the experimental brain concentration of rivastigmine plus NAP 226-90 with the in vitro rivastigmine IC50 value because of the time-dependent inhibition occurring with drugs of this kind. As reported by Ogura et al. (2000), an IC50 value of 4.3 nM for rivastigmine was estimated in rat brain in vitro after 48 h incubation. The increases in ACh extracellular levels observed in our experiments after the administration of donepezil and rivastigmine are comparable with those reported in the literature. Liang and Tang (2004), administering donepezil 4.0 μmol/kg, a dose about twice as high as that used in the present experiments, obtained an 80% increase in acetylcholine levels in the rat cortex, and similar increase was obtained with rivastigmine 1.1 μmol/kg, about one third of the dose used in our experiments. Giacobini et al. (1996) observed a 200% increase after the administration of donepezil

0.5 mg/kg s.c. In the present experiments the activity of PEC was about half as large than that reported by Greig et al. (2005). These variations are common in microdialysis experiments, given the variability in ACh release between rats, and other methodological variables such as the difference in the properties and preparation of the microdialysis membranes (Khan and Shuaib, 2001). The question arises whether a simple relationship between the increase in ACh levels and cholinesterase inhibition exists. In our experiments, the 3.5 fold increase of extracellular ACh levels found after donepezil and rivastigmine administration was associated with an AChE inhibition between 22 and 40%, respectively. It should be mentioned that, as shown by Kosasa et al. (1999) in the hippocampus, the maximum increase in ACh levels does not necessarily correspond to the maximum AChE inhibition, but the enzyme inhibition tends to anticipate the acetylcholine increase. Giacobini et al. (1996), investigating the effects of donepezil on extracellular acetylcholine levels, observed a 200% increase with a 15% AChE inhibition, and a 2100% increase with a 35% AChE inhibition. Scali et al. (1997), studying the effect of metrifonate, an irreversible non selective cholinesterase inhibitor, reported no significant cortical ACh increase with 30 mg/kg which inhibited cholinesterase activity by 16% but a 5-fold increase with 80 mg/kg which caused a 77% cholinesterase inhibition. Liang and Tang (2004) observed an 80% increase in ACh levels after the administration of donepezil and rivastigmine temporally associated with an AChE inhibition of 15 and 40%, respectively. We may therefore conclude that the data present in the literature show that no simple and straightforward correlation between the degree of cholinesterase inhibition and the increase in ACh levels seems to exist. Age-related differences in sensitivity to cholinesterase inhibitors, preferential affinity for different AChE molecular forms (Ogane et al., 1992; Zhao and Tang, 2002), relative abundance of the two enzymes and difference in their tissue

distribution (Ballard et al., 2005), as well as dilution effects during cholinesterase determination are some of the factors which may account for the lack of a precise relationship between ACh increase and AChE inhibition found after inhibitors administration. Therefore, the data so far available do not allow to define which is the minimal cholinesterase inhibition resulting in a significant increase in ACh extracellular levels (Pepeu, 2000).

PEC caused a 25–39% inhibition of BuChE which was accompanied by about two fold increase in cortical ACh extracellular level. The possibility to increase ACh levels by inhibiting BuChE was shown by Giacobini (2003) by infusing the selective BuChE inhibitor MF-8622 directly in the cortex of the rat. The present experiments demonstrate that a partial inhibition of BuChE is sufficient to increase ACh release to levels comparable to those obtained with the inhibition of AChE. However, BuChE activity in the brain is less than 10% of AChE activity, as shown in Table 1, or 20% as reported by Giacobini and Holmstedt (1958) in the rat spinal cord. Mesulam et al. (2002) demonstrated that AChE knockout mice are vital, and utilize BuChE to hydrolyze ACh. In our experiments the rats were normal, with full AChE activity, nevertheless partial inhibition of BuChE activity was able to increase ACh levels in the cortex. This finding suggests that the importance of BuChE as a "co-regulator" of synaptic ACh levels should be reconsidered, particularly under the light of the diffuse (volume) transmission which is a feature of central cholinergic mechanisms (Steriade and Descarries, 2006). PEC at the dose of 5 mg/kg did not significantly inhibit AChE. A non significant 5–12% inhibition, possibly ascribable to the variability of the two different detection methods used, was observed. This degree of inhibition is not usually accompanied by any increase in acetylcholine level (Pepeu, 2000).

Furthermore, our experiments confirm that NP-0361 at the dose of 20 mg/kg i.p. only exerts a statistically significant 39% inhibition of AChE. Conversely, the administration of NP-0336 at the dose of 80 ,g/kg i.p. is followed by statistically significant 15% BuChE inhibition only. Lower doses of the two drugs (10 mg/kg of NP-0361 and 40 mg/kg of NP-0336) were ineffective.

Both AChE and BuChE inhibitions were accompanied by an almost doubling of the extracellular levels of cortical ACh, lasting about 1 h, measured by transversal microdialysis coupled to HPLC detection and quantification.

The increase in ACh extracellular levels elicited by the administration of NP-0361 is smaller than the expected from a 39% AChE inhibition. By comparison, treatment with rivastigmine 1.0 mg/kg increases about 6 fold the ACh levels accompanied by a 50% of AChE inhibition. It is possible that the sedation observed in the rats treated with NP-0361 20 mg/kg, is also accompanied by the decrease activity of the cortical cholinergic system and the ensuing reduction in ACh release.

Conversely, it is remarkable that 15% BuChE inhibition is sufficient to increase ACh extracellular levels, considering that BuChE activity is only 10% of total cortical cholinesterase activity (Cerbai et al., 2007). However, the above results on BuChE inhibition, obtained after the administration of the selective BuChE inhibitor PEC, show a 3 fold increase in ACh extracellular levels (Cerbai et al., 2007).

A role of BuChE in neurotransmission is demonstrated also by the increase sensitivity to AChE inhibitors observed in BuChE knockout mice (Duysen et al., 2007). The increase in ACh levels after BuChE inhibition supports the hypothesis, proposed by O'Brien et al. (2003), that BuChE might be a major regulator of attention, based on studies on Alzheimer's patients with reduced BuChE activity due to polymorphism. Our results may also help explaining the findings by Bartorelli et al. (2005), that AD patients

deteriorating on selective AChE inhibitor treatment can benefit from switching to a dual AChE–BuChE inhibitor, such as rivastigmine, in terms of stabilization of disease and improvement in cognitive functions. Finally, it is pertinent to mention that BuChE is increased in the cerebral cortex of Alzheimer's disease patients (Perry et al., 1978) and it is associated with the amyloid plaques. It has been suggested that BuChE, together with AChE (Alvarez et al., 1997), may participate in the transformation of the β-amyloid deposit into neuritic plaques (Guillozet et al., 1997). Inhibition of the enzyme may therefore delay plaque formation, thus suggesting the possibility to use BuChE inhibitors in the treatment of Alzheimer's disease not only to increase the availability of ACh at the synapses, but also to reduce the number of plaques.

6. Reference List

1. Adams J, Collaco-Moraes Y, de Belleroche J (1996) Cyclooxygenase-2 induction in cerebral cortex: an intracellular response to synaptic excitation. J Neurochem 66: 6-13.

2. Aggleton JP, Mishkin M (1985) Mamillary-body lesions and visual recognition in monkeys. Exp Brain Res 58: 190-197.

3. Aisen PS (1997) Inflammation and Alzheimer's disease: mechanisms and therapeutic strategies. Gerontology 43: 143-149.

4. Akirav I, Sandi C, Richter-Levin G (2001) Differential activation of hippocampus and amygdala following spatial learning under stress. Eur J Neurosci 14: 719-725.

5. Alkondon M, Albuquerque EX (1993) Diversity of nicotinic acetylcholine receptors in rat hippocampal neurons. I. Pharmacological and functional evidence for distinct structural subtypes. J Pharmacol Exp Ther 265: 1455-1473.

6. Alkondon M, Reinhardt S, Lobron C, Hermsen B, Maelicke A, Albuquerque EX (1994) Diversity of nicotinic acetylcholine receptors in rat hippocampal neurons. II. The rundown and inward rectification of agonist-elicited whole-cell currents and identification of receptor subunits by in situ hybridization. J Pharmacol Exp Ther 271: 494-506.

7. Alonso M, Viola H, Izquierdo I, Medina JH (2002b) Aversive experiences are associated with a rapid and transient activation of ERKs in the rat hippocampus. Neurobiol Learn Mem 77: 119-124.

8. Alonso M, Viola H, Izquierdo I, Medina JH (2002a) Aversive experiences are associated with a rapid and transient activation of ERKs in the rat hippocampus. Neurobiol Learn Mem 77: 119-124.

9. Alvarez A, Opazo C, Alarcon R, Garrido J, Inestrosa NC (1997) Acetylcholinesterase promotes the aggregation of amyloid-beta-peptide fragments by forming a complex with the growing fibrils. J Mol Biol 272: 348-361.

10. Anderton BH, Betts J, Blackstock WP, Brion JP, Chapman S, Connell J, Dayanandan R, Gallo JM, Gibb G, Hanger DP, Hutton M, Kardalinou E, Leroy K, Lovestone S, Mack T, Reynolds CH, Van Slegtenhorst M (2001) Sites of phosphorylation in tau and factors affecting their regulation. Biochem Soc Symp 73-80.

11. Apergis-Schoute AM, Debiec J, Doyere V, LeDoux JE, Schafe GE (2005) Auditory fear conditioning and long-term potentiation in the lateral amygdala

require ERK/MAP kinase signaling in the auditory thalamus: a role for presynaptic plasticity in the fear system. J Neurosci 25: 5730-5739.

12. Arendt T, Bruckner MK, Lange M, Bigl V (1992) Changes in acetylcholinesterase and butyrylcholinesterase in Alzheimer's disease resemble embryonic development--a study of molecular forms. Neurochem Int 21: 381-396.

13. Atkins CM, Selcher JC, Petraitis JJ, Trzaskos JM, Sweatt JD (1998a) The MAPK cascade is required for mammalian associative learning. Nat Neurosci 1: 602-609.

14. Atkins CM, Selcher JC, Petraitis JJ, Trzaskos JM, Sweatt JD (1998b) The MAPK cascade is required for mammalian associative learning. Nat Neurosci 1: 602-609.

15. Atzori C, Ghetti B, Piva R, Srinivasan AN, Zolo P, Delisle MB, Mirra SS, Migheli A (2001) Activation of the JNK/p38 pathway occurs in diseases characterized by tau protein pathology and is related to tau phosphorylation but not to apoptosis. J Neuropathol Exp Neurol 60: 1190-1197.

16. Baddeley A (1992) Working memory. Science 255: 556-559.

17. Bading H, Greenberg ME (1991) Stimulation of protein tyrosine phosphorylation by NMDA receptor activation. Science 253: 912-914.

18. Ballmaier M, Casamenti F, Scali C, Mazzoncini R, Zoli M, Pepeu G, Spano PF (2002) Rivastigmine antagonizes deficits in prepulse inhibition induced by selective immunolesioning of cholinergic neurons in nucleus basalis magnocellularis. Neuroscience 114: 91-98.

19. Banati RB, Gehrmann J, Czech C, Monning U, Jones LL, Konig G, Beyreuther K, Kreutzberg GW (1993) Early and rapid de novo synthesis of Alzheimer beta A4-amyloid precursor protein (APP) in activated microglia. Glia 9: 199-210.

20. Baratti CM, Huygens P, Mino J, Merlo A, Gardella J (1979) Memory facilitation with posttrial injection of oxotremorine and physostigmine in mice. Psychopharmacology (Berl) 64: 85-88.

21. Bard F, Cannon C, Barbour R, Burke RL, Games D, Grajeda H, Guido T, Hu K, Huang J, Johnson-Wood K, Khan K, Kholodenko D, Lee M, Lieberburg I, Motter R, Nguyen M, Soriano F, Vasquez N, Weiss K, Welch B, Seubert P, Schenk D, Yednock T (2000) Peripherally administered antibodies against amyloid beta-peptide enter the central nervous system and reduce pathology in a mouse model of Alzheimer disease. Nat Med 6: 916-919.

22. Barger SW, Harmon AD (1997) Microglial activation by Alzheimer amyloid precursor protein and modulation by apolipoprotein E. Nature 388: 878-881.

23. Barros DM, Pereira P, Medina JH, Izquierdo I (2002) Modulation of working memory and of long- but not short-term memory by cholinergic mechanisms in the basolateral amygdala. Behav Pharmacol 13: 163-167.

24. Bartolini L, Casamenti F, Pepeu G (1996) Aniracetam restores object recognition impaired by age, scopolamine, and nucleus basalis lesions. Pharmacol Biochem Behav 53: 277-283.

25. Bartorelli L, Giraldi C, Saccardo M, Cammarata S, Bottini G, Fasanaro AM, Trequattrini A (2005a) Effects of switching from an AChE inhibitor to a dual AChE-BuChE inhibitor in patients with Alzheimer's disease. Curr Med Res Opin 21: 1809-1818.

26. Bartorelli L, Giraldi C, Saccardo M, Cammarata S, Bottini G, Fasanaro AM, Trequattrini A (2005b) Effects of switching from an AChE inhibitor to a dual AChE-BuChE inhibitor in patients with Alzheimer's disease. Curr Med Res Opin 21: 1809-1818.

27. Bartus RT, Dean RL, Pontecorvo MJ, Flicker C (1985) The cholinergic hypothesis: a historical overview, current perspective, and future directions. Ann N Y Acad Sci 444: 332-358.

28. Baumann K, Mandelkow EM, Biernat J, Piwnica-Worms H, Mandelkow E (1993) Abnormal Alzheimer-like phosphorylation of tau-protein by cyclin-dependent kinases cdk2 and cdk5. FEBS Lett 336: 417-424.

29. Bellucci A, Luccarini I, Scali C, Prosperi C, Giovannini MG, Pepeu G, Casamenti F (2006) Cholinergic dysfunction, neuronal damage and axonal loss in TgCRND8 mice. Neurobiol Dis 23: 260-272.

30. Berkeley JL, Gomeza J, Wess J, Hamilton SE, Nathanson NM, Levey AI (2001) M1 muscarinic acetylcholine receptors activate extracellular signal-regulated kinase in CA1 pyramidal neurons in mouse hippocampal slices. Mol Cell Neurosci 18: 512-524.

31. Berman DE, Dudai Y (2001) Memory extinction, learning anew, and learning the new: dissociations in the molecular machinery of learning in cortex. Science 291: 2417-2419.

32. Berman DE, Hazvi S, Neduva V, Dudai Y (2000) The role of identified neurotransmitter systems in the response of insular cortex to unfamiliar taste: activation of ERK1-2 and formation of a memory trace. J Neurosci 20: 7017-7023.

33. Berman DE, Hazvi S, Rosenblum K, Seger R, Dudai Y (1998b) Specific and differential activation of mitogen-activated protein kinase cascades by unfamiliar taste in the insular cortex of the behaving rat. J Neurosci 18: 10037-10044.

34. Berman DE, Hazvi S, Rosenblum K, Seger R, Dudai Y (1998c) Specific and differential activation of mitogen-activated protein kinase cascades by unfamiliar taste in the insular cortex of the behaving rat. J Neurosci 18: 10037-10044.

35. Berman DE, Hazvi S, Rosenblum K, Seger R, Dudai Y (1998a) Specific and differential activation of mitogen-activated protein kinase cascades by unfamiliar taste in the insular cortex of the behaving rat. J Neurosci 18: 10037-10044.

36. Berntson GG, Sarter M, Cacioppo JT (1998) Anxiety and cardiovascular reactivity: the basal forebrain cholinergic link. Behav Brain Res 94: 225-248.

37. Bevilaqua LR, Bonini JS, Rossato JI, Izquierdo LA, Cammarota M, Izquierdo I (2005a) The entorhinal cortex plays a role in extinction. Neurobiol Learn Mem.

38. Bevilaqua LR, Bonini JS, Rossato JI, Izquierdo LA, Cammarota M, Izquierdo I (2005b) The entorhinal cortex plays a role in extinction. Neurobiol Learn Mem.

39. Biernat J, Gustke N, Drewes G, Mandelkow EM, Mandelkow E (1993) Phosphorylation of Ser262 strongly reduces binding of tau to microtubules: distinction between PHF-like immunoreactivity and microtubule binding. Neuron 11: 153-163.

40. Blum S, Moore AN, Adams F, Dash PK (1999a) A mitogen-activated protein kinase cascade in the CA1/CA2 subfield of the dorsal hippocampus is essential for long-term spatial memory. J Neurosci 19: 3535-3544.

41. Blum S, Moore AN, Adams F, Dash PK (1999b) A mitogen-activated protein kinase cascade in the CA1/CA2 subfield of the dorsal hippocampus is essential for long-term spatial memory. J Neurosci 19: 3535-3544.

42. Blum S, Moore AN, Adams F, Dash PK (1999c) A mitogen-activated protein kinase cascade in the CA1/CA2 subfield of the dorsal hippocampus is essential for long-term spatial memory. J Neurosci 19: 3535-3544.

43. Blum S, Moore AN, Adams F, Dash PK (1999d) A mitogen-activated protein kinase cascade in the CA1/CA2 subfield of the dorsal hippocampus is essential for long-term spatial memory. J Neurosci 19: 3535-3544.

44. Boulter J, Connolly J, Deneris E, Goldman D, Heinemann S, Patrick J (1987) Functional expression of two neuronal nicotinic acetylcholine receptors from cDNA clones identifies a gene family. Proc Natl Acad Sci U S A 84: 7763-7767.

45. Boulton TG, Nye SH, Robbins DJ, Ip NY, Radziejewska E, Morgenbesser SD, DePinho RA, Panayotatos N, Cobb MH, Yancopoulos GD (1991) ERKs: a family of protein-serine/threonine kinases that are activated and tyrosine phosphorylated in response to insulin and NGF. Cell 65: 663-675.

46. Boulton TG, Yancopoulos GD, Gregory JS, Slaughter C, Moomaw C, Hsu J, Cobb MH (1990a) An insulin-stimulated protein kinase similar to yeast kinases involved in cell cycle control. Science 249: 64-67.

47. Boulton TG, Yancopoulos GD, Gregory JS, Slaughter C, Moomaw C, Hsu J, Cobb MH (1990b) An insulin-stimulated protein kinase similar to yeast kinases involved in cell cycle control. Science 249: 64-67.

48. Brann MR, Buckley NJ, Bonner TI (1988) The striatum and cerebral cortex express different muscarinic receptor mRNAs. FEBS Lett 230: 90-94.

49. Brodaty H, Ames D, Snowdon J, Woodward M, Kirwan J, Clarnette R, Lee E, Lyons B, Grossman F (2003) A randomized placebo-controlled trial of risperidone for the treatment of aggression, agitation, and psychosis of dementia. J Clin Psychiatry 64: 134-143.

50. Brown DA, Abogadie FC, Allen TG, Buckley NJ, Caulfield MP, Delmas P, Haley JE, Lamas JA, Selyanko AA (1997) Muscarinic mechanisms in nerve cells. Life Sci 60: 1137-1144.

51. Burghaus L, Schutz U, Krempel U, de Vos RA, Jansen Steur EN, Wevers A, Lindstrom J, Schroder H (2000) Quantitative assessment of nicotinic acetylcholine receptor proteins in the cerebral cortex of Alzheimer patients. Brain Res Mol Brain Res 76: 385-388.

52. Butterfield DA, Boyd-Kimball D (2004) Amyloid beta-peptide(1-42) contributes to the oxidative stress and neurodegeneration found in Alzheimer disease brain. Brain Pathol 14: 426-432.

53. Buwalda B, de Groote L, Van der Zee EA, Matsuyama T, Luiten PG (1995) Immunocytochemical demonstration of developmental distribution of muscarinic acetylcholine receptors in rat parietal cortex. Brain Res Dev Brain Res 84: 185-191.

54. Buxbaum JD, Oishi M, Chen HI, Pinkas-Kramarski R, Jaffe EA, Gandy SE, Greengard P (1992) Cholinergic agonists and interleukin 1 regulate processing and secretion of the Alzheimer beta/A4 amyloid protein precursor. Proc Natl Acad Sci U S A 89: 10075-10078.

55. Calabresi P, Centonze D, Gubellini P, Pisani A, Bernardi G (1998) Endogenous ACh enhances striatal NMDA-responses via M1-like muscarinic receptors and PKC activation. Eur J Neurosci 10: 2887-2895.

56. Cammarota M, Bevilaqua LR, Ardenghi P, Paratcha G, Levi dS, Izquierdo I, Medina JH (2000b) Learning-associated activation of nuclear MAPK, CREB and Elk-1, along with Fos production, in the rat hippocampus after a one-trial avoidance learning: abolition by NMDA receptor blockade. Brain Res Mol Brain Res 76: 36-46.

57. Cammarota M, Bevilaqua LR, Ardenghi P, Paratcha G, Levi dS, Izquierdo I, Medina JH (2000a) Learning-associated activation of nuclear MAPK, CREB and Elk-1, along with Fos production, in the rat hippocampus after a one-trial avoidance learning: abolition by NMDA receptor blockade. Brain Res Mol Brain Res 76: 36-46.

58. Casamenti F, Di Patre PL, Bartolini L, Pepeu G (1988) Unilateral and bilateral nucleus basalis lesions: differences in neurochemical and behavioural recovery. Neuroscience 24: 209-215.

59. Casamenti F, Prosperi C, Scali C, Giovannelli L, Pepeu G (1998) Morphological, biochemical and behavioural changes induced by neurotoxic and inflammatory insults to the nucleus basalis. Int J Dev Neurosci 16: 705-714.

60. Castro NG, Albuquerque EX (1993) Brief-lifetime, fast-inactivating ion channels account for the alpha-bungarotoxin-sensitive nicotinic response in hippocampal neurons. Neurosci Lett 164: 137-140.

61. Ceccarelli I, Casamenti F, Massafra C, Pepeu G, Scali C, Aloisi AM (1999) Effects of novelty and pain on behavior and hippocampal extracellular ACh levels in male and female rats. Brain Res 815: 169-176.

62. Cerbai F, Giovannini MG, Melani C, Enz A, Pepeu G (2007) N1phenethyl-norcymserine, a selective butyrylcholinesterase inhibitor, increases acetylcholine release in rat cerebral cortex: a comparison with donepezil and rivastigmine. Eur J Pharmacol 572: 142-150.

63. Chishti MA, Yang DS, Janus C, Phinney AL, Horne P, Pearson J, Strome R, Zuker N, Loukides J, French J, Turner S, Lozza G, Grilli M, Kunicki S, Morissette C, Paquette J, Gervais F, Bergeron C, Fraser PE, Carlson GA, George-Hyslop PS, Westaway D (2001) Early-onset amyloid deposition and cognitive deficits in transgenic mice expressing a double mutant form of amyloid precursor protein 695. J Biol Chem 276: 21562-21570.

64. Chuiko GM, Podgornaya VA, Zhelnin YY (2003) Acetylcholinesterase and butyrylcholinesterase activities in brain and plasma of freshwater teleosts: cross-species and cross-family differences. Comp Biochem Physiol B Biochem Mol Biol 135: 55-61.

65. Churcher I (2006) Tau therapeutic strategies for the treatment of Alzheimer's disease. Curr Top Med Chem 6: 579-595.

66. Clarke PB (1993) Nicotinic receptors in mammalian brain: localization and relation to cholinergic innervation. Prog Brain Res 98: 77-83.

67. Clarke PB, Pert A (1985) Autoradiographic evidence for nicotine receptors on nigrostriatal and mesolimbic dopaminergic neurons. Brain Res 348: 355-358.

68. Cleveland DW, Hwo SY, Kirschner MW (1977) Purification of tau, a microtubule-associated protein that induces assembly of microtubules from purified tubulin. J Mol Biol 116: 207-225.

69. Collins AC, Wilkins LH, Slobe BS, Cao JZ, Bullock AE (1996) Long-term ethanol and nicotine treatment elicit tolerance to ethanol. Alcohol Clin Exp Res 20: 990-999.

70. Comery TA, Martone RL, Aschmies S, Atchison KP, Diamantidis G, Gong X, Zhou H, Kreft AF, Pangalos MN, Sonnenberg-Reines J, Jacobsen JS, Marquis KL (2005) Acute gamma-secretase inhibition improves contextual fear conditioning in the Tg2576 mouse model of Alzheimer's disease. J Neurosci 25: 8898-8902.

71. Court JA, Martin-Ruiz C, Graham A, Perry E (2000) Nicotinic receptors in human brain: topography and pathology. J Chem Neuroanat 20: 281-298.

72. Dajas-Bailador FA, Mogg AJ, Wonnacott S (2002a) Intracellular Ca2+ signals evoked by stimulation of nicotinic acetylcholine receptors in SH-SY5Y cells: contribution of voltage-operated Ca2+ channels and Ca2+ stores. J Neurochem 81: 606-614.

73. Dajas-Bailador FA, Soliakov L, Wonnacott S (2002b) Nicotine activates the extracellular signal-regulated kinase 1/2 via the alpha7 nicotinic acetylcholine receptor and protein kinase A, in SH-SY5Y cells and hippocampal neurones. J Neurochem 80: 520-530.

74. Damsma G, Westerink BH, de Vries JB, Van den Berg CJ, Horn AS (1987) Measurement of acetylcholine release in freely moving rats by means of automated intracerebral dialysis. J Neurochem 48: 1523-1528.

75. Daniels WM, Hendricks J, Salie R, Taljaard JJ (2001) The role of the MAP-kinase superfamily in beta-amyloid toxicity. Metab Brain Dis 16: 175-185.

76. Darvesh S, Grantham DL, Hopkins DA (1998) Distribution of butyrylcholinesterase in the human amygdala and hippocampal formation. J Comp Neurol 393: 374-390.

77. Darvesh S, Hopkins DA (2003) Differential distribution of butyrylcholinesterase and acetylcholinesterase in the human thalamus. J Comp Neurol 463: 25-43.

78. Decker MW, McGaugh JL (1991) The role of interactions between the cholinergic system and other neuromodulatory systems in learning and memory. Synapse 7: 151-168.

79. Delbono O, Gopalakrishnan M, Renganathan M, Monteggia LM, Messi ML, Sullivan JP (1997) Activation of the recombinant human alpha 7 nicotinic acetylcholine receptor significantly raises intracellular free calcium. J Pharmacol Exp Ther 280: 428-438.

80. Delmas P, Niel JP, Gola M (1996) Muscarinic activation of a novel voltage-sensitive inward current in rabbit prevertebral sympathetic neurons. Eur J Neurosci 8: 598-610.

81. Dineley KT, Westerman M, Bui D, Bell K, Ashe KH, Sweatt JD (2001) Beta-amyloid activates the mitogen-activated protein kinase cascade via hippocampal alpha7 nicotinic acetylcholine receptors: In vitro and in vivo mechanisms related to Alzheimer's disease. J Neurosci 21: 4125-4133.

82. Drubin D, Kirschner M (1986) Purification of tau protein from brain. Methods Enzymol 134: 156-160.

83. Drutel G, Peitsaro N, Karlstedt K, Wieland K, Smit MJ, Timmerman H, Panula P, Leurs R (2001) Identification of rat H3 receptor isoforms with different brain expression and signaling properties. Mol Pharmacol 59: 1-8.

84. Eglen RM, Choppin A, Dillon MP, Hegde S (1999) Muscarinic receptor ligands and their therapeutic potential. Curr Opin Chem Biol 3: 426-432.

85. Eikelenboom P, Rozemuller JM, van Muiswinkel FL (1998) Inflammation and Alzheimer's disease: relationships between pathogenic mechanisms and clinical expression. Exp Neurol 154: 89-98.

86. ELLMAN GL, COURTNEY KD, ANDRES V, Jr., FEATHER-STONE RM (1961) A new and rapid colorimetric determination of acetylcholinesterase activity. Biochem Pharmacol 7: 88-95.

87. English JD, Sweatt JD (1996) Activation of p42 mitogen-activated protein kinase in hippocampal long term potentiation. J Biol Chem 271: 24329-24332.

88. English JD, Sweatt JD (1997) A requirement for the mitogen-activated protein kinase cascade in hippocampal long term potentiation. J Biol Chem 272: 19103-19106.

89. Ennaceur A, Delacour J (1987) Effect of combined or separate administration of piracetam and choline on learning and memory in the rat. Psychopharmacology (Berl) 92: 58-67.

90. Ennaceur A, Meliani K (1992) Effects of physostigmine and scopolamine on rats' performances in object-recognition and radial-maze tests. Psychopharmacology (Berl) 109: 321-330.

91. Enslen H, Davis RJ (2001) Regulation of MAP kinases by docking domains. Biol Cell 93: 5-14.

92. Etcheberrigaray R, Tan M, Dewachter I, Kuiperi C, Van dA, I, Wera S, Qiao L, Bank B, Nelson TJ, Kozikowski AP, Van Leuven F, Alkon DL (2004) Therapeutic effects of PKC activators in Alzheimer's disease transgenic mice. Proc Natl Acad Sci U S A 101: 11141-11146.

93. Everitt BJ, Robbins TW (1997a) Central cholinergic system and cognition. Annual Review of Psychology 48: 649-684.

94. Everitt BJ, Robbins TW (1997b) Central cholinergic systems and cognition. Annu Rev Psychol 48: 649-684.

95. Fadda F, Cocco S, Stancampiano R (2000) Hippocampal acetylcholine release correlates with spatial learning performance in freely moving rats. Neuroreport 11: 2265-2269.

96. Fagarasan MO, Efthimiopoulos S (1996) Mechanism of amyloid beta-peptide (1-42) toxicity in PC12 cells. Mol Psychiatry 1: 398-403.

97. Ferrer I, Barrachina M, Puig B (2002) Glycogen synthase kinase-3 is associated with neuronal and glial hyperphosphorylated tau deposits in Alzheimer's disease, Pick's disease, progressive supranuclear palsy and corticobasal degeneration. Acta Neuropathol 104: 583-591.

98. Ferrer I, Blanco R, Carmona M, Puig B, Barrachina M, Gomez C, Ambrosio S (2001) Active, phosphorylation-dependent mitogen-activated protein kinase (MAPK/ERK), stress-activated protein kinase/c-Jun N-terminal kinase (SAPK/JNK), and p38 kinase expression in Parkinson's disease and Dementia with Lewy bodies. J Neural Transm 108: 1383-1396.

99. Ferrer I, Gomez-Isla T, Puig B, Freixes M, Ribe E, Dalfo E, Avila J (2005b) Current advances on different kinases involved in tau phosphorylation, and implications in Alzheimer's disease and tauopathies. Curr Alzheimer Res 2: 3-18.

100. Ferrer I, Gomez-Isla T, Puig B, Freixes M, Ribe E, Dalfo E, Avila J (2005a) Current advances on different kinases involved in tau phosphorylation, and implications in Alzheimer's disease and tauopathies. Curr Alzheimer Res 2: 3-18.

101. Fiore RS, Bayer VE, Pelech SL, Posada J, Cooper JA, Baraban JM (1993a) p42 mitogen-activated protein kinase in brain: prominent localization in neuronal cell bodies and dendrites. Neuroscience 55: 463-472.

102. Fiore RS, Bayer VE, Pelech SL, Posada J, Cooper JA, Baraban JM (1993b) p42 mitogen-activated protein kinase in brain: prominent localization in neuronal cell bodies and dendrites. Neuroscience 55: 463-472.

103. Fiore RS, Murphy TH, Sanghera JS, Pelech SL, Baraban JM (1993c) Activation of p42 mitogen-activated protein kinase by glutamate receptor stimulation in rat primary cortical cultures. J Neurochem 61: 1626-1633.

104. Fiszer U, Mix E, Fredrikson S, Kostulas V, Olsson T, Link H (1994) gamma delta+ T cells are increased in patients with Parkinson's disease. J Neurol Sci 121: 39-45.

105. Flicker C, Dean RL, Watkins DL, Fisher SK, Bartus RT (1983) Behavioral and neurochemical effects following neurotoxic lesions of a major cholinergic input to the cerebral cortex in the rat. Pharmacol Biochem Behav 18: 973-981.

106. Flores CM, Rogers SW, Pabreza LA, Wolfe BB, Kellar KJ (1992) A subtype of nicotinic cholinergic receptor in rat brain is composed of alpha 4 and beta 2 subunits and is up-regulated by chronic nicotine treatment. Mol Pharmacol 41: 31-37.

107. Flynn DD, Ferrari-DiLeo G, Mash DC, Levey AI (1995) Differential regulation of molecular subtypes of muscarinic receptors in Alzheimer's disease. J Neurochem 64: 1888-1891.

108. Frank MG, Baratta MV, Sprunger DB, Watkins LR, Maier SF (2007) Microglia serve as a neuroimmune substrate for stress-induced potentiation of CNS pro-inflammatory cytokine responses. Brain Behav Immun 21: 47-59.

109. Fratiglioni L, Wang HX (2000) Smoking and Parkinson's and Alzheimer's disease: review of the epidemiological studies. Behav Brain Res 113: 117-120.

110. Galli KM, Galli G, Bosisio E, Cighetti G, Paoletti R (1984) Evaluation of enzyme activities by gas chromatography-mass spectrometry: HMGCoA reductase and cholesterol 7 alpha-hydroxylase. J Chromatogr 289: 267-276.

111. George-Hyslop P, Haines J, Rogaev E, Mortilla M, Vaula G, Pericak-Vance M, Foncin JF, Montesi M, Bruni A, Sorbi S, . (1992) Genetic evidence for a novel familial Alzheimer's disease locus on chromosome 14. Nat Genet 2: 330-334.

112. Gervais FG, Xu D, Robertson GS, Vaillancourt JP, Zhu Y, Huang J, LeBlanc A, Smith D, Rigby M, Shearman MS, Clarke EE, Zheng H, Van Der Ploeg LH, Ruffolo SC, Thornberry NA, Xanthoudakis S, Zamboni RJ, Roy S, Nicholson DW (1999) Involvement of caspases in proteolytic cleavage of Alzheimer's amyloid-beta precursor protein and amyloidogenic A beta peptide formation. Cell 97: 395-406.

113. Giacobini E (2003) Cholinesterases: new roles in brain function and in Alzheimer's disease. Neurochem Res 28: 515-522.

114. Giacobini E, Spiegel R, Enz A, Veroff AE, Cutler NR (2002) Inhibition of acetyl- and butyryl-cholinesterase in the cerebrospinal fluid of patients with Alzheimer's disease by rivastigmine: correlation with cognitive benefit. J Neural Transm 109: 1053-1065.

115. Giovannini MG, Bartolini L, Bacciottini L, Greco L, Blandina P (1999) Effects of histamine H3 receptor agonists and antagonists on cognitive performance and scopolamine-induced amnesia. Behav Brain Res 104: 147-155.

116. Giovannini MG, Bartolini L, Kopf SR, Pepeu G (1998) Acetylcholine release from the frontal cortex during exploratory activity. Brain Res 784: 218-227.

117. Giovannini MG, Blitzer RD, Wong T, Asoma K, Tsokas P, Morrison JH, Iyengar R, Landau EM (2001d) Mitogen-activated protein kinase regulates early phosphorylation and delayed expression of Ca2+/calmodulin-dependent protein kinase II in long-term potentiation. J Neurosci 21: 7053-7062.

118. Giovannini MG, Blitzer RD, Wong T, Asoma K, Tsokas P, Morrison JH, Iyengar R, Landau EM (2001c) Mitogen-activated protein kinase regulates early phosphorylation and delayed expression of Ca2+/calmodulin-dependent protein kinase II in long-term potentiation. J Neurosci 21: 7053-7062.

119. Giovannini MG, Blitzer RD, Wong T, Asoma K, Tsokas P, Morrison JH, Iyengar R, Landau EM (2001a) Mitogen-activated protein kinase regulates early phosphorylation and delayed expression of Ca2+/calmodulin-dependent protein kinase II in long-term potentiation. J Neurosci 21: 7053-7062.

120. Giovannini MG, Blitzer RD, Wong T, Asoma K, Tsokas P, Morrison JH, Iyengar R, Landau EM (2001b) Mitogen-activated protein kinase regulates early phosphorylation and delayed expression of Ca2+/calmodulin-dependent protein kinase II in long-term potentiation. J Neurosci 21: 7053-7062.

121. Giovannini MG, Camilli F, Mundula A, Pepeu G (1994) Glutamatergic regulation of acetylcholine output in different brain regions: a microdialysis study in the rat. Neurochem Int 25: 23-26.

122. Giovannini MG, Efoudebe M, Passani MB, Baldi E, Bucherelli C, Giachi F, Corradetti R, Blandina P (2003c) Improvement in fear memory by histamine-elicited ERK2 activation in hippocampal CA3 cells. J Neurosci 23: 9016-9023.

123. Giovannini MG, Efoudebe M, Passani MB, Baldi E, Bucherelli C, Giachi F, Corradetti R, Blandina P (2003a) Improvement in fear memory by histamine-elicited ERK2 activation in hippocampal CA3 cells. J Neurosci 23: 9016-9023.

124. Giovannini MG, Efoudebe M, Passani MB, Baldi E, Bucherelli C, Giachi F, Corradetti R, Blandina P (2003b) Improvement in fear memory by histamine-elicited ERK2 activation in hippocampal CA3 cells. J Neurosci 23: 9016-9023.

125. Giovannini MG, Rakovska A, Benton RS, Pazzagli M, Bianchi L, Pepeu G (2001e) Effects of novelty and habituation on acetylcholine, GABA, and glutamate release from the frontal cortex and hippocampus of freely moving rats. Neuroscience 106: 43-53.

126. Giovannini MG, Scali C, Prosperi C, Bellucci A, Vannucchi MG, Rosi S, Pepeu G, Casamenti F (2002) Beta-amyloid-induced inflammation and cholinergic hypofunction in the rat brain in vivo: involvement of the p38MAPK pathway. Neurobiol Dis 11: 257-274.

127. Goldgaber D, Harris HW, Hla T, Maciag T, Donnelly RJ, Jacobsen JS, Vitek MP, Gajdusek DC (1989) Interleukin 1 regulates synthesis of amyloid beta-protein precursor mRNA in human endothelial cells. Proc Natl Acad Sci U S A 86: 7606-7610.

128. Gomeza J, Shannon H, Kostenis E, Felder C, Zhang L, Brodkin J, Grinberg A, Sheng H, Wess J (1999a) Pronounced pharmacologic deficits in M2 muscarinic acetylcholine receptor knockout mice. Proc Natl Acad Sci U S A 96: 1692-1697.

129. Gomeza J, Zhang L, Kostenis E, Felder C, Bymaster F, Brodkin J, Shannon H, Xia B, Deng C, Wess J (1999b) Enhancement of D1 dopamine receptor-mediated locomotor stimulation in M(4) muscarinic acetylcholine receptor knockout mice. Proc Natl Acad Sci U S A 96: 10483-10488.

130. Gonzalez-Scarano F, Baltuch G (1999) Microglia as mediators of inflammatory and degenerative diseases. Annu Rev Neurosci 22: 219-240.

131. Gopalakrishnan M, Molinari EJ, Sullivan JP (1997) Regulation of human alpha4beta2 neuronal nicotinic acetylcholine receptors by cholinergic channel ligands and second messenger pathways. Mol Pharmacol 52: 524-534.

132. Graff-Radford NR, Tranel D, Van Hoesen GW, Brandt JP (1990) Diencephalic amnesia. Brain 113 (Pt 1): 1-25.

133. Graham SH, Chen J, Lan JQ, Simon RP (1996) A dose-response study of neuroprotection using the AMPA antagonist NBQX in rat focal cerebral ischemia. J Pharmacol Exp Ther 276: 1-4.

134. Graybiel AM, Ragsdale CW, Jr. (1982) Pseudocholinesterase staining in the primary visual pathway of the macaque monkey. Nature 299: 439-442.

135. Guan ZZ, Zhang X, Ravid R, Nordberg A (2000) Decreased protein levels of nicotinic receptor subunits in the hippocampus and temporal cortex of patients with Alzheimer's disease. J Neurochem 74: 237-243.

136. Guillozet AL, Smiley JF, Mash DC, Mesulam MM (1997a) Butyrylcholinesterase in the life cycle of amyloid plaques. Ann Neurol 42: 909-918.

137. Guillozet AL, Smiley JF, Mash DC, Mesulam MM (1997b) Butyrylcholinesterase in the life cycle of amyloid plaques. Ann Neurol 42: 909-918.

138. Haass C, Hung AY, Schlossmacher MG, Oltersdorf T, Teplow DB, Selkoe DJ (1993) Normal cellular processing of the beta-amyloid precursor protein results in the secretion of the amyloid beta peptide and related molecules. Ann N Y Acad Sci 695: 109-116.

139. Haass C, Selkoe DJ (1993) Cellular processing of beta-amyloid precursor protein and the genesis of amyloid beta-peptide. Cell 75: 1039-1042.

140. Haddad JJ (2004) Mitogen-activated protein kinases and the evolution of Alzheimer's: a revolutionary neurogenetic axis for therapeutic intervention? Prog Neurobiol 73: 359-377.

141. Hafner S, Adler HS, Mischak H, Janosch P, Heidecker G, Wolfman A, Pippig S, Lohse M, Ueffing M, Kolch W (1994) Mechanism of inhibition of Raf-1 by protein kinase A. Mol Cell Biol 14: 6696-6703.

142. Haj-Dahmane S, Andrade R (1996) Muscarinic activation of a voltage-dependent cation nonselective current in rat association cortex. J Neurosci 16: 3848-3861.

143. Halliday GM, Shepherd CE, McCann H, Reid WG, Grayson DA, Broe GA, Kril JJ (2000) Effect of anti-inflammatory medications on neuropathological findings in Alzheimer disease. Arch Neurol 57: 831-836.

144. Halliwell JV (1990) Physiological mechanisms of cholinergic action in the hippocampus. Prog Brain Res 84: 255-272.

145. Hamilton SE, Hardouin SN, Anagnostaras SG, Murphy GG, Richmond KN, Silva AJ, Feigl EO, Nathanson NM (2001) Alteration of cardiovascular and neuronal function in M1 knockout mice. Life Sci 68: 2489-2493.

146. Hamilton SE, Loose MD, Qi M, Levey AI, Hille B, McKnight GS, Idzerda RL, Nathanson NM (1997) Disruption of the m1 receptor gene ablates muscarinic receptor-dependent M current regulation and seizure activity in mice. Proc Natl Acad Sci U S A 94: 13311-13316.

147. Hammer R, Berrie CP, Birdsall NJ, Burgen AS, Hulme EC (1980) Pirenzepine distinguishes between different subclasses of muscarinic receptors. Nature 283: 90-92.

148. Han J, Lee JD, Bibbs L, Ulevitch RJ (1994) A MAP kinase targeted by endotoxin and hyperosmolarity in mammalian cells. Science 265: 808-811.

149. Hanger DP, Brion JP, Gallo JM, Cairns NJ, Luthert PJ, Anderton BH (1991) Tau in Alzheimer's disease and Down's syndrome is insoluble and abnormally phosphorylated. Biochem J 275 (Pt 1): 99-104.

150. Harrington CR, Louwagie J, Rossau R, Vanmechelen E, Perry RH, Perry EK, Xuereb JH, Roth M, Wischik CM (1994) Influence of apolipoprotein E genotype on senile dementia of the Alzheimer and Lewy body types. Significance for etiological theories of Alzheimer's disease. Am J Pathol 145: 1472-1484.

151. Harris ME, Hensley K, Butterfield DA, Leedle RA, Carney JM (1995) Direct evidence of oxidative injury produced by the Alzheimer's beta-amyloid peptide (1-40) in cultured hippocampal neurons. Exp Neurol 131: 193-202.

152. Harrison JE, O'Callaghan FJ, Hancock E, Osborne JP, Bolton PF (1999) Cognitive deficits in normally intelligent patients with tuberous sclerosis. Am J Med Genet 88: 642-646.

153. Hauss-Wegrzyniak B, Lukovic L, Bigaud M, Stoeckel ME (1998) Brain inflammatory response induced by intracerebroventricular infusion of lipopolysaccharide: an immunohistochemical study. Brain Res 794: 211-224.

154. Heckers S, Ohtake T, Wiley RG, Lappi DA, Geula C, Mesulam MM (1994) Complete and selective cholinergic denervation of rat neocortex and hippocampus but not amygdala by an immunotoxin against the p75 NGF receptor. J Neurosci 14: 1271-1289.

155. Hellstrom-Lindahl E, Court J, Keverne J, Svedberg M, Lee M, Marutle A, Thomas A, Perry E, Bednar I, Nordberg A (2004a) Nicotine reduces A beta in the brain and cerebral vessels of APPsw mice. Eur J Neurosci 19: 2703-2710.

156. Hellstrom-Lindahl E, Mousavi M, Ravid R, Nordberg A (2004b) Reduced levels of Abeta 40 and Abeta 42 in brains of smoking controls and Alzheimer's patients. Neurobiol Dis 15: 351-360.

157. Hensley K, Floyd RA, Zheng NY, Nael R, Robinson KA, Nguyen X, Pye QN, Stewart CA, Geddes J, Markesbery WR, Patel E, Johnson GV, Bing G (1999) p38 kinase is activated in the Alzheimer's disease brain. J Neurochem 72: 2053-2058.

158. Hersch SM, Gutekunst CA, Rees HD, Heilman CJ, Levey AI (1994) Distribution of m1-m4 muscarinic receptor proteins in the rat striatum: light and electron microscopic immunocytochemistry using subtype-specific antibodies. J Neurosci 14: 3351-3363.

159. Higuchi M, Ishihara T, Zhang B, Hong M, Andreadis A, Trojanowski J, Lee VM (2002) Transgenic mouse model of tauopathies with glial pathology and nervous system degeneration. Neuron 35: 433-446.

160. Hirsch EC, Breidert T, Rousselet E, Hunot S, Hartmann A, Michel PP (2003) The role of glial reaction and inflammation in Parkinson's disease. Ann N Y Acad Sci 991: 214-228.

161. Ho L, Purohit D, Haroutunian V, Luterman JD, Willis F, Naslund J, Buxbaum JD, Mohs RC, Aisen PS, Pasinetti GM (2001) Neuronal cyclooxygenase 2 expression in the hippocampal formation as a function of the clinical progression of Alzheimer disease. Arch Neurol 58: 487-492.

162. Hoek RM, Ruuls SR, Murphy CA, Wright GJ, Goddard R, Zurawski SM, Blom B, Homola ME, Streit WJ, Brown MH, Barclay AN, Sedgwick JD (2000) Down-regulation of the macrophage lineage through interaction with OX2 (CD200). Science 290: 1768-1771.

163. Hsiao K, Chapman P, Nilsen S, Eckman C, Harigaya Y, Younkin S, Yang F, Cole G (1996) Correlative memory deficits, Abeta elevation, and amyloid plaques in transgenic mice. Science 274: 99-102.

164. Hull M, Lieb K, Fiebich BL (2002) Pathways of inflammatory activation in Alzheimer's disease: potential targets for disease modifying drugs. Curr Med Chem 9: 83-88.

165. Igaz LM, Bekinschtein P, Izquierdo I, Medina JH (2004) One-trial aversive learning induces late changes in hippocampal CaMKIIalpha, Homer 1a, Syntaxin 1a and ERK2 protein levels. Brain Res Mol Brain Res 132: 1-12.

166. Ishiguro K, Kobayashi S, Omori A, Takamatsu M, Yonekura S, Anzai K, Imahori K, Uchida T (1994) Identification of the 23 kDa subunit of tau protein kinase II as a putative activator of cdk5 in bovine brain. FEBS Lett 342: 203-208.

167. Izquierdo I (1989) Mechanism of action of scopolamine as an amnesic. Trends in Pharmacological Sciences 10: 175-177.

168. Izquierdo I, Barros DM, Mello e Souza, de Souza MM, Izquierdo LA, Medina JH (1998a) Mechanisms for memory types differ. Nature 393: 635-636.

169. Izquierdo I, Barros DM, Mello e Souza, de Souza MM, Izquierdo LA, Medina JH (1998b) Mechanisms for memory types differ. Nature 393: 635-636.

170. Izquierdo I, Izquierdo LA, Barros DM, Mello e Souza, de Souza MM, Quevedo J, Rodrigues C, Sant'Anna MK, Madruga M, Medina JH (1998d) Differential involvement of cortical receptor mechanisms in working, short-term and long-term memory. Behav Pharmacol 9: 421-427.

171. Izquierdo I, Izquierdo LA, Barros DM, Mello e Souza, de Souza MM, Quevedo J, Rodrigues C, Sant'Anna MK, Madruga M, Medina JH (1998c) Differential involvement of cortical receptor mechanisms in working, short-term and long-term memory. Behav Pharmacol 9: 421-427.

172. Izquierdo I, Izquierdo LA, Barros DM, Mello e Souza, de Souza MM, Quevedo J, Rodrigues C, Sant'Anna MK, Madruga M, Medina JH (1998e) Differential involvement of cortical receptor mechanisms in working, short-term and long-term memory. Behav Pharmacol 9: 421-427.

173. Izquierdo I, Medina JH (1997) Memory formation: the sequence of biochemical events in the hippocampus and its connection to activity in other brain structures. Neurobiol Learn Mem 68: 285-316.

174. Izquierdo I, Quillfeldt JA, Zanatta MS, Quevedo J, Schaeffer E, Schmitz PK, Medina JH (1997) Sequential role of hippocampus and amygdala, entorhinal cortex and parietal cortex in formation and retrieval of memory for inhibitory avoidance in rats. Eur J Neurosci 9: 786-793.

175. Johnson CD, Russell RL (1975) A rapid, simple radiometric assay for cholinesterase, suitable for multiple determinations. Anal Biochem 64: 229-238.

176. Kaang BK, Kandel ER, Grant SG (1993a) Activation of cAMP-responsive genes by stimuli that produce long-term facilitation in Aplysia sensory neurons. Neuron 10: 427-435.

177. Kaang BK, Kandel ER, Grant SG (1993b) Activation of cAMP-responsive genes by stimuli that produce long-term facilitation in Aplysia sensory neurons. Neuron 10: 427-435.

178. Kaminska B (2005) MAPK signalling pathways as molecular targets for anti-inflammatory therapy--from molecular mechanisms to therapeutic benefits. Biochim Biophys Acta 1754: 253-262.

179. Kaminska B, Kaczmarek L, Zangenehpour S, Chaudhuri A (1999) Rapid phosphorylation of Elk-1 transcription factor and activation of MAP kinase signal transduction pathways in response to visual stimulation. Mol Cell Neurosci 13: 405-414.

180. Kanterewicz BI, Urban NN, McMahon DB, Norman ED, Giffen LJ, Favata MF, Scherle PA, Trzskos JM, Barrionuevo G, Klann E (2000) The extracellular signal-regulated kinase cascade is required for NMDA receptor-independent LTP in area CA1 but not area CA3 of the hippocampus. J Neurosci 20: 3057-3066.

181. Kelly A, Laroche S, Davis S (2003) Activation of mitogen-activated protein kinase/extracellular signal-regulated kinase in hippocampal circuitry is required for consolidation and reconsolidation of recognition memory. J Neurosci 23: 5354-5360.

182. Kim JB, Sig CJ, Yu YM, Nam K, Piao CS, Kim SW, Lee MH, Han PL, Park JS, Lee JK (2006) HMGB1, a novel cytokine-like mediator linking acute neuronal death and delayed neuroinflammation in the postischemic brain. J Neurosci 26: 6413-6421.

183. Kimura H, McGeer PL, Peng F, McGeer EG (1980) Choline acetyltransferase-containing neurons in rodent brain demonstrated by immunohistochemistry. Science 208: 1057-1059.

184. Kobayashi S, Ishiguro K, Omori A, Takamatsu M, Arioka M, Imahori K, Uchida T (1993) A cdc2-related kinase PSSALRE/cdk5 is homologous with the 30 kDa subunit of tau protein kinase II, a proline-directed protein kinase associated with microtubule. FEBS Lett 335: 171-175.

185. Krapivinsky G, Krapivinsky L, Manasian Y, Ivanov A, Tyzio R, Pellegrino C, Ben Ari Y, Clapham DE, Medina I (2003) The NMDA receptor is coupled to the ERK pathway by a direct interaction between NR2B and RasGRF1. Neuron 40: 775-784.

186. Kubo T, Maeda A, Sugimoto K, Akiba I, Mikami A, Takahashi H, Haga T, Haga K, Ichiyama A, Kangawa K, . (1986) Primary structure of porcine cardiac

muscarinic acetylcholine receptor deduced from the cDNA sequence. FEBS Lett 209: 367-372.

187. Kummer JL, Rao PK, Heidenreich KA (1997) Apoptosis induced by withdrawal of trophic factors is mediated by p38 mitogen-activated protein kinase. J Biol Chem 272: 20490-20494.

188. Kushner I (1991) The acute phase response: from Hippocrates to cytokine biology. Eur Cytokine Netw 2: 75-80.

189. Kyriakis JM, Banerjee P, Nikolakaki E, Dai T, Rubie EA, Ahmad MF, Avruch J, Woodgett JR (1994a) The stress-activated protein kinase subfamily of c-Jun kinases. Nature 369: 156-160.

190. Kyriakis JM, Banerjee P, Nikolakaki E, Dai T, Rubie EA, Ahmad MF, Avruch J, Woodgett JR (1994b) The stress-activated protein kinase subfamily of c-Jun kinases. Nature 369: 156-160.

191. Leanza G, Nilsson OG, Nikkhah G, Wiley RG, Bjorklund A (1996) Effects of neonatal lesions of the basal forebrain cholinergic system by 192 immunoglobulin G-saporin: biochemical, behavioural and morphological characterization. Neuroscience 74: 119-141.

192. Leanza G, Nilsson OG, Wiley RG, Bjorklund A (1995) Selective lesioning of the basal forebrain cholinergic system by intraventricular 192 IgG-saporin: behavioural, biochemical and stereological studies in the rat. Eur J Neurosci 7: 329-343.

193. LeDoux JE (1995) Emotion: clues from the brain. Annu Rev Psychol 46: 209-235.

194. Lee CY (1979) Recent advances in chemistry and pharmacology of snake toxins. Adv Cytopharmacol 3: 1-16.

195. Lee JD, Ulevitch RJ, Han J (1995) Primary structure of BMK1: a new mammalian map kinase. Biochem Biophys Res Commun 213: 715-724.

196. Lev S, Moreno H, Martinez R, Canoll P, Peles E, Musacchio JM, Plowman GD, Rudy B, Schlessinger J (1995) Protein tyrosine kinase PYK2 involved in Ca(2+)-induced regulation of ion channel and MAP kinase functions. Nature 376: 737-745.

197. Levey AI, Edmunds SM, Heilman CJ, Desmond TJ, Frey KA (1994) Localization of muscarinic m3 receptor protein and M3 receptor binding in rat brain. Neuroscience 63: 207-221.

198. Levey AI, Edmunds SM, Hersch SM, Wiley RG, Heilman CJ (1995a) Light and electron microscopic study of m2 muscarinic acetylcholine receptor in the basal forebrain of the rat. J Comp Neurol 351: 339-356.

199. Levey AI, Edmunds SM, Koliatsos V, Wiley RG, Heilman CJ (1995b) Expression of m1-m4 muscarinic acetylcholine receptor proteins in rat hippocampus and regulation by cholinergic innervation. J Neurosci 15: 4077-4092.

200. Levey AI, Kitt CA, Simonds WF, Price DL, Brann MR (1991) Identification and localization of muscarinic acetylcholine receptor proteins in brain with subtype-specific antibodies. J Neurosci 11: 3218-3226.

201. Lew J, Huang QQ, Qi Z, Winkfein RJ, Aebersold R, Hunt T, Wang JH (1994) A brain-specific activator of cyclin-dependent kinase 5. Nature 371: 423-426.

202. Li B, Stribley JA, Ticu A, Xie W, Schopfer LM, Hammond P, Brimijoin S, Hinrichs SH, Lockridge O (2000) Abundant tissue butyrylcholinesterase and its possible function in the acetylcholinesterase knockout mouse. J Neurochem 75: 1320-1331.

203. Lim GP, Yang F, Chu T, Chen P, Beech W, Teter B, Tran T, Ubeda O, Ashe KH, Frautschy SA, Cole GM (2000) Ibuprofen suppresses plaque pathology and inflammation in a mouse model for Alzheimer's disease. J Neurosci 20: 5709-5714.

204. Lohse MJ (1993) Molecular mechanisms of membrane receptor desensitization. Biochim Biophys Acta 1179: 171-188.

205. Lue LF, Walker DG, Rogers J (2001) Modeling microglial activation in Alzheimer's disease with human postmortem microglial cultures. Neurobiol Aging 22: 945-956.

206. Lukas RJ (1995) Diversity and patterns of regulation of nicotinic receptor subtypes. Ann N Y Acad Sci 757: 153-168.

207. Lukiw WJ, Bazan NG (1998) Strong nuclear factor-kappaB-DNA binding parallels cyclooxygenase-2 gene transcription in aging and in sporadic Alzheimer's disease superior temporal lobe neocortex. J Neurosci Res 53: 583-592.

208. Luo Y, Bolon B, Kahn S, Bennett BD, Babu-Khan S, Denis P, Fan W, Kha H, Zhang J, Gong Y, Martin L, Louis JC, Yan Q, Richards WG, Citron M, Vassar R (2001) Mice deficient in BACE1, the Alzheimer's beta-secretase, have normal phenotype and abolished beta-amyloid generation. Nat Neurosci 4: 231-232.

209. Lyons A, Downer EJ, Crotty S, Nolan YM, Mills KH, Lynch MA (2007) CD200 ligand receptor interaction modulates microglial activation in vivo and in vitro: a role for IL-4. J Neurosci 27: 8309-8313.

210. Maren S (1996a) Synaptic transmission and plasticity in the amygdala. An emerging physiology of fear conditioning circuits. Mol Neurobiol 13: 1-22.

211. Maren S (1996b) Synaptic transmission and plasticity in the amygdala. An emerging physiology of fear conditioning circuits. Mol Neurobiol 13: 1-22.

212. Maren S (2001) Is there savings for pavlovian fear conditioning after neurotoxic basolateral amygdala lesions in rats? Neurobiol Learn Mem 76: 268-283.

213. Markesbery WR (1999) The role of oxidative stress in Alzheimer disease. Arch Neurol 56: 1449-1452.

214. Markram H, Segal M (1990) Long-lasting facilitation of excitatory postsynaptic potentials in the rat hippocampus by acetylcholine. J Physiol 427: 381-393.

215. Marks MJ, Stitzel JA, Romm E, Wehner JM, Collins AC (1986) Nicotinic binding sites in rat and mouse brain: comparison of acetylcholine, nicotine, and alpha-bungarotoxin. Mol Pharmacol 30: 427-436.

216. Martin-Ruiz CM, Court JA, Molnar E, Lee M, Gotti C, Mamalaki A, Tsouloufis T, Tzartos S, Ballard C, Perry RH, Perry EK (1999) Alpha4 but not alpha3 and alpha7 nicotinic acetylcholine receptor subunits are lost from the temporal cortex in Alzheimer's disease. J Neurochem 73: 1635-1640.

217. Mash DC, Flynn DD, Potter LT (1985) Loss of M2 muscarine receptors in the cerebral cortex in Alzheimer's disease and experimental cholinergic denervation. Science 228: 1115-1117.

218. Masliah E, Sisk A, Mallory M, Mucke L, Schenk D, Games D (1996) Comparison of neurodegenerative pathology in transgenic mice overexpressing V717F beta-amyloid precursor protein and Alzheimer's disease. J Neurosci 16: 5795-5811.

219. Matsui M, Motomura D, Karasawa H, Fujikawa T, Jiang J, Komiya Y, Takahashi S, Taketo MM (2000) Multiple functional defects in peripheral autonomic organs in mice lacking muscarinic acetylcholine receptor gene for the M3 subtype. Proc Natl Acad Sci U S A 97: 9579-9584.

220. McDonald MP, Wenk GL, Crawley JN (1997) Analysis of galanin and the galanin antagonist M40 on delayed non-matching-to-position performance in rats lesioned with the cholinergic immunotoxin 192 IgG-saporin. Behav Neurosci 111: 552-563.

221. McGaugh JL, Izquierdo I (2000) The contribution of pharmacology to research on the mechanisms of memory formation. Trends Pharmacol Sci 21: 208-210.

222. McGaughy J, Kaiser T, Sarter M (1996) Behavioral vigilance following infusions of 192 IgG-saporin into the basal forebrain: selectivity of the behavioral impairment and relation to cortical AChE-positive fiber density. Behav Neurosci 110: 247-265.

223. McGeer PL, McGeer EG (1995) The inflammatory response system of brain: implications for therapy of Alzheimer and other neurodegenerative diseases. Brain Res Brain Res Rev 21: 195-218.

224. McGeer PL, McGeer EG (1998) Glial cell reactions in neurodegenerative diseases: pathophysiology and therapeutic interventions. Alzheimer Dis Assoc Disord 12 Suppl 2: S1-S6.

225. McGeer PL, Schulzer M, McGeer EG (1996) Arthritis and anti-inflammatory agents as possible protective factors for Alzheimer's disease: a review of 17 epidemiologic studies. Neurology 47: 425-432.

226. McIntyre CK, Marriott LK, Gold PE (2003) Cooperation between memory systems: acetylcholine release in the amygdala correlates positively with performance on a hippocampus-dependent task. Behav Neurosci 117: 320-326.

227. McIntyre CK, Pal SN, Marriott LK, Gold PE (2002) Competition between memory systems: acetylcholine release in the hippocampus correlates negatively with good performance on an amygdala-dependent task. J Neurosci 22: 1171-1176.

228. Mesulam MM, Guillozet A, Shaw P, Levey A, Duysen EG, Lockridge O (2002) Acetylcholinesterase knockouts establish central cholinergic pathways and can use butyrylcholinesterase to hydrolyze acetylcholine. Neuroscience 110: 627-639.

229. Mesulam MM, Mufson EJ, Wainer BH, Levey AI (1983) Central cholinergic pathways in the rat: an overview based on an alternative nomenclature (Ch1-Ch6). Neuroscience 10: 1185-1201.

230. Misztal G, Paw B (1996) Determination of fludarabine phosphate in human plasma using reversed phase high-performance liquid chromatography. Pharmazie 51: 733-734.

231. Miyakawa T, Yamada M, Duttaroy A, Wess J (2001) Hyperactivity and intact hippocampus-dependent learning in mice lacking the M1 muscarinic acetylcholine receptor. J Neurosci 21: 5239-5250.

232. Morishima Y, Gotoh Y, Zieg J, Barrett T, Takano H, Flavell R, Davis RJ, Shirasaki Y, Greenberg ME (2001) Beta-amyloid induces neuronal apoptosis via a mechanism that involves the c-Jun N-terminal kinase pathway and the induction of Fas ligand. J Neurosci 21: 7551-7560.

233. Moser N, Wevers A, Lorke DE, Reinhardt S, Maelicke A, Schroder H (1996) Alpha4-1 subunit mRNA of the nicotinic acetylcholine receptor in the rat olfactory bulb: cellular expression in adult, pre- and postnatal stages. Cell Tissue Res 285: 17-25.

234. Mrak RE, Griffinbc WS (2001) The role of activated astrocytes and of the neurotrophic cytokine S100B in the pathogenesis of Alzheimer's disease. Neurobiol Aging 22: 915-922.

235. Mrzljak L, Levey AI, Goldman-Rakic PS (1993) Association of m1 and m2 muscarinic receptor proteins with asymmetric synapses in the primate cerebral cortex: morphological evidence for cholinergic modulation of excitatory neurotransmission. Proc Natl Acad Sci U S A 90: 5194-5198.

236. Muir JL, Everitt BJ, Robbins TW (1996) The cerebral cortex of the rat and visual attentional function: dissociable effects of mediofrontal, cingulate, anterior dorsolateral, and parietal cortex lesions on a five-choice serial reaction time task. Cereb Cortex 6: 470-481.

237. Mullan M, Houlden H, Windelspecht M, Fidani L, Lombardi C, Diaz P, Rossor M, Crook R, Hardy J, Duff K, . (1992) A locus for familial early-onset Alzheimer's disease on the long arm of chromosome 14, proximal to the alpha 1-antichymotrypsin gene. Nat Genet 2: 340-342.

238. Naor C, Dudai Y (1996b) Transient impairment of cholinergic function in the rat insular cortex disrupts the encoding of taste in conditioned taste aversion. Behav Brain Res 79: 61-67.

239. Naor C, Dudai Y (1996a) Transient impairment of cholinergic function in the rat insular cortex disrupts the encoding of taste in conditioned taste aversion. Behav Brain Res 79: 61-67.

240. Nordberg A (1994) Human nicotinic receptors--their role in aging and dementia. Neurochem Int 25: 93-97.

241. Nordberg A (2001) Nicotinic receptor abnormalities of Alzheimer's disease: therapeutic implications. Biol Psychiatry 49: 200-210.

242. Nordberg A, Hellstrom-Lindahl E, Lee M, Johnson M, Mousavi M, Hall R, Perry E, Bednar I, Court J (2002) Chronic nicotine treatment reduces beta-amyloidosis in the brain of a mouse model of Alzheimer's disease (APPsw). J Neurochem 81: 655-658.

243. Ono K, Hasegawa K, Yamada M, Naiki H (2002) Nicotine breaks down preformed Alzheimer's beta-amyloid fibrils in vitro. Biol Psychiatry 52: 880-886.

244. Orgogozo JM, Gilman S, Dartigues JF, Laurent B, Puel M, Kirby LC, Jouanny P, Dubois B, Eisner L, Flitman S, Michel BF, Boada M, Frank A, Hock C (2003) Subacute meningoencephalitis in a subset of patients with AD after Abeta42 immunization. Neurology 61: 46-54.

245. Pasinetti GM, Aisen PS (1998) Cyclooxygenase-2 expression is increased in frontal cortex of Alzheimer's disease brain. Neuroscience 87: 319-324.

246. Passani MB, Bacciottini L, Mannaioni PF, Blandina P (2000) Central histaminergic system and cognition. Neurosci Biobehav Rev 24: 107-113.

247. Passetti F, Dalley JW, O'Connell MT, Everitt BJ, Robbins TW (2000) Increased acetylcholine release in the rat medial prefrontal cortex during performance of a visual attentional task. Eur J Neurosci 12: 3051-3058.

248. Patterson D, Gardiner K, Kao FT, Tanzi R, Watkins P, Gusella JF (1988) Mapping of the gene encoding the beta-amyloid precursor protein and its relationship to the Down syndrome region of chromosome 21. Proc Natl Acad Sci U S A 85: 8266-8270.

249. Peavy RD, Conn PJ (1998) Phosphorylation of mitogen-activated protein kinase in cultured rat cortical glia by stimulation of metabotropic glutamate receptors. J Neurochem 71: 603-612.

250. Pepeu G, Giovannini MG (2004) Changes in acetylcholine extracellular levels during cognitive processes. Learn Mem 11: 21-27.

251. Peralta EG, Ashkenazi A, Winslow JW, Smith DH, Ramachandran J, Capon DJ (1987) Distinct primary structures, ligand-binding properties and tissue-specific expression of four human muscarinic acetylcholine receptors. EMBO J 6: 3923-3929.

252. Perry EK, Morris CM, Court JA, Cheng A, Fairbairn AF, McKeith IG, Irving D, Brown A, Perry RH (1995) Alteration in nicotine binding sites in Parkinson's disease, Lewy body dementia and Alzheimer's disease: possible index of early neuropathology. Neuroscience 64: 385-395.

253. Perry EK, Perry RH, Blessed G, Tomlinson BE (1978c) Changes in brain cholinesterases in senile dementia of Alzheimer type. Neuropathol Appl Neurobiol 4: 273-277.

254. Perry EK, Perry RH, Blessed G, Tomlinson BE (1978a) Changes in brain cholinesterases in senile dementia of Alzheimer type. Neuropathol Appl Neurobiol 4: 273-277.

255. Perry EK, Perry RH, Blessed G, Tomlinson BE (1978b) Changes in brain cholinesterases in senile dementia of Alzheimer type. Neuropathol Appl Neurobiol 4: 273-277.

256. Potter LT (1967) A radiometric microassay of acetylcholinesterase. J Pharmacol Exp Ther 156: 500-506.

257. Raman M, Chen W, Cobb MH (2007) Differential regulation and properties of MAPKs. Oncogene 26: 3100-3112.

258. Ramirez G, Rey S, von Bernhardi R (2008) Proinflammatory stimuli are needed for induction of microglial cell-mediated AbetaPP_{244-C} and Abeta-neurotoxicity in hippocampal cultures. J Alzheimers Dis 15: 45-59.

259. Rawlins JN, Olton DS (1982) The septo-hippocampal system and cognitive mapping. Behav Brain Res 5: 331-358.

260. Rebeck GW, Perls TT, West HL, Sodhi P, Lipsitz LA, Hyman BT (1994) Reduced apolipoprotein epsilon 4 allele frequency in the oldest old Alzheimer's patients and cognitively normal individuals. Neurology 44: 1513-1516.

261. Reever CM, Ferrari-DiLeo G, Flynn DD (1997) The M5 (m5) receptor subtype: fact or fiction? Life Sci 60: 1105-1112.

262. Rogers J, Lue LF (2001) Microglial chemotaxis, activation, and phagocytosis of amyloid beta-peptide as linked phenomena in Alzheimer's disease. Neurochem Int 39: 333-340.

263. Rogers J, Mastroeni D, Leonard B, Joyce J, Grover A (2007) Neuroinflammation in Alzheimer's disease and Parkinson's disease: are microglia pathogenic in either disorder? Int Rev Neurobiol 82: 235-246.

264. Rogers J, Shen Y (2000) A perspective on inflammation in Alzheimer's disease. Ann N Y Acad Sci 924: 132-135.

265. Rogers J, Strohmeyer R, Kovelowski CJ, Li R (2002) Microglia and inflammatory mechanisms in the clearance of amyloid beta peptide. Glia 40: 260-269.

266. Rosenblum K, Berman DE, Hazvi S, Lamprecht R, Dudai Y (1997b) NMDA receptor and the tyrosine phosphorylation of its 2B subunit in taste learning in the rat insular cortex. J Neurosci 17: 5129-5135.

267. Rosenblum K, Berman DE, Hazvi S, Lamprecht R, Dudai Y (1997a) NMDA receptor and the tyrosine phosphorylation of its 2B subunit in taste learning in the rat insular cortex. J Neurosci 17: 5129-5135.

268. Rosi S, Giovannini MG, Lestage PJ, Munoz C, Corte LD, Pepeu G (2004) S 18986, a positive modulator of AMPA receptors with cognition-enhancing properties, increases ACh release in the hippocampus of young and aged rat. Neurosci Lett 361: 120-123.

269. Rosi S, Pert CB, Ruff MR, McGann-Gramling K, Wenk GL (2005) Chemokine receptor 5 antagonist D-Ala-peptide T-amide reduces microglia and astrocyte activation within the hippocampus in a neuroinflammatory rat model of Alzheimer's disease. Neuroscience 134: 671-676.

270. Rosi S, Vazdarjanova A, Ramirez-Amaya V, Worley PF, Barnes CA, Wenk GL (2006) Memantine protects against LPS-induced neuroinflammation, restores behaviorally-induced gene expression and spatial learning in the rat. Neuroscience 142: 1303-1315.

271. Rossner S, Schliebs R, Hartig W, Bigl V (1995) 192IGG-saporin-induced selective lesion of cholinergic basal forebrain system: neurochemical effects on

cholinergic neurotransmission in rat cerebral cortex and hippocampus. Brain Res Bull 38: 371-381.

272. Rouse ST, Marino MJ, Potter LT, Conn PJ, Levey AI (1999) Muscarinic receptor subtypes involved in hippocampal circuits. Life Sci 64: 501-509.

273. Ruitenberg A, Kalmijn S, de Ridder MA, Redekop WK, van Harskamp F, Hofman A, Launer LJ, Breteler MM (2001) Prognosis of Alzheimer's disease: the Rotterdam Study. Neuroepidemiology 20: 188-195.

274. Saba-El-Leil MK, Vella FD, Vernay B, Voisin L, Chen L, Labrecque N, Ang SL, Meloche S (2003a) An essential function of the mitogen-activated protein kinase Erk2 in mouse trophoblast development. EMBO Rep 4: 964-968.

275. Saba-El-Leil MK, Vella FD, Vernay B, Voisin L, Chen L, Labrecque N, Ang SL, Meloche S (2003b) An essential function of the mitogen-activated protein kinase Erk2 in mouse trophoblast development. EMBO Rep 4: 964-968.

276. Saba-El-Leil MK, Vella FD, Vernay B, Voisin L, Chen L, Labrecque N, Ang SL, Meloche S (2003c) An essential function of the mitogen-activated protein kinase Erk2 in mouse trophoblast development. EMBO Rep 4: 964-968.

277. Salvemini D, Misko TP, Masferrer JL, Seibert K, Currie MG, Needleman P (1993) Nitric oxide activates cyclooxygenase enzymes. Proc Natl Acad Sci U S A 90: 7240-7244.

278. Sarter M, Bruno JP (1997b) Cognitive functions of cortical acetylcholine: toward a unifying hypothesis. Brain Res Brain Res Rev 23: 28-46.

279. Sarter M, Bruno JP (1997a) Cognitive functions of cortical acetylcholine: toward a unifying hypothesis. Brain Res Brain Res Rev 23: 28-46.

280. Sarter M, Bruno JP (1997c) Cognitive functions of cortical acetylcholine: toward a unifying hypothesis. Brain Res Brain Res Rev 23: 28-46.

281. Sarter M, Bruno JP (2000) Cortical cholinergic inputs mediating arousal, attentional processing and dreaming: differential afferent regulation of the basal forebrain by telencephalic and brainstem afferents. Neuroscience 95: 933-952.

282. Sarter M, Bruno JP, Givens B (2003) Attentional functions of cortical cholinergic inputs: what does it mean for learning and memory? Neurobiol Learn Mem 80: 245-256.

283. Scali C, Casamenti F, Bellucci A, Costagli C, Schmidt B, Pepeu G (2002) Effect of subchronic administration of metrifonate, rivastigmine and donepezil on brain acetylcholine in aged F344 rats. J Neural Transm 109: 1067-1080.

284. Scali C, Giovannini MG, Prosperi C, Bartolini L, Pepeu G (1997) Tacrine administration enhances extracellular acetylcholine in vivo and restores the cognitive impairment in aged rats. Pharmacol Res 36: 463-469.

285. Scali C, Prosperi C, Giovannelli L, Bianchi L, Pepeu G, Casamenti F (1999) Beta(1-40) amyloid peptide injection into the nucleus basalis of rats induces microglia reaction and enhances cortical gamma-aminobutyric acid release in vivo. Brain Res 831: 319-321.

286. Schafe GE, Atkins CM, Swank MW, Bauer EP, Sweatt JD, LeDoux JE (2000a) Activation of ERK/MAP kinase in the amygdala is required for memory consolidation of pavlovian fear conditioning. J Neurosci 20: 8177-8187.

287. Schafe GE, Atkins CM, Swank MW, Bauer EP, Sweatt JD, LeDoux JE (2000b) Activation of ERK/MAP kinase in the amygdala is required for memory consolidation of pavlovian fear conditioning. J Neurosci 20: 8177-8187.

288. Schafe GE, Nadel NV, Sullivan GM, Harris A, LeDoux JE (1999a) Memory consolidation for contextual and auditory fear conditioning is dependent on protein synthesis, PKA, and MAP kinase. Learn Mem 6: 97-110.

289. Schafe GE, Nadel NV, Sullivan GM, Harris A, LeDoux JE (1999b) Memory consolidation for contextual and auditory fear conditioning is dependent on protein synthesis, PKA, and MAP kinase. Learn Mem 6: 97-110.

290. Schenk D, Barbour R, Dunn W, Gordon G, Grajeda H, Guido T, Hu K, Huang J, Johnson-Wood K, Khan K, Kholodenko D, Lee M, Liao Z, Lieberburg I, Motter R, Mutter L, Soriano F, Shopp G, Vasquez N, Vandevert C, Walker S, Wogulis M, Yednock T, Games D, Seubert P (1999) Immunization with amyloid-beta attenuates Alzheimer-disease-like pathology in the PDAPP mouse. Nature 400: 173-177.

291. Schenk D, Hagen M, Seubert P (2004) Current progress in beta-amyloid immunotherapy. Curr Opin Immunol 16: 599-606.

292. Schwartz RD, Kellar KJ (1985) In vivo regulation of [3H]acetylcholine recognition sites in brain by nicotinic cholinergic drugs. J Neurochem 45: 427-433.

293. Seger R, Krebs EG (1995b) The MAPK signaling cascade. FASEB J 9: 726-735.

294. Seger R, Krebs EG (1995a) The MAPK signaling cascade. FASEB J 9: 726-735.

295. Selcher JC, Atkins CM, Trzaskos JM, Paylor R, Sweatt JD (1999a) A necessity for MAP kinase activation in mammalian spatial learning. Learn Mem 6: 478-490.

296. Selcher JC, Atkins CM, Trzaskos JM, Paylor R, Sweatt JD (1999b) A necessity for MAP kinase activation in mammalian spatial learning. Learn Mem 6: 478-490.

297. Selcher JC, Atkins CM, Trzaskos JM, Paylor R, Sweatt JD (1999c) A necessity for MAP kinase activation in mammalian spatial learning. Learn Mem 6: 478-490.

298. Selcher JC, Atkins CM, Trzaskos JM, Paylor R, Sweatt JD (1999d) A necessity for MAP kinase activation in mammalian spatial learning. Learn Mem 6: 478-490.

299. Selcher JC, Nekrasova T, Paylor R, Landreth GE, Sweatt JD (2001a) Mice lacking the ERK1 isoform of MAP kinase are unimpaired in emotional learning. Learn Mem 8: 11-19.

300. Selcher JC, Nekrasova T, Paylor R, Landreth GE, Sweatt JD (2001b) Mice lacking the ERK1 isoform of MAP kinase are unimpaired in emotional learning. Learn Mem 8: 11-19.

301. Selkoe DJ (1994) Amyloid beta-protein precursor: new clues to the genesis of Alzheimer's disease. Curr Opin Neurobiol 4: 708-716.

302. Selkoe DJ (1999) Translating cell biology into therapeutic advances in Alzheimer's disease. Nature 399: A23-A31.

303. Sharma G, Vijayaraghavan S (2001) Nicotinic cholinergic signaling in hippocampal astrocytes involves calcium-induced calcium release from intracellular stores. Proc Natl Acad Sci U S A 98: 4148-4153.

304. Sharrocks AD, Yang SH, Galanis A (2000) Docking domains and substrate-specificity determination for MAP kinases. Trends Biochem Sci 25: 448-453.

305. Shen J, Barnes CA, Wenk GL, McNaughton BL (1996) Differential effects of selective immunotoxic lesions of medial septal cholinergic cells on spatial working and reference memory. Behav Neurosci 110: 1181-1186.

306. Sheng JG, Jones RA, Zhou XQ, McGinness JM, Van Eldik LJ, Mrak RE, Griffin WS (2001) Interleukin-1 promotion of MAPK-p38 overexpression in experimental animals and in Alzheimer's disease: potential significance for tau protein phosphorylation. Neurochem Int 39: 341-348.

307. Sheng JG, Zhu SG, Jones RA, Griffin WS, Mrak RE (2000) Interleukin-1 promotes expression and phosphorylation of neurofilament and tau proteins in vivo. Exp Neurol 163: 388-391.

308. Singh TJ, Zaidi T, Grundke-Iqbal I, Iqbal K (1995) Modulation of GSK-3-catalyzed phosphorylation of microtubule-associated protein tau by non-proline-dependent protein kinases. FEBS Lett 358: 4-8.

309. Sinha S, Lieberburg I (1999) Cellular mechanisms of beta-amyloid production and secretion. Proc Natl Acad Sci U S A 96: 11049-11053.

310. Stancampiano R, Cocco S, Cugusi C, Sarais L, Fadda F (1999) Serotonin and acetylcholine release response in the rat hippocampus during a spatial memory task. Neuroscience 89: 1135-1143.

311. Steinberg BA, Augustine JR (1997) Behavioral, anatomical, and physiological aspects of recovery of motor function following stroke. Brain Res Brain Res Rev 25: 125-132.

312. Steiner H (2004) Uncovering gamma-secretase. Curr Alzheimer Res 1: 175-181.

313. Stewart WF, Kawas C, Corrada M, Metter EJ (1997) Risk of Alzheimer's disease and duration of NSAID use. Neurology 48: 626-632.

314. Stoehr JD, Mobley SL, Roice D, Brooks R, Baker LM, Wiley RG, Wenk GL (1997) The effects of selective cholinergic basal forebrain lesions and aging upon expectancy in the rat. Neurobiol Learn Mem 67: 214-227.

315. Street JS, Clark WS, Gannon KS, Cummings JL, Bymaster FP, Tamura RN, Mitan SJ, Kadam DL, Sanger TM, Feldman PD, Tollefson GD, Breier A (2000) Olanzapine treatment of psychotic and behavioral symptoms in patients with Alzheimer disease in nursing care facilities: a double-blind, randomized, placebo-controlled trial. The HGEU Study Group. Arch Gen Psychiatry 57: 968-976.

316. Streit WJ (2002) Microglia and the response to brain injury. Ernst Schering Res Found Workshop 11-24.

317. Sudweeks SN, Yakel JL (2000) Functional and molecular characterization of neuronal nicotinic ACh receptors in rat CA1 hippocampal neurons. J Physiol 527 Pt 3: 515-528.

318. Sugita S, Uchimura N, Jiang ZG, North RA (1991) Distinct muscarinic receptors inhibit release of gamma-aminobutyric acid and excitatory amino acids in mammalian brain. Proc Natl Acad Sci U S A 88: 2608-2611.

319. Sun A, Liu M, Nguyen XV, Bing G (2003) P38 MAP kinase is activated at early stages in Alzheimer's disease brain. Exp Neurol 183: 394-405.

320. Takahashi M, Tomizawa K, Ishiguro K, Takamatsu M, Fujita SC, Imahori K (1995) Involvement of tau protein kinase I in paired helical filament-like phosphorylation of the juvenile tau in rat brain. J Neurochem 64: 1759-1768.

321. Takata K, Kitamura Y, Tsuchiya D, Kawasaki T, Taniguchi T, Shimohama S (2004) High mobility group box protein-1 inhibits microglial Abeta clearance and enhances Abeta neurotoxicity. J Neurosci Res 78: 880-891.

322. Tariot PN, Farlow MR, Grossberg GT, Graham SM, McDonald S, Gergel I (2004) Memantine treatment in patients with moderate to severe Alzheimer disease already receiving donepezil: a randomized controlled trial. JAMA 291: 317-324.

323. Terry AV, Jr., Buccafusco JJ (2003) The cholinergic hypothesis of age and Alzheimer's disease-related cognitive deficits: recent challenges and their implications for novel drug development. J Pharmacol Exp Ther 306: 821-827.

324. Thiermann H, Szinicz L, Eyer P, Zilker T, Worek F (2005) Correlation between red blood cell acetylcholinesterase activity and neuromuscular transmission in organophosphate poisoning. Chem Biol Interact 157-158: 345-347.

325. Tocco G, Freire-Moar J, Schreiber SS, Sakhi SH, Aisen PS, Pasinetti GM (1997) Maturational regulation and regional induction of cyclooxygenase-2 in rat brain: implications for Alzheimer's disease. Exp Neurol 144: 339-349.

326. Trejo J, Massamiri T, Deng T, Dewji NN, Bayney RM, Brown JH (1994) A direct role for protein kinase C and the transcription factor Jun/AP-1 in the regulation of the Alzheimer's beta-amyloid precursor protein gene. J Biol Chem 269: 21682-21690.

327. Troy CM, Rabacchi SA, Xu Z, Maroney AC, Connors TJ, Shelanski ML, Greene LA (2001) beta-Amyloid-induced neuronal apoptosis requires c-Jun N-terminal kinase activation. J Neurochem 77: 157-164.

328. Ulloa L, Messmer D (2006) High-mobility group box 1 (HMGB1) protein: friend and foe. Cytokine Growth Factor Rev 17: 189-201.

329. Unwin N (1996) Projection structure of the nicotinic acetylcholine receptor: distinct conformations of the alpha subunits. J Mol Biol 257: 586-596.

330. Usarek E, Kuzma-Kozakiewicz M, Schwalenstocker B, Kazmierczak B, Munch C, Ludolph AC, Baranczyk-Kuzma A (2006) Tau isoforms expression in transgenic mouse model of amyotrophic lateral sclerosis. Neurochem Res 31: 597-602.

331. Utsugisawa K, Nagane Y, Tohgi H, Yoshimura M, Ohba H, Genda Y (1999) Changes with aging and ischemia in nicotinic acetylcholine receptor subunit alpha7 mRNA expression in postmortem human frontal cortex and putamen. Neurosci Lett 270: 145-148.

332. Utsuki T, Shoaib M, Holloway HW, Ingram DK, Wallace WC, Haroutunian V, Sambamurti K, Lahiri DK, Greig NH (2002) Nicotine lowers the secretion of the Alzheimer's amyloid beta-protein precursor that contains amyloid beta-peptide in rat. J Alzheimers Dis 4: 405-415.

333. Van Broeckhoven C, Backhovens H, Cruts M, De Winter G, Bruyland M, Cras P, Martin JJ (1992) Mapping of a gene predisposing to early-onset Alzheimer's disease to chromosome 14q24.3. Nat Genet 2: 335-339.

334. Van der Zee EA, Compaan JC, Bohus B, Luiten PG (1995) Alterations in the immunoreactivity for muscarinic acetylcholine receptors and colocalized PKC gamma in mouse hippocampus induced by spatial discrimination learning. Hippocampus 5: 349-362.

335. Van der Zee EA, Luiten PG (1999a) Muscarinic acetylcholine receptors in the hippocampus, neocortex and amygdala: a review of immunocytochemical localization in relation to learning and memory. Prog Neurobiol 58: 409-471.

336. Van der Zee EA, Luiten PG (1999b) Muscarinic acetylcholine receptors in the hippocampus, neocortex and amygdala: a review of immunocytochemical localization in relation to learning and memory. Prog Neurobiol 58: 409-471.

337. Vassar R, Bennett BD, Babu-Khan S, Kahn S, Mendiaz EA, Denis P, Teplow DB, Ross S, Amarante P, Loeloff R, Luo Y, Fisher S, Fuller J, Edenson S, Lile J, Jarosinski MA, Biere AL, Curran E, Burgess T, Louis JC, Collins F, Treanor J, Rogers G, Citron M (1999) Beta-secretase cleavage of Alzheimer's amyloid precursor protein by the transmembrane aspartic protease BACE. Science 286: 735-741.

338. Vilaro MT, Mengod G, Palacios JM (1993) Advances and limitations of the molecular neuroanatomy of cholinergic receptors: the example of multiple muscarinic receptors. Prog Brain Res 98: 95-101.

339. Vnek N, Rothblat LA (1996) The hippocampus and long-term object memory in the rat. J Neurosci 16: 2780-2787.

340. Walker DG, Kim SU, McGeer PL (1995) Complement and cytokine gene expression in cultured microglial derived from postmortem human brains. J Neurosci Res 40: 478-493.

341. Walz R, Roesler R, Quevedo J, Rockenbach IC, Amaral OB, Vianna MR, Lenz G, Medina JH, Izquierdo I (1999) Dose-dependent impairment of inhibitory avoidance retention in rats by immediate post-training infusion of a mitogen-activated protein kinase kinase inhibitor into cortical structures. Behav Brain Res 105: 219-223.

342. Walz R, Roesler R, Quevedo J, Sant'Anna MK, Madruga M, Rodrigues C, Gottfried C, Medina JH, Izquierdo I (2000c) Time-dependent impairment of inhibitory avoidance retention in rats by posttraining infusion of a mitogen-activated protein kinase kinase inhibitor into cortical and limbic structures. Neurobiol Learn Mem 73: 11-20.

343. Walz R, Roesler R, Quevedo J, Sant'Anna MK, Madruga M, Rodrigues C, Gottfried C, Medina JH, Izquierdo I (2000d) Time-dependent impairment of inhibitory avoidance retention in rats by posttraining infusion of a mitogen-activated protein kinase kinase inhibitor into cortical and limbic structures. Neurobiol Learn Mem 73: 11-20.

344. Walz R, Roesler R, Quevedo J, Sant'Anna MK, Madruga M, Rodrigues C, Gottfried C, Medina JH, Izquierdo I (2000a) Time-dependent impairment of inhibitory avoidance retention in rats by posttraining infusion of a mitogen-activated protein kinase kinase inhibitor into cortical and limbic structures. Neurobiol Learn Mem 73: 11-20.

345. Walz R, Roesler R, Quevedo J, Sant'Anna MK, Madruga M, Rodrigues C, Gottfried C, Medina JH, Izquierdo I (2000b) Time-dependent impairment of inhibitory avoidance retention in rats by posttraining infusion of a mitogen-

activated protein kinase kinase inhibitor into cortical and limbic structures. Neurobiol Learn Mem 73: 11-20.

346. Watabe AM, Zaki PA, O'Dell TJ (2000a) Coactivation of beta-adrenergic and cholinergic receptors enhances the induction of long-term potentiation and synergistically activates mitogen-activated protein kinase in the hippocampal CA1 region. J Neurosci 20: 5924-5931.

347. Watabe AM, Zaki PA, O'Dell TJ (2000b) Coactivation of beta-adrenergic and cholinergic receptors enhances the induction of long-term potentiation and synergistically activates mitogen-activated protein kinase in the hippocampal CA1 region. J Neurosci 20: 5924-5931.

348. Wess J (1993) Mutational analysis of muscarinic acetylcholine receptors: structural basis of ligand/receptor/G protein interactions. Life Sci 53: 1447-1463.

349. Wevers A, Jeske A, Lobron C, Birtsch C, Heinemann S, Maelicke A, Schroder R, Schroder H (1994) Cellular distribution of nicotinic acetylcholine receptor subunit mRNAs in the human cerebral cortex as revealed by non-isotopic in situ hybridization. Brain Res Mol Brain Res 25: 122-128.

350. White NM, McDonald RJ (2002) Multiple parallel memory systems in the brain of the rat. Neurobiol Learn Mem 77: 125-184.

351. Whitehouse PJ, Kalaria RN (1995) Nicotinic receptors and neurodegenerative dementing diseases: basic research and clinical implications. Alzheimer Dis Assoc Disord 9 Suppl 2: 3-5.

352. Whiting PJ, Schoepfer R, Conroy WG, Gore MJ, Keyser KT, Shimasaki S, Esch F, Lindstrom JM (1991) Expression of nicotinic acetylcholine receptor subtypes in brain and retina. Brain Res Mol Brain Res 10: 61-70.

353. Wilcock GK (2003) Memantine for the treatment of dementia. Lancet Neurol 2: 503-505.

354. Wilensky AE, Schafe GE, LeDoux JE (2000) The amygdala modulates memory consolidation of fear-motivated inhibitory avoidance learning but not classical fear conditioning. J Neurosci 20: 7059-7066.

355. Wilkie GI, Hutson P, Sullivan JP, Wonnacott S (1996) Pharmacological characterization of a nicotinic autoreceptor in rat hippocampal synaptosomes. Neurochem Res 21: 1141-1148.

356. Willaime-Morawek S, Brami-Cherrier K, Mariani J, Caboche J, Brugg B (2003) C-Jun N-terminal kinases/c-Jun and p38 pathways cooperate in ceramide-induced neuronal apoptosis. Neuroscience 119: 387-397.

357. Williams NG, Zhong H, Minneman KP (1998) Differential coupling of alpha1-, alpha2-, and beta-adrenergic receptors to mitogen-activated protein kinase

pathways and differentiation in transfected PC12 cells. J Biol Chem 273: 24624-24632.

358. Winder DG, Martin KC, Muzzio IA, Rohrer D, Chruscinski A, Kobilka B, Kandel ER (1999) ERK plays a regulatory role in induction of LTP by theta frequency stimulation and its modulation by beta-adrenergic receptors. Neuron 24: 715-726.

359. Winocur G, Oxbury S, Roberts R, Agnetti V, Davis C (1984) Amnesia in a patient with bilateral lesions to the thalamus. Neuropsychologia 22: 123-143.

360. Wrenn CC, Wiley RG (1998) The behavioral functions of the cholinergic basal forebrain: lessons from 192 IgG-saporin. Int J Dev Neurosci 16: 595-602.

361. Xia Z, Dickens M, Raingeaud J, Davis RJ, Greenberg ME (1995) Opposing effects of ERK and JNK-p38 MAP kinases on apoptosis. Science 270: 1326-1331.

362. Xiao J, Perry G, Troncoso J, Monteiro MJ (1996) alpha-calcium-calmodulin-dependent kinase II is associated with paired helical filaments of Alzheimer's disease. J Neuropathol Exp Neurol 55: 954-963.

363. Yamada M, Miyakawa T, Duttaroy A, Yamanaka A, Moriguchi T, Makita R, Ogawa M, Chou CJ, Xia B, Crawley JN, Felder CC, Deng CX, Wess J (2001) Mice lacking the M3 muscarinic acetylcholine receptor are hypophagic and lean. Nature 410: 207-212.

364. Yamagata K, Andreasson KI, Kaufmann WE, Barnes CA, Worley PF (1993) Expression of a mitogen-inducible cyclooxygenase in brain neurons: regulation by synaptic activity and glucocorticoids. Neuron 11: 371-386.

365. Yankner BA, Caceres A, Duffy LK (1990) Nerve growth factor potentiates the neurotoxicity of beta amyloid. Proc Natl Acad Sci U S A 87: 9020-9023.

366. Yao Y, Li W, Wu J, Germann UA, Su MS, Kuida K, Boucher DM (2003) Extracellular signal-regulated kinase 2 is necessary for mesoderm differentiation. Proc Natl Acad Sci U S A 100: 12759-12764.

367. Yasoshima Y, Yamamoto T (1997) Rat gustatory memory requires protein kinase C activity in the amygdala and cortical gustatory area. NeuroReport 8: 1363-1367.

368. Yeomans J, Forster G, Blaha C (2001) M5 muscarinic receptors are needed for slow activation of dopamine neurons and for rewarding brain stimulation. Life Sci 68: 2449-2456.

369. Zang Z, Creese I (1997) Differential regulation of expression of rat hippocampal muscarinic receptor subtypes following fimbria-fornix lesion. Biochem Pharmacol 53: 1379-1382.

370. Zheng JQ, Felder M, Connor JA, Poo MM (1994) Turning of nerve growth cones induced by neurotransmitters. Nature 368: 140-144.

371. Zhou G, Bao ZQ, Dixon JE (1995b) Components of a new human protein kinase signal transduction pathway. J Biol Chem 270: 12665-12669.

372. Zhou G, Bao ZQ, Dixon JE (1995a) Components of a new human protein kinase signal transduction pathway. J Biol Chem 270: 12665-12669.

373. Zhu JJ, Qin Y, Zhao M, Van Aelst L, Malinow R (2002) Ras and Rap control AMPA receptor trafficking during synaptic plasticity. Cell 110: 443-455.

374. Zhu X, Castellani RJ, Takeda A, Nunomura A, Atwood CS, Perry G, Smith MA (2001a) Differential activation of neuronal ERK, JNK/SAPK and p38 in Alzheimer disease: the 'two hit' hypothesis. Mech Ageing Dev 123: 39-46.

375. Zhu X, Raina AK, Rottkamp CA, Aliev G, Perry G, Boux H, Smith MA (2001b) Activation and redistribution of c-jun N-terminal kinase/stress activated protein kinase in degenerating neurons in Alzheimer's disease. J Neurochem 76: 435-441.

376. Zhu X, Rottkamp CA, Boux H, Takeda A, Perry G, Smith MA (2000) Activation of p38 kinase links tau phosphorylation, oxidative stress, and cell cycle-related events in Alzheimer disease. J Neuropathol Exp Neurol 59: 880-888.

377. Zola-Morgan S, Squire LR (1993) Neuroanatomy of memory. Annu Rev Neurosci 16: 547-563.